Investigating the techno-economic and environmental performance of hydrogen deployment paradigms in Canada

by

Ian Maynard

A thesis submitted to the Faculty of Graduate and Postdoctoral Affairs in partial fulfillment of the requirements for the degree of

Master of Applied Science

in

Mechanical Engineering

Carleton University
Ottawa, Ontario

© 2022
Ian Maynard

Abstract

This thesis presents a multi-scale investigation of the cost and performance of two hydrogen transition pathways. It adopts a systems perspective to: 1) simulate hydrogen transition in one Canadian region that is pursuing hydrogen as a way to exit natural gas, and 2) optimize the deployment of hydrogen-backed microgrids to meet electrical and thermal loads in Canada's remote and northern communities, which currently rely on diesel. These constitute two applications where hydrogen deployment could be demonstrated in the near-term, because current fossil alternatives are expensive and undesirable. Chapter 2 simulates production pathways for green hydrogen in Canada's Atlantic Maritimes. It employs empirical growth rates to estimate the installed capacity, cost, and emissions of an integrated energy system that couples offshore wind with electrolysis. Various scenarios are considered: hydrogen storage, grid integration, and freight transportation. Hydrogen production is found to be at least three times costlier than grid integration. Projects could be implemented by 2050 and at <2 $/kg$H_2$ with aggressive growth rates, learning rates, and electrolyzer capital costs of 500 $/kW. Chapter 3 develops a method to estimate the thermal loads in remote and northern communities. It applies this method to 40 communities and develops a regression model that estimates thermal loads. Chapter 4 builds an optimization model that deploys wind turbines and reversible fuel cells to meet the electrical and thermal loads of those 40 communities. Results show that hydrogen-backed microgrids are viable and cheaper than their diesel equivalents, but they entail overbuilding of wind capacity to serve electrical and thermal needs. The cost of avoided emissions from these microgrids are equal to or greater than the federal carbon price in 2030. Five communities have costs of avoided emissions of <200 CAD/tCO_2, while 30 have costs of <500 CAD/tCO_2.

Preface

This integrated thesis includes three chapters that have been formatted for publication in the peer-reviewed literature as research articles. Until the articles are published, readers must cite these chapters as follows:

- Chapter 2 can be cited as:

  Maynard I, Abdulla A. Expanding green hydrogen production to supplant liquid or gaseous fuels in a net-zero transition. *Renewable Energy*. [Submitted]

- Chapter 3 can be cited as:

  Maynard I, Abdulla A. A method for estimating thermal energy loads in Canada's remote and northern communities. *Environmental Research Letters*. [Submitted]

- Chapter 4 can be cited as:

  Maynard I, Schell KR, Abdulla A. Optimizing hydrogen microgrids to facilitate diesel exit and meet the energy needs of remote and northern communities. *Nature Sustainability*. [In preparation]

Acknowledgments

I would like to express my gratitude to my thesis supervisor, Ahmed Abdulla, who has guided me and helped make this journey an exciting learning experience. I would also like to thank Ryan Kilpatrick for offering assistance and collaboration that helped steer the execution of this thesis and heavily influenced the last two chapters. Kristen Schell also has my thanks, as she provided essential insight and knowledge of Python and optimization methods. Finally, I would like to thank all my friends and family who have helped support me throughout this graduate program.

I'd also like to acknowledge the support I received to conduct this work from the Natural Sciences and Engineering Research Council [grant number RGPIN-2021-03805]. This was also supported by the Carleton University Office of the Vice President Research and International and the Carleton University Faculty of Engineering and Design through a Multi-disciplinary Research Catalyst Fund.

Nomenclature

Variable	Description	Unit
Nomenclature for Chapter 2		
A	Area swept by blades	m^2
$C_{CO_2}^{avoidance}$	Cost of CO_2 avoidance (schematic)	USD
$C_{CO_2}^{social}$	Social cost of CO_2 (schematic)	USD
C_E^{capex}	Electrolyzer CAPEX (schematic)	USD
C_E^{opex}	Electrolyzer OPEX (schematic)	USD
C_{Total}	Total cost at project completion (schematic)	USD
C_T^{capex}	Turbine CAPEX (schematic)	USD
C_T^{opex}	Turbine OPEX (schematic)	USD
C_{LCOH}	Levelized costs of hydrogen (schematic)	USD
C_{in}	Cut-in speed	m/s
C_{out}	Cut-out speed	m/s
C_p	Power coefficient	
CF_e	Electrolyzer capacity factor	%
CF_t	Turbine capacity factor	%
$D_{elec,\,fossil\,(2050)}$	Electric power generated by fossil resources in the Maritimes in 2050	GWh
D_{H_2}	H_2 demand	m^3
$D_{H_2,ind}$	Industrial H_2 demand	m^3
D_{supp}	Diesel supplanted by hydrogen	m^3
D_y	Distance traveled in the Maritimes each year (y)	km
d_m	Number of days in a month (m)	
$E_{CO_2}^{avoided}$	CO_2 emissions avoided	kg
EF_s	Emission factor per emitting source (s)	gCO_2/kg, gCO_2/m^3, gCO_2/L
$Elec_s$	Annual electricity production per emitting source (s)	GWh
EM_s	Annual emissions per emitting source (s)	kg
EM_s^{total}	Annual emissions of all sources (s)	kg
$EN_{i,m}$	Number of electrolyzers for each month (m) and year (i)	

Variable	Description	Unit
G	Annual project growth rate	%
H_{Supp}	Amount of hydrogen to supplant diesel transportation	m^3
h_{hub}	Hub height	m
HC_s	Heat content per emitting source (s)	GJ/t, GJ/ML, GJ/L
HR_s	Heat rate per emitting source (s)	Btu/kWh
i	Year	
i_{start}	Start year	
L	Annual reduction in cost (schematic)	USD
L_{array}	Array losses	%
L_{aux}	Auxiliary loads	%
L_s	Total summer climate losses	GWh / (Installed MW)
L_w	Total winter climate losses	GWh / (Installed MW)
MP_r	% of distance driven in Maritimes per route (r)	%
MD_r	Distance driven in Maritimes per route (r)	km
m	Month	
NG_{supp}	Natural gas supplanted by hydrogen in m^3	m^3
$NS_{r,y}$	# of shipments for each route (r) in each year (y)	
P_{air}^{hub}	Air pressure at hub	Pa
P_{elec}	Average daily array power output (schematic)	GWh
P_{elec}^{annual}	Annual electrical production by the turbine array	Wh
P_{elec}^{array}	Average daily net array electrical production	Wh
P_{elec}^{net}	Average daily net turbine electrical production	Wh
P_{elec}^{raw}	Average daily turbine raw electrical production	Wh
P_{H_2}	Average daily hydrogen output (schematic)	m^3
$P_{H_2}^{kg}$	Average daily hydrogen production	kg
$P_{H_2}^{m^3}$	Average daily hydrogen output	m^3
R	Blade radius	m

Variable	Description	Unit
s	Fossil-fuel based emitting sources for scenario γ	
TD_r	Total distance traveled in each route (r)	km
TN_i	Number of turbines for each iteration year (i)	
$TN_i(i=1)$	Number of starting turbines at the beginning of simulation	
TN_{max}	Max number of turbines (specific to each scenario)	
T_{air}^{hub}	Air temp at hub	°C
T_{apr}	Average temperature - April	°C
T_{aug}	Average temperature - August	°C
T_{dec}	Average temperature - December	°C
T_{feb}	Average temperature - February	°C
T_{jan}	Average temperature - January	°C
T_{jul}	Average temperature - July	°C
T_{jun}	Average temperature - June	°C
T_{mar}	Average temperature - March	°C
T_{may}	Average temperature - May	°C
T_{nov}	Average temperature - November	°C
T_{oct}	Average temperature - October	°C
T_{sep}	Average temperature - September	°C
V_w	Wind speed	m/s
w	Percentage of time a wind speed occurs during the day	%
z	Surface roughness	m
ρ_{air}^{hub}	Air density at hub	kg/m^3

Nomenclature for Chapter 4

Variable	Description	Unit
CAP_{dfs}^{DF}	CAPEX of diesel furnace for each size, dfs	USD/kW
CAP_{gs}^{G}	CAPEX of diesel genset for each size, gs	USD/kW
CAP_{hfs}^{HF}	CAPEX of hydrogen furnace for each size, hfs	USD/kW
CAP_{rs}^{R}	CAPEX of RFC for each size, rs	USD/kW
CAP_{ws}^{W}	CAPEX of wind turbine for each size, ws	USD/kW

Variable	Description	Unit
cc	Total microgrid capital costs (Annualized)	USD
cc^{DF}	Diesel furnace capital costs (Annualized)	USD
cc^{G}	Diesel genset capital costs (Annualized)	USD
cc^{HF}	Hydrogen furnace capital costs (Annualized)	USD
cc^{R}	RFC capital costs (Annualized)	USD
cc^{W}	Wind turbine capital costs (Annualized)	USD
ce_{gs}^{G}	Total electrical capacity of the diesel gensets for each size, gs	kW
ce_{rs}^{R}	Total electrical capacity of the RFCs for each size, rs	kW
ce_{ws}^{W}	Total electrical capacity of the wind turbines for each size, ws	kW
ct_{dfs}^{DF}	Total thermal capacity of the diesel furnaces for each size, dfs	kW
ct_{hfs}^{HF}	Total thermal capacity of the hydrogen furnaces for each size, hfs	kW
D_E	Conversion of diesel to electricity	kWh/ L diesel
D_T	Conversion of diesel to heat	kWh/ L diesel
DFS	Set of the diesel furnace sizes, dfs	
E_H	Conversion of electricity to hydrogen	kg H_2/ kWh
Eta^{DF}	Efficiency of diesel furnace	%
Eta^{HF}	Efficiency of hydrogen furnace	%
f^{DF}	Fuel consumption of diesel furnace	L
f^{G}	Fuel consumption of diesel genset	L
GS	Set of diesel genset sizes, gs	
H_E	Conversion of hydrogen to electricity	kg H_2/ kWh
H_T	Conversion of hydrogen to heat	kg H_2/ kWh
HFS	Set of hydrogen furnace sizes, hfs	
Ke_{gs}^{G}	Max electrical capacity for each size diesel genset, gs	kW
Ke_{rs}^{R}	Max electrical capacity for each size RFC, rs	kW
Ke_{ws}^{W}	Max electrical capacity for each size wind turbine, ws	kW
Kt_{dfs}^{DF}	Max thermal capacity for each size diesel furnace, dfs	kW

Variable	Description	Unit
Kt_{hfs}^{HF}	Max thermal capacity for each size hydrogen furnace, hfs	kW
L^{DF}	Lifetime of diesel furnace	Years
L^{G}	Lifetime of diesel genset	Years
L^{HF}	Lifetime of hydrogen furnace	Years
L^{R}	Lifetime of RFC	Years
L^{W}	Lifetime of wind turbine	Years
L_t	Electrical load at each time, t	kWh
LT_t	Thermal load at each time, t	kWh
M	Arbitrarily large number for the binary constraint to function	
ne_{gs}^{G}	Number of diesel gensets of each size, gs	
ne_{rs}^{R}	Number of RFCs of each size, rs	
ne_{ws}^{W}	Number of wind turbines of each size, ws	
nt_{dfs}^{DF}	Number of diesel furnaces of each size, dfs	
nt_{hfs}^{HF}	Number of hydrogen furnaces of each size, hfs	
oc	Total microgrid operating costs	USD
oc^{DF}	Diesel furnace operating costs	USD
oc^{G}	Diesel genset operating costs	USD
oc^{HF}	Hydrogen furnace operating costs	USD
oc^{R}	RFC operating costs	USD
oc^{W}	Wind turbine operating costs	USD
OP^{D}	Cost of diesel	USD/ L diesel
OP_{dfs}^{DF}	OPEX of diesel furnace of each size, dfs	USD/kW
OP_{gs}^{G}	OPEX of diesel genset of each size, gs	USD/kW
OP_{hfs}^{HF}	OPEX of hydrogen furnace of each size, hfs	USD/kW
OP_{rs}^{R}	OPEX of RFC of each size, rs	USD/kW
OP_{ws}^{W}	OPEX of wind turbine of each size, ws	USD/kW
pl_t	Level of power at each time, t ("$+$" = power excess, "$-$" = power deficit)	kWh
R_{min}	Minimum amount of hydrogen in the hydrogen tank (value set to 0)	kg H_2
r	Discount rate	%

Variable	Description	Unit
RS	Set of the RFC sizes, rs	
SLT	Set of the time range for the summer thermal load $(0 \leq t \leq 335)$	
SoR	State of RFC (amount of hydrogen stored in the hydrogen tank)	kg H_2
T	Set of time for the four-week period $(0 \leq t \leq 671)$	
Ue_{gs}^{G}	Unit electrical capacity of each size diesel genset, gs	
Ue_{rs}^{R}	Unit electrical capacity of each size RFC, rs	
Ue_{ws}^{W}	Unit electrical capacity of each size wind turbine, ws	
Ut_{dfs}^{DF}	Unit thermal capacity of each size diesel furnace, dfs	
Ut_{hfs}^{HF}	Unit thermal capacity of each size hydrogen furnace, hfs	
$W_{t,ws}$	Max wind output at each time, t and for each size, ws	
W_E	Production of water when creating electricity from hydrogen	L H_2O/ kg H_2
W_H	Consumption of water when creating hydrogen from electricty	L H_2O/ kg H_2
WS	Set of wind turbine sizes, ws	
wt_t	Water tank level at each time, t	L H_2O
wtr_{cap}^{a}	Annual water consumption with water capture	L H_2O
wtr_{nocap}^{a}	Annual water consumption without water capture	L H_2O
wtr_{cap}^{s}	Summer water consumption with water capture	L H_2O
wtr_{nocap}^{s}	Summer water consumption without water capture	L H_2O
wtr_{cap}^{w}	Winter water consumption with water capture	L H_2O
wtr_{nocap}^{w}	Winter water consumption without water capture	L H_2O
y_t	Binary variable for each time, t	
Δ_t^{SoR}	SoR duty for each time, t	kg H_2

Variable	Description	Unit
τ	Number of typical days represented by each day in the four-week period (13 to estimate values from four weeks to a year)	

Contents

List of Tables

List of Figures

List of Appendices

Chapter 1. Thesis introduction

1.1 Background and context

With its signing of the Paris Agreement in 2015 [1] and its passing of Bill C-12 in 2021 [2], Canada has set its sights on reducing its greenhouse gas emissions (GHG) to achieve an ambitious target of net-zero emissions by 2050. One pathway for reducing GHG emissions, especially from sectors of the economy that are difficult to electrify—like industry, transport, and heat—is to use hydrogen that is produced in low-carbon ways. One prominent set of such pathways is referred to as green hydrogen, which refers to hydrogen that is produced through water electrolysis with zero-carbon or low-carbon sources of energy. Although green hydrogen production is expensive today, an analysis by the International Energy Agency (IEA) finds that green hydrogen production costs could fall 30% by 2030, as low-cost renewables are deployed and hydrogen production technologies experience cost reductions [3].

Canada is witnessing growing interest in low-carbon hydrogen production, but most analyses have focused either on specific case studies—such as converting a specific bus system or a specific industrial facility to use the fuel—or on the concept of "hydrogen hubs" that would serve several co-located energy users. Each one of these case studies requires its own techno-economic analysis. Meanwhile, few technical analyses exist that outline the cost, performance, and infrastructure needs of broad, sectoral transitions. The thesis comprises a multi-scale analysis of two niche hydrogen applications that are likely candidates for near-term demonstration. At a large-scale, it simulates hydrogen transition pathways for an entire region—the Atlantic Maritimes—that will need fossil fuel exist strategies to achieve its net-zero emission targets. At a smaller-scale, it optimizes the deployment of hydrogen-backed microgrids for remote and northern communities that

need to engage in a diesel exit, since that fuel is the predominant method of providing both electric power and thermal energy to those communities.

1.2 Research objectives

This thesis explores the techno-economic and environmental performance of hydrogen transition pathways at two different scales. The objectives of chapter 2 are:

- To explore the cost and performance of implementing an integrated energy system that employs offshore wind and hydrogen to supplant natural gas or diesel usage within the Atlantic Maritimes.
- To incorporate realistic parameters for growth rates and technological learning rates into the simulation to determine whether the completion of various hydrogen transition pathways is feasible by 2050.
- To estimate the cost of this integrated energy system and compare it to the cost of hydrogen production through alternative pathways, and to determine the component costs that are required to make this system competitive with other hydrogen production methods.

The objectives for chapter 3 are:

- To develop and test a method for generating hourly thermal load profiles for remote and northern communities across Canada.
- To determine the significance of thermal loads and the role of low-carbon heat provision in any effective energy transition in these communities.

The objectives for chapter 4 are:

- To develop a mixed integer linear program to optimize the deployment of hydrogen-backed microgrids (wind, reversible fuel cell, and hydrogen furnace) in

selected remote and northern communities, and to compare their costs to those of diesel microgrids.

- To determine for which communities and under what conditions hydrogen-backed microgrids might be feasible in the near future.

1.3 Structure of thesis

Chapter 2 of this thesis focuses on simulating hydrogen transition pathways that supplant natural gas use in the Atlantic Maritimes. Chapter 3 presents a method to develop hourly thermal load profiles for a large subset of remote and northern communities in Canada. These thermal load profiles are used as inputs into an optimization model of hydrogen-backed microgrids that produce no operational emissions: this model is presented in chapter 4. Concluding remarks and recommendations for future work are presented in chapter 5.

Chapter 2. Expanding green hydrogen production to supplant liquid or gaseous fuels in the net-zero transition

2.1. Introduction

Many jurisdictions worldwide have proposed ambitious emission reduction targets, with Canada [2], the European Union [4] the United Kingdom [5], and the United States [6] pledging to achieve net-zero emissions by 2050. In addition to deploying more low-carbon electricity generators to serve a highly electrified energy system, there is recognition that emissions from some sectors of the economy—like industry and heavy-duty freight—are hard-to abate; these sectors will continue to require liquid or gaseous fuels for the foreseeable future [7]. The conversation regarding these sectors has shifted to low-carbon fuel options, including hydrogen which can be electrochemically reacted in fuel cells or combusted in furnaces or engines to produce heat or work.

We simulate the infrastructure buildout that would be required to supplant fuels with green (i.e., non-fossil-derived) hydrogen in the Atlantic Maritimes region of Canada, the implications of analyzing which go beyond the local context. The region has a more diverse electricity generation mix than many Canadian provinces, some of which are largely dependent on a single resource like hydropower. By contrast and like other jurisdictions globally, the Maritimes have legacy coal and nuclear generation that will have to be retired over the coming decades due to age or stringent decarbonization targets [8, 9]. In addition, like many other economies, the region is reliant on natural gas imports—in this case, from the U.S. Northeast [10], where gas infrastructure is constrained and subject to spikes in demand and price during cold winters. Moreover, like most other jurisdictions globally, the region's proposed net-zero transition pathway projects a large expansion in low-carbon renewable energy sources: wind, solar, and

hydro are expected to satisfy most of the region's electricity demand in 2050 [11]. As such, any expansion in renewable hydrogen production will unfold at the same time as power sector decarbonization and demand electrification. Finally, the Maritimes are of a similar size to many other regions (and nations) globally, making results generalizable to a wider geographic context.

Specifically, we seek to fill two analytical gaps. First, most visions assume implementation by 2050 is possible. Even if the investment that would be required to meet this target were available, historical evidence suggests that there are constraints or limits to technological upscaling. Here, we employ growth and learning rates derived from industrial experience and provide more realistic assessments of time to completion. Second, few visions set hydrogen production targets by 2050; the few targets that do exist are divorced from low-carbon fuel demand. We seek to focus the minds of investors and policymakers by estimating the amount of infrastructure that would be required to meet expected demand and its cost. In section 2.2, we summarize the existing literature and the policy context surrounding green hydrogen in Canada and the Maritimes, much of which is applicable to other nations as well. Section 2.3 describes the data and methods; section 2.4 presents results; and section 2.5 provides concluding remarks and policy implications.

2.2 Background

2.2.1. Explaining Canada's interest in hydrogen

Hydrogen has become prominent in Canada, partly due to the country's economic and political characteristics. The Canadian economy is reliant on the production and export of liquid and gaseous fuels [12]; energy policy is developed and implemented at the provincial, rather than the federal, level [13]; and energy politics are "fragmented", if

not polarized [14]. Apart from hydropower, it is difficult to find an energy technology around which politics and policy are aligned. This lack of alignment has been a constraint to deep decarbonization: it is rare for multiple, disparate provinces to see a role for themselves when it comes to almost any energy technology. Fortuitously, hydrogen technologies fall into this category, as evidenced by the large number of hydrogen strategy documents released and pilot projects initiated. In 2020, the Federal Government released its "Hydrogen Strategy for Canada" [15]. The provinces of Alberta and Québec proposed hydrogen projects that relied on different production pathways, with the former exploiting its fossil reserves [16] and the latter relying on its water resources and low-cost hydroelectric power [17]. The Atlantic Maritimes, comprising the three provinces of New Brunswick, Nova Scotia, and Prince Edward Island (PEI), published a feasibility study for hydrogen production, storage, and utilization [18]. British Columbia released its hydrogen strategy in 2021 [19], and Ontario's strategy was published in April 2022 [20].

2.2.2. An integrated energy system (IES) to produce green hydrogen

One pathway to produce green hydrogen is to electrolyze water in polymer electrolyte membrane (PEM) electrolyzers, powered by low-carbon sources of electricity. Here, we simulate hydrogen production pathways that deploy offshore wind (OSW) and integrate it with PEM electrolysis. OSW is especially promising since many coastal regions across the world envision an aggressive expansion in this resource. This is true of the Atlantic Maritimes, too: forecasts of expansion in low-carbon electric power are underpinned by offshore wind, solar, tidal, and potentially new nuclear power—but few projects exist in the pipeline to achieve that vision. Together, solar and wind are expected

to grow from their current share of 15% to 45% by 2050 (Figure 2.1A). Coal and oil, meanwhile, would be phased out.

Our focus on hydrogen is strategic and relevant to a wider geographic context. One of the major challenges to hydrogen adoption is the need (and cost) of deploying hydrogen distribution infrastructure. Many of the natural gas pipelines in the Maritimes are relatively new and made of hydrogen-compatible materials, like polyethylene [18]. However, the bulk of the gas distribution system is the cast-iron, bidirectional Maritimes and Northeast Pipeline (M&NP), which stretches from the U.S. state of Maine into the Atlantic, terminating past the Sable Island Bank approximately 200km offshore (Figure 2.2). Until 2018, natural gas was produced off Nova Scotia's coast and exported through this pipeline to the U.S. [21] (Figure 2.1B). Natural gas pipelines in the Maritimes, including M&NP, could be repurposed or converted to hydrogen—this would reduce the cost and difficulty of siting new pipeline infrastructure.

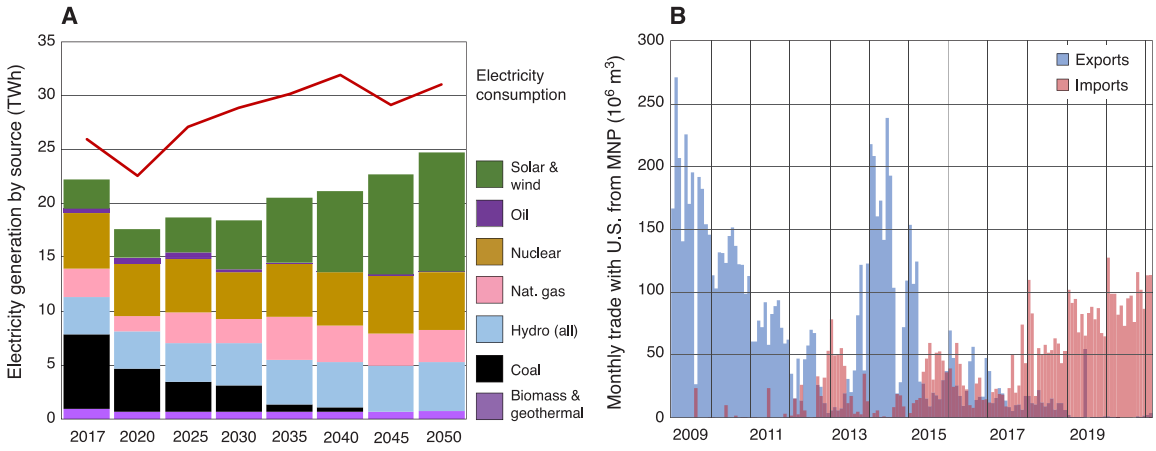

Figure 2.1. A) The Atlantic Maritimes has a diverse electricity mix; net-zero emission targets will require the retirement of coal, the replacement of nuclear that is set to retire in 2040, and radical expansion in variable renewable energy sources. **B)** The bidirectional Maritimes and Northeast Pipeline (M&NP) is the infrastructure through which natural

gas from the Scotian shelf was locally consumed and exported to the U.S. A decline in offshore natural gas production has made the region dependent on natural gas imports from the U.S.

Three other considerations make OSW deployment in the Maritimes promising. First, the wind resource is among the best in the world: previous studies have simulated average annual capacity factors of >50% in this region [22]. Second is the ability to reduce challenges from incumbent interests (like fishing and commercial shipping) and from coastal residents. Because the Scotian shelf is vast and the existing M&NP runs 200km offshore to the Sable Island Bank (Figure 2.2), it would be possible to deploy both OSW array and electrolyzers out of sight of coastal residents: being able to see wind turbines has emerged as a key constraint to their offshore deployment in the U.S. [23] and Japan [24], but this problem has also restricted the deployment of onshore wind power in Canada [25]. Deploying an IES out of sight was a consideration of this research, enabled by the existence of a relatively young and underutilized pipeline infrastructure.

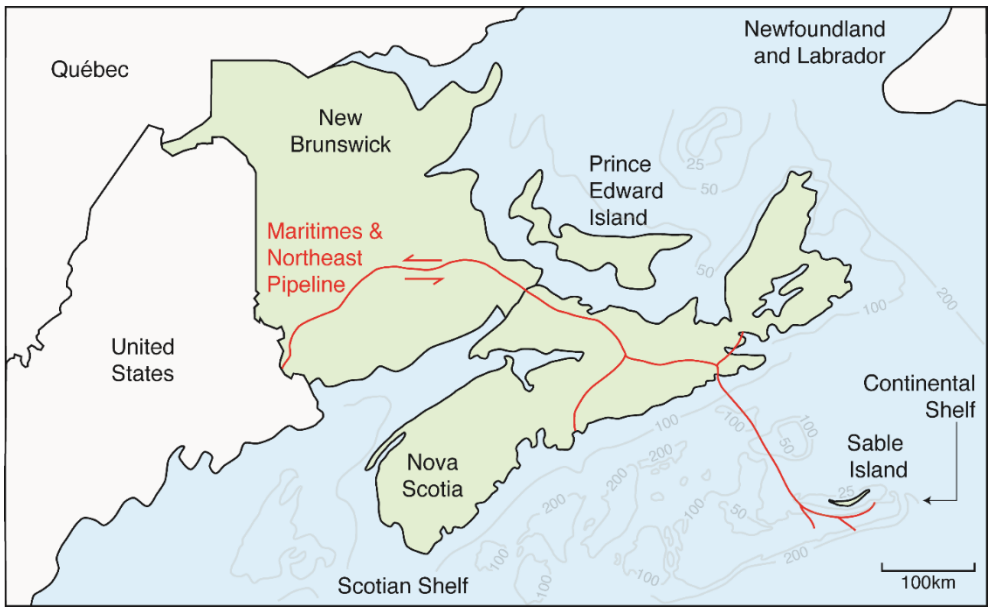

Figure 2.2. The Atlantic Maritimes include New Brunswick, Nova Scotia, and Prince Edward Island. High mean wind speeds, dormant seabed natural gas pipelines, and the existence of a large, shallow continental shelf make the region a promising location for hydrogen production through water electrolysis powered by OSW.

Finally, the Maritimes desire to become a hub for the global offshore wind industry [26] and, as home to two of Canada's largest ports and a hub for its shipbuilding industry, the region is better suited to this task than others.

2.2.3. Literature review

In one of Canada's most recent pushes towards hydrogen, it signed a deal with Germany to export hydrogen by 2025 to assist with Germany's energy needs. World Energy GH2, the company behind the project, plans to build up 164 turbines along the coast of the Port au Port Peninsula in Newfoundland and produce green hydrogen [27]. Another notable hydrogen-focused project within the Maritimes was a wind-hydrogen

village which served as an experiment to convert wind power to hydrogen for a more sustainable energy source for remote and off-grid locations [28]. A recent study analyzed the potential for offshore wind for all of Canada with high accuracy estimates from satellite-derived wind maps like Cross-Calibrated Multi-Platform (CCMP) images and found that the Pacific and Atlantic Oceans offer two of the best Canadian wind resources. The Atlantic Ocean offers drastically more energy potential due to its larger size and higher wind speeds [29]. Another study focused on the continental shelf of Atlantic Canada and discovered that most of its geology is not suitable for pile-driven (i.e., fixed) foundations, rendering floating offshore wind a more appropriate solution. One potential location that exists within this region suitable for these types of foundations is around Sable Island, NS [30].

Other research that focuses on the economics of expanding offshore wind include the use of optimization models that minimize the cost of combined generation and transmission expansion planning [31] or financial simulations that estimate the combination of costs and incentives at which a rapid expansion of the technology might occur [32]. Unlike previous research, this study is interested in the scale and speed of expansion under a range of scenarios and assuming historical experience is repeated. To that end, uncertainty analysis was considered central to the research, and building an optimization model was considered inappropriate in this case. A recursive simulation was deemed a better choice. We wanted to focus on both the technological performance as well as the economic impact of rapidly expanding such systems, specifically at predefined, empirical growth rates.

2.3. Data and methods

2.3.1. Scenarios and energy systems under investigation

We explore five IES deployment scenarios, summarized in Table 2.1 below, that scale up the deployment of OSW and PEM electrolysis to meet different energy system objectives.

Table 2.1. Description of the five scenarios under investigation in this research.

Scenario	Description
α	IES meets **monthly** energy demand served by natural gas. Monthly demand is the most granular data available. U.S. market absorbs excess hydrogen.
β_{tot}	IES meets **total annual** energy demand served by natural gas. This entails investments in storage and compression capacity.
β_{ind}	IES meets the **industrial sector's annual** energy demand that is served by natural gas. This entails investments in storage and compression capacity.
γ	IES feeds **electricity** into the grid through subsea cables. OSW farm sized to replace fossil generation, including sufficient electrolysis and hydrogen storage to provide the grid with two-weeks' worth of OSW output through fuel cells.
δ	IES meets the **freight transportation sector's annual demand** for hydrogen, but only for freight miles traveled within the region.

The reference turbine chosen is the International Energy Agency's (IEA) 15 MW_e OSW turbine [33]. The floating OSW array would be deployed on the Scotian shelf, where water depths of approximately 200m make such deployments feasible with today's mooring technologies [34]. Depending on scenario, different amounts of power generated by the OSW array are fed into polymer electrolyte membrane (PEM) electrolyzers that electrochemically split purified water into hydrogen and oxygen. Specifically, this research models the size and performance of electrolyzers based on Siemens' Silyzer 300, a commercial offering [35]. The hydrogen is then injected into the bidirectional M&NP pipeline, employing existing infrastructure to serve energy needs at lower carbon

intensity. Cost estimates for converting large, cast-iron natural gas pipelines to carry hydrogen were not found, so this cost was not included in the assessment.

A recursive simulation model was chosen so that empirical growth rates, derived from the literature on past expansions of onshore and offshore wind power capacity, could be used to constrain the upscaling of the system. Given the interest in determining the completion years, rather than forcing buildouts to complete by 2050, this recursive simulation approach was deemed to be a more appropriate method than an optimization model that forces the system to scale up beyond what empirical evidence suggests is possible. This would help show if and by how much each scenario would exceed the 2050 target.

2.3.2. Simulation of scenario α

The model comprises a recursive simulation that begins in 2025 and ends when a scenario's objectives are achieved. Deployment begins in 2025 with either one or five $15MW_e$ OSW turbines; this represents either mild or aggressive deployment: the latter scenario is supported by historical experience: constructing the Block Island Wind Farm in Rhode Island, which comprises five smaller turbines (6MWe each), took approximately 18 months from the installation of the first fixed foundation jacket to commissioning [36].

In scenario α, the simulation proceeds to build OSW and electrolyzer capacity until monthly energy demand from natural gas is met. Monthly wind power production is estimated using six years of wind speed forecast data for the Scotian shelf, taken from the National Center for Atmospheric Research [37]. Wind electricity and treated seawater are

inputs to PEM electrolyzers modeled on [35]. A schematic of this simulation can be seen in Figure 2.3.

If the objective of meeting monthly energy demand from natural gas is not met, the simulation proceeds to the next year, 2026, applying growth and technological learning rates. The choice of growth rates is derived from the range of the IEA's expectations for OSW [22], while estimates of OSW cost and learning rates are derived from the National Renewable Energy Laboratory's (NREL's) Annual Technology Baseline estimates for OSW [38]. Auxiliary power needs for OSW turbines are estimated to be 5% at best and 10% at worst. Array losses are estimated to be 0% at best and 10% at worst, reflecting the large number of possible OSW farm layouts. Without a site-specific analysis that accommodates all stakeholder concerns, which is outside the scope of this analysis, a precise layout cannot be developed. However, the size of the Scotian shelf can accommodate these arrays if typical inter-array distances are assumed [39].

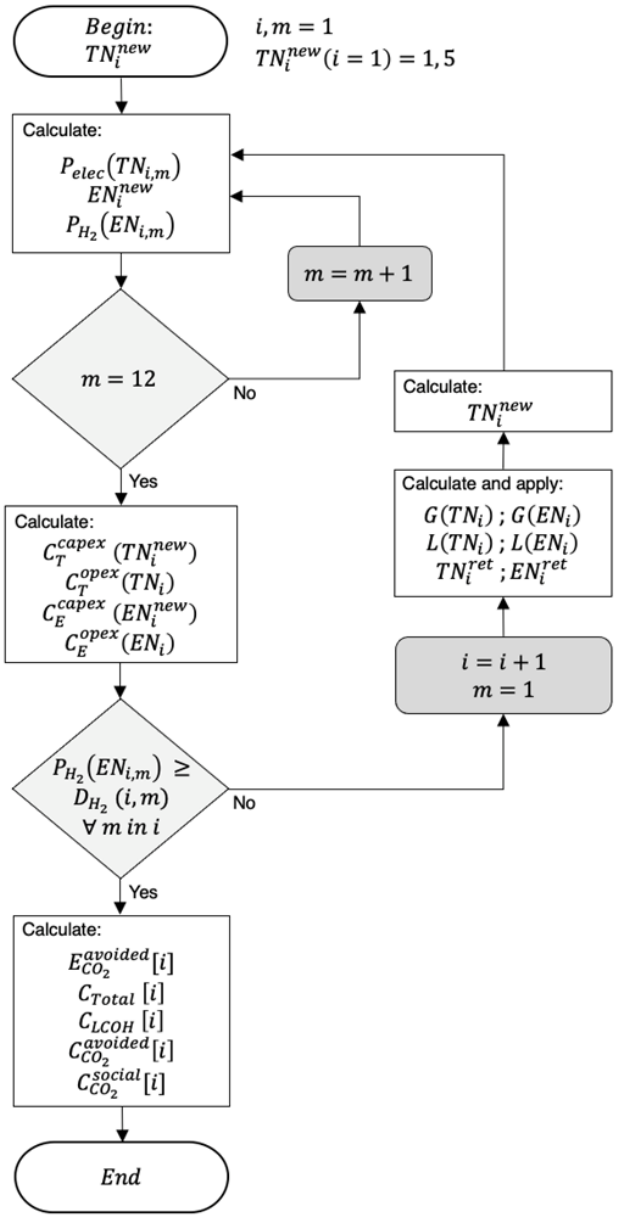

Figure 2.3. Schematic of the simulation model employed for scenario α, where sufficient OSW and electrolyzer capacity is built to meet monthly energy demand from natural gas. Similar schematics for the other scenarios can be found in Appendix A.2. Nomenclature for the schematic can be found in Table 2.2.

Table 2.2. Nomenclature of variables shown in Figure 2.3 and their values.

Variable	Factor	Value
$C_{CO_2}^{avoidance}$	Cost of CO_2 avoidance in USD	
$C_{CO_2}^{social}$	Social cost of CO_2 in USD	
C_E^{capex}	Electrolyzer CAPEX in USD	
C_E^{opex}	Electrolyzer OPEX in USD	
C_{Total}	Total cost at project completion in USD	
C_T^{capex}	Turbine CAPEX in USD	
C_T^{opex}	Turbine OPEX in USD	
C_{LCOH}	Levelized costs of hydrogen in USD	
D_{H_2}	H_2 demand in m^3	
$EN_{i,m}$	Number of electrolyzers	
$E_{CO_2}^{avoided}$	CO_2 emissions avoided in tonnes	
G	Annual growth rate of project	25%, 30%, 36%
i	Year	
L	Annual reduction in cost	(NREL ATB for OSW, applied to electrolyzers)
L_{array}	Array losses	0%, 5%, 10%
L_{aux}	Auxiliary loads	5%, 10%
L_s	Total summer climate losses	0.0559 GWh/MW_e
L_w	Total winter climate losses	0.2436 GWh/MW_e
m	Month	1-12
NG_{supp}	Natural gas supplemented by hydrogen in m^3	
P_{elec}	Average daily array power output in GWh	
P_{H_2}	Average daily hydrogen output in m^3	
TN_i	Number of turbines	
$TN_i(i = 1)$	Number of starting turbines	1, 5

Estimates of PEM electrolyzer cost span a wide range. Lower cost estimates are derived from recent estimates by the Hydrogen Council [40] that reflect the group's expectations once electrolyzer manufacturing is scaled up and economies of scale are

exploited. Higher cost estimates are derived from realized commercial projects, summarized in a paper by Felgenhauer et al. [41].

The simulation scales up the deployment of this integrated energy system in annual timesteps, until the scenario objective is met. Once unit lifetimes are exceeded, units are retired and new investments in capacity are made. Once the scenario objective is met, the following performance metrics are recorded: completion year; installed capacity of OSW turbines at project completion; installed capacity of electrolyzers at project completion; total project cost, cost per kg H_2 in 2025; cost per kg H_2 at project completion, and number of tons of CO_2 emissions avoided.

2.3.3. Simulation of scenarios β_{tot} and β_{ind}

The progression of these two scenarios and the data employed are the same as in section 2.3.2 above. One difference is in the simulation's stopping condition. In scenario β_{tot}, the simulation proceeds until total annual—rather than monthly—energy demand is met. IES construction halts once the project can supply enough hydrogen per year to meet annual energy demand that is currently served by natural gas. In scenario β_{ind}, the simulation proceeds until the Maritimes' industrial sector's annual energy demand from natural gas is met by hydrogen. This sector's annual energy demand from natural gas accounts for 68% of the regions' total natural gas demand.

Another difference between these scenarios and α is that investments in storage and compression capacity are required. The storage system employed in these scenarios utilizes underground caverns to store compressed hydrogen. In addition to constructing the caverns and compressors, yearly compression and conditioning costs must be

included—these are much lower than capital costs [42, 43]. Schematics for these two scenarios can be found in Appendix A.2.

2.3.4. Simulation of scenario γ

This scenario sees the IES integrate the electricity produced from the OSW farm into the grid through subsea cables. The OSW farm is sized to supplant all expected fossil-fuel generation in the Maritimes in 2050, based on the Canada Energy Regulator's Reference (i.e., business as usual) scenario [11]. To ensure resource adequacy in the face of intermittent generation and occasional wind droughts, the simulation invests in sufficient electrolysis and hydrogen storage capacity to provide the electric grid with sufficient hydrogen energy to provide two-weeks' worth of OSW farm output. This 14-day period is longer than the longest wind droughts simulated around the Sable Island Bank, which last for less than six days [37]. The progression of the scenario and the data employed are the same as in section 2.3.2, and a schematic of this scenario can be found in Appendix A.2.

This scenario enables a comparison between hydrogen production and electric power integration—this comparison is necessary because the Maritimes plan to integrate much greater amounts of low-carbon electric power into the grid. The region is projected to continue to generate electricity from legacy coal and nuclear infrastructure until the 2040s. While there are no plans to invest in new coal units, the region's nuclear power plans are uncertain: New Brunswick's 660MWe Point Lepreau Nuclear Generation Station is due to retire in 2042 after recent license renewal [44]. This research assumes that a new generation of small modular reactors (SMRs) will be commissioned on the same site by 2050, as the province expects [45].

2.3.5. Simulation of scenario δ

One option for decarbonizing heavy-duty freight is to employ hydrogen-combusting or fuel cell-electric trucks. In this scenario, IES expansion stops once sufficient hydrogen is produced to meet the energy demand of hydrogen trucks that carry freight from or to the region. The scenario satisfies the energy demand of the trip segment that occurs within the Maritimes only.

Data on freight shipments to and from the three provinces that comprise the Maritimes is retrieved from the Canadian Freight Analysis Framework [46]. This database provides the origin, destination, distance, and tonnage of each freight truck shipment that occurred in Canada over the course of a year. The database was filtered to consider only those shipments for which either the origin or the destination was in the Maritimes. The web mapping platform Google Maps was then employed to determine the distance each freight shipment traveled within the Maritimes. For inbound shipments, this was the distance from the region's borders to the shipment's destination; for outbound shipments, this was the distance from the origin to the region's borders. A fuel economy of 5.9 miles per gallon of diesel was assumed [47]. Any large expansion in hydrogen production to accommodate hydrogen trucks would unfold in a more organized, national (or global) fashion, and it would be served by a portfolio of resources rather than one IES. Appendix A.19 provides further details regarding this calculation.

2.3.6. Consumption data

Among the five scenarios, three replace natural gas, one produces electricity, and one replaces diesel. Natural gas consumption was obtained from Statistics Canada for January 2016 to December 2021 [48]. To estimate 2050 consumption, a linear trend was

employed, using data points from all six years available and extrapolating that linear trend to 2050. Predicted electrical consumption data from 2025 to 2050 was retrieved from the Canada Energy Regulator's (CER) reference scenario [11]. Diesel consumption from 2011 to 2017 was retrieved from the Canadian Freight Analysis Framework (CFAF) from Statistics Canada [46]. Similar to the natural gas data, the 2050 consumption values were extrapolated by assuming a linear trend, employing the seven available years. Further information regarding consumption data is in Appendices A.9, A.16, and A.19.

2.3.7. Component performance data

Wind turbine performance is calculated using data from the National Center for Atmospheric Research's (NCAR) Global Forecast System (GFS) database, which provides wind speeds, at the height of 100m, in 6-hour intervals [37]. We consider data for a location on the Scotian shelf at coordinates 44° N and 61° W; it is assumed that the entire shelf experiences the same wind speeds. Wind speeds are extrapolated to the hub height of the turbine, 150m, assuming a roughness of 0.0002 m.

Performance of the electrolyzers comes directly from Siemens' rating of the chosen electrolyzer: it produces 335 kg of hydrogen per hour when consuming 17.5 MWh [35]. A capacity factor of 80% is assumed, allowing for electrolyzer downtime or repairs. Further information into component performance can be found in Appendices A.5, A.6, and A.8.

2.3.8. Component cost data

Seven cost categories are considered as component costs within this techno-economic analysis. Turbine and electrolyzer capital expenditure (CAPEX) and Fixed

Operation and Maintenance (FO&M) are relevant for each of the five scenarios. CAPEX includes offshore wind overnight capital costs (OCC), construction financing, and grid connection costs. These costs are in 2018 USD with inflation considered by the authors. The costs decrease each year in line with the estimates of the 2020 Annual Technology Baseline (ATB) from the National Renewable Energy Laboratory (NREL) [38]. Electrolyzer costs are calculated similarly in that they decrease in cost every year at the same rates as that experienced by the turbines.

Storage, which is considered in four scenarios, is split into compressor CAPEX, conditioning, and cavern storage CAPEX. Depending on the size of the storage system, compressor costs range from about \$500/kW to \$1,300/kW, conditioning costs range from \$0.01/kgH_2 to \$0.02/kgH_2, and cavern CAPEX is constant at about \$9/kgH_2. Due to uncertainty regarding how these costs might evolve over time, no learning rates are applied. Table 2.3 below shows the ranges of inputs used for the cost analysis.

Table 2.3. Input data used in this analysis

Input	Unit	Lower	Middle	Upper	Reference
Annual project growth rate		25%	30%	36%	[22]
Turbine performance	GWh	71.5		75.7	Model
Turbine CAPEX[a]	USD/kW	\$3172.54	\$3774.80	\$5459.65	[38]
Turbine FO&M[a]	USD/kWyr	\$58.26	\$68.40	\$95.28	
Electrolyzer CAPEX[a]	USD/kW	\$500	\$2000	\$6500	[40, 41, 49]

Input	Unit	Lower	Middle	Upper	Reference
Electrolyzer FO&M[a]	USD/kWyr	$14.25	$57	$360	[40, 41, 49]
Discount rate	%	3	5	7	[50]
Turbine lifetime	Year	20	25	30	[51, 52]
Electrolyzer lifetime	Year	5	10	15	[35]
Compressor efficiency	kWh/kgH_2	1.6	4.4	18	[43]
PEM fuel cell efficiency	%	50	60	70	[53]

[a] Starting cost in 2025

For this study, we take the costs of offshore wind turbine classes 8 through 12 as representative of the type of systems that would be deployed on the Scotian Shelf, given its water depths. The lower bound costs come from the class 8 advanced estimates; the middle costs are from the class 10 moderate estimates; and the upper bound cost come from class 12 conservative estimates. Further information on cost data can be found in the Appendix A.11.

2.3.9. Emission data

Calculating the avoided emissions varies depending on the scenario. For the natural gas scenarios, α, β_{tot}, and β_{ind}, emissions are simply calculated by multiplying the amount of natural gas that is replaced by its emission factor, 1921 gCO_2/m^3 natural gas. This comes from Canada's Greenhouse Gas Inventory [54]. Scenario γ is more complex, as there are several sources that the renewable energy is replacing. These sources include coal, natural gas, oil, and biomass which are found from CER's reference

scenario. Because the scenario extends only to 2050, each year afterwards remains at the 2050 emissions level [11]. These four sources are replaced in descending order of total carbon emissions from that source (coal, then natural gas, oil, and biomass) to reduce as much emissions as possible. Diesel emissions are calculated by multiplying the amount of diesel replaced by its emission factor of 2,680,500 gCO_2/m^3 diesel [54]. Further information on emission data can be found in Appendix A.9.

2.4. Results and Discussion

2.4.1. Natural gas substitution scenario α

To replace natural gas demand in 2050 in the Atlantic Maritimes with hydrogen requires the production and distribution of approximately 432,000 tH_2 per year—for context, Canada currently produces 3 million tH_2 per year using steam methane reforming. This hydrogen would replace about 1.1 million tons of natural gas (tNG) annually, a substitution that eliminates 3 million tCO_2, or 11% of the Maritimes' total current emissions.

Meeting monthly natural gas demand in the Maritimes with no hydrogen storage (scenario α) requires an IES with installed OSW capacity between 5,800 and 6,800 MW, depending on turbine performance (i.e., auxiliary power requirements and array losses). Installed PEM electrolyzer capacity of approximately 4,800 MW is required. This IES would produce approximately 562,000 tH_2, with the system overbuilt to meet monthly energy demand, as per the scenario's stopping condition. The excess hydrogen must be accommodated, most likely through blending into the U.S. natural gas system.

Figure 2.4A shows the average daily hydrogen production per month. These daily hydrogen production values fluctuate throughout the year due to the differing wind profiles of each month, with the lowest production occurring in July and the highest production in December. The number of offshore wind turbines is also plotted, and the completion years are highlighted.

Maximum electric power and hydrogen production occur during the winter months when the wind resource is richer. This is fortuitous, since winter is when both electricity and natural gas demand are highest in the Maritimes: residential consumers in New Brunswick and Nova Scotia rely heavily on electric space heating, but natural gas is used in other sectors like industry. Winter is also when natural gas demand is highest in the U.S. Northeast, where the fuel is used for heating. Especially cold weather in the region increases natural gas demand, boosts storage withdrawals, and causes freeze-offs, driving prices higher [55].

The above results assume that the IES begins with one turbine in 2025. Upscaling this system at an average annual growth rate of 25% requires about 40 years, with project completion achieved in 2065. Assuming a more aggressive average annual growth rate of 36%, the buildout would require about 30 years and completion would be achieved by 2055. This means that a sustained commitment to deploying OSW and PEM electrolyzers—two systems that sit at relatively high technological readiness levels and are commercially available—would take decades. Achieving full deployment of this system by 2050, Canada's net-zero emission target, is only possible with aggressive average annual growth rates and when turbine and electrolyzer performance is exceptional. Table 2.4 summarizes the results for scenarios α, β_{tot}, and β_{ind}.

Here, we present results for the cases with one starting turbine. Results for the cases with five starting turbines are provided in Appendix A.18. Broadly, starting with five turbines in 2025 speeds up the buildout by three to four years, depending on scenario, but comes at a premium of between 2% and 7%, which in real terms is anywhere from $0.8 to $10.6 billion.

2.4.2. Natural gas substitution scenarios β_{tot} and β_{ind}

Employing hydrogen storage (scenario β_{tot}) mitigates system costs by approximately 16% to 24%, since it reduces the installed capacity of OSW turbines and PEM electrolyzers by about 20%, as shown in Figure 2.4B. This reduction considers the cost of constructing and operating cavern-based hydrogen storage, compression, and conditioning.

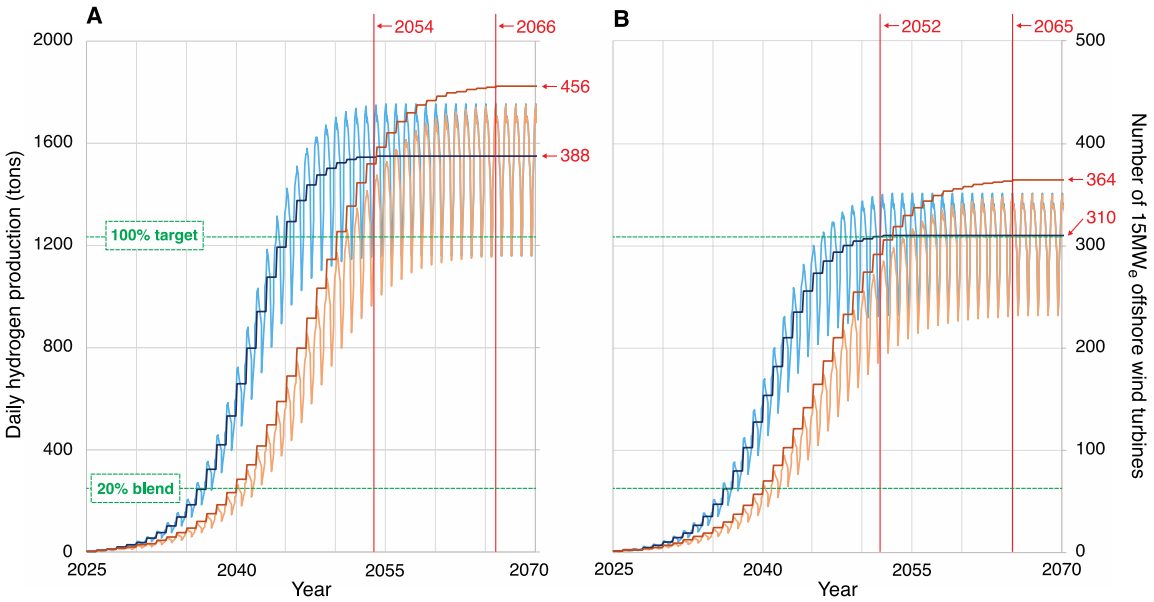

Figure 2.4. A) An IES that converts OSW power to hydrogen while meeting monthly natural demand in the Maritimes (scenario α) entails overbuilding: between 390 and 460 turbines are required, depending on their performance, and aggressive growth and

learning rates are required to achieve a completion date close to the 2050 net-zero target. **B)** A system that is designed to produce just enough hydrogen to meet annual demand (scenario β_{tot}) reduces system size and project costs by a fifth and cuts completion time by 1-2 years. Dark lines represent number of turbines; lighter lines represent average daily hydrogen production rates for each month; these vary seasonally due to differences in wind resource.

The total amount of hydrogen produced and distributed annually in scenario β_{tot} is approximately 449,000 tH2. This amount satisfies annual demand and produces sufficient excess hydrogen to meet two-weeks' worth of demand, as a safety factor. Across scenarios, storage cuts the time to completion by one to two years, though this estimate ignores the often-substantial cost of siting, permitting, and commissioning cavern-based storage. Since the industrial sector accounts for about 68% of natural gas demand in the region, constructing the IES to satisfy industrial sector demand only (scenario β_{ind}), rather than total natural gas demand, mitigates the size and cost of the overall system by 32%, with the system producing and distributing 303,000 tH2 annually. Figure 2.5 summarizes the key costs associated with all three natural gas substitution scenarios.

Median hydrogen production cost in 2025—the year the projects begin—is high (66 $/kg$H_2$), but as expected, hydrogen costs fall substantially as the project expands, reaching a median of <6 $/kg$H_2$, with a tenth percentile of 2.6 to 2.8 $/kg$H_2$ and a ninetieth percentile of 11.6 to 12 $/kg$H_2$. The probability of costs falling below 2 $/kg$H_2$ is approximately 2%; this ambitious target is equivalent to the cost of producing hydrogen using today's dominant (and carbon-intensive) technology—steam methane reforming [40]. Therefore, only by assuming best-case component performance and

cheap initial CAPEX is the cost of hydrogen production competitive with the commercial alternative in the absence of carbon constraints.

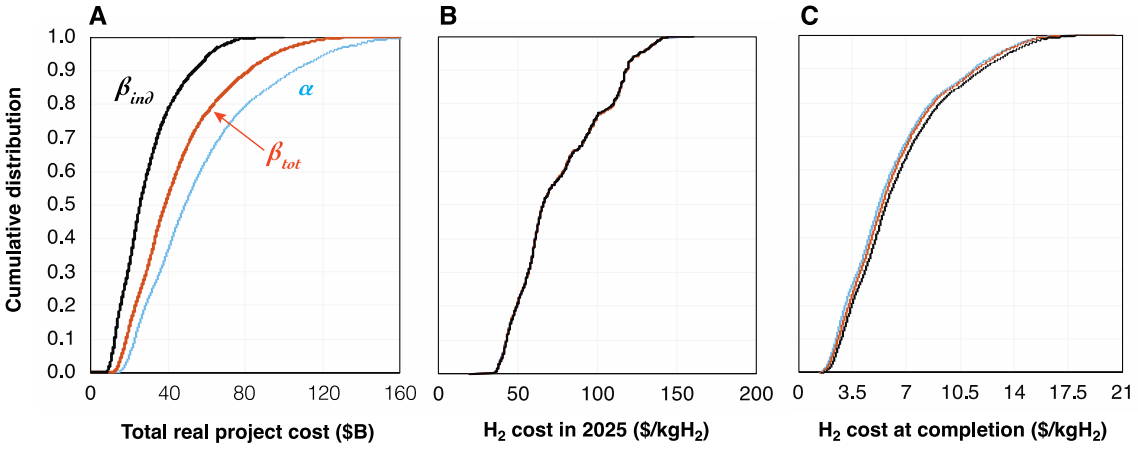

Figure 2.5. Cumulative distribution functions of the **A)** total real cost of the project, **B)** hydrogen production cost in 2025 (the initial year in the simulation), and **C)** the hydrogen production cost at project completion for the three natural gas substitution scenarios. Median estimates of hydrogen production costs at project completion range from 5.2 $/kg$H_2$ to 5.7 $/kg$H_2$, even after learning has occurred in both OSW and PEM electrolysis. All costs are in USD.

The storage system employed in scenarios β_{tot} and β_{ind} utilize underground caverns to store compressed hydrogen. The storage requirements differ across scenarios, depending on turbine performance and system growth rate. The amount of storage for β_{tot} is approximately 22,300 tH_2 and incurs cavern construction costs of approximately $190 million. For context, 12,000 tH_2 would satisfy approximately two weeks' worth of gaseous fuel demand in the Maritimes. β_{ind} employs storage of about 28,000 tH_2, which includes a two-week reserve of industry gaseous fuel demand of about 9,100 tH_2. This scenario sees cavern construction costs of about $240 million dollars. The cost estimates used for cavern construction can be found in Appendix A.13. Even considering the

uncertainty associated with storage cost, scenarios β_{tot} and β_{ind} are cheaper than scenario α across cases. Storage is sized to meet the largest monthly H_2 deficit, which happens to be larger for β_{ind} than β_{tot} due to the more cyclical nature of industrial fuel demand in this region. In other words, β_{tot} generates smaller deficits throughout the year and thus requires a smaller storage system.

Table 2.4. Summary of completion date and infrastructure required for scenarios that seek to substitute natural gas energy demand with hydrogen

Scenario	$\boldsymbol{\alpha}$		$\boldsymbol{\beta_{tot}}$		$\boldsymbol{\beta_{ind}}$	
	Worst	*Best*	*Worst*	*Best*	*Worst*	*Best*
Completion year	2066	2054	2065	2052	2061	2050
Installed capacity of OSW (MW)	6,840	5,820	5,460	4,650	3,690	3,135
Installed capacity of electrolyzers (MW)	4,778	4,795	3,815	3,833	2,573	2,590
Number of 15 MW OSW turbines	456	388	364	310	246	209
Number of 17.5 MW PEM electrolyzers	273	274	218	219	147	148

The avoided cost of CO_2 emissions across scenarios is high. At best, it sits at 176 \$/tCO_2 for scenario α, 187 \$/tCO_2 for scenario β_{tot}, and 205 \$/tCO_2 for scenario β_{ind}. At worst, when component performance is poor and costs are high, avoided costs sit at approximately 2,500 \$/tCO_2 for scenario α and approximately 2,600 \$/tCO_2 for scenarios β_{tot} and β_{ind}. Even in the best-case scenario, avoided costs are larger than the current federal carbon price in Canada (50 CAD/tCO_2). However, this federal carbon price is set to reach 170 CAD/tCO_2 by 2030 (this is equivalent to approximately 130 USD/tCO_2 at current exchange rates [56]). As mentioned earlier in this section, any excess production must be blended into the extensive natural gas network of the U.S. Northeast. As a result, despite its higher cost, scenario α is expected to lead to greater CO_2 avoidance than would be possible if we fully substituted natural gas consumption in just the Maritimes.

Moreover, the pipeline systems within the Maritimes can absorb some excess production through storage.

2.4.3. Producing hydrogen vs. integrating electric power into the grid: scenario γ

In scenario γ, the OSW farm feeds its power primarily to the electric power grid and is sized to supplant all fossil-fuel generation in the region. Upon the project's completion, the electricity generated annually is sufficient to displace about 5 TWh of non-renewable electric power generation, which is expected to comprise 22% of the region's annual electricity generation in 2050. This electricity production is highest during the winter months, which is beneficial in the Maritimes—a region with a winter-peaking power system due to the predominance of electric heat.

This IES, once fully built, could avoid the emission of 2.7 million metric tons of CO_2 per year, which is approximately 9% of the region's current emissions [57]. It is substantially smaller than the IES constructed in scenarios α, β_{tot}, and β_{ind}, and comprises 73 OSW turbines and 3 PEM electrolyzers in the best-case scenario, as shown in Table 2.5 below.

Table 2.5. Summary of completion date and infrastructure required for scenarios that seek to substitute fossil-fueled electric power generation with OSW power.

Scenario	$\boldsymbol{\gamma}$	
	Worst	*Best*
Completion year	2052	2044
Installed capacity of OSW (MW)	1,290	1,095
Installed capacity of electrolyzers (MW)	70	53
Number of 15 MW OSW turbines	86	73
Number of 17.5 MW PEM electrolyzers	4	3

This smaller system is completed faster, with project completion achieved six to fourteen years prior to the completion of the hydrogen production pathways. In terms of emission avoidance, the performance of this scenario is similar to that of the hydrogen production pathways discussed in sections 2.4.1 and 2.4.2, with scenario γ avoiding approximately the same amount of emissions as scenario β_{tot} over the cumulative, 40-year span of the simulation, and more than β_{ind} despite the smaller size of the system. This is because the OSW farm in scenario γ displaces a more carbon-intense fuel mix over the next two decades than the natural gas scenarios—here, the fuel mix includes substantial coal, as well as some oil and biomass.

This scenario's total real project cost is substantially reduced due to its smaller size. Scenario γ costs anywhere between 7% and 30% of scenarios α, β_{tot}, and β_{ind}. Moreover, while the annual cost of electricity from this system starts at a steep value of up to 9.1 $/kWh in 2025, it drops to anywhere from 3 to 17 ¢/kWh at project completion. By the time of project completion and across scenarios, there is a 70% chance that this system will yield levelized annual costs of electricity that are lower than 0.1 $/kWh. Figure 2.6 summarizes these results.

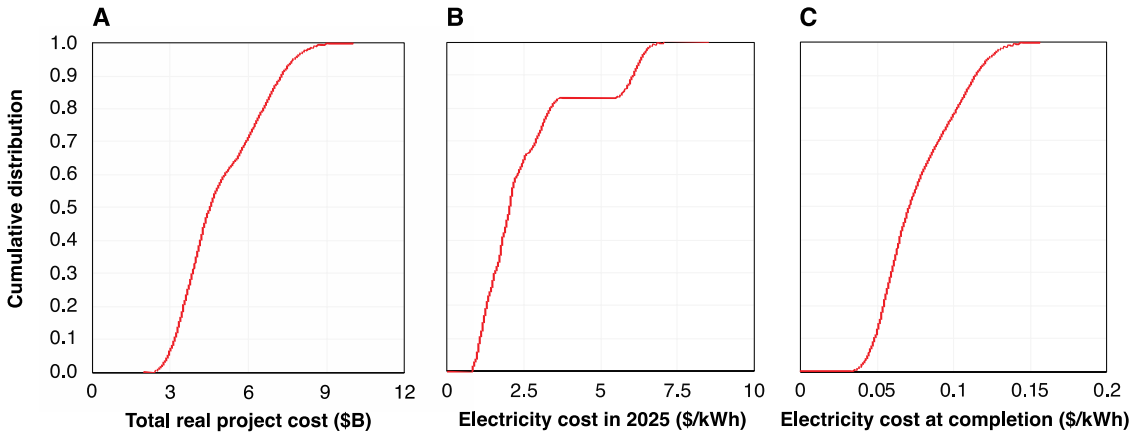

Figure 2.6. Cumulative distribution functions of the **A)** total real cost of scenario γ, **B)** electric power production costs in 2025 (the initial year in the simulation), and **C)** the electric power production costs at project completion. The median estimate of power costs at project completion is approximately 7 ¢/kWh. All costs are in USD.

As for hydrogen storage, this scenario produces and stores 6,400 to 9,000 tH_2 to achieve its resource adequacy objective, which is to have sufficient hydrogen on hand to provide electric power to the grid that is equal to two-weeks' worth of OSW farm output.

2.4.4. Hydrogen required to satisfy demand of heavy transportation: scenario δ

Hydrogen production amounts are much larger in the scenario where the IES must meet the demand of freight transport for vehicle miles traveled within the region. This necessitates an IES that is two orders of magnitude larger than the one considered in scenarios α, β_{tot}, and β_{ind}, involving between 195 and 230 GW of OSW capacity and approximately 160 GW of electrolyzer capacity. To deploy this larger system, the time to completion is extended by decades, with completion years of between 2073 and 2095 in the best and worst-case scenarios, respectively. To fulfill the local (i.e., in-region)

demand of heavy freight that is converted to employ hydrogen rather than diesel, 18 million tH2 is required annually.

2.4.5. Validation

Turbine performance is validated by comparing the annual output from the model to the predicted annual output indicated by the IEA 15 MW reference turbine documents [33]. IEA states this turbine can output 77.4 GWh and the turbine produced within the model produces 71.5 to 75.7 GWh, depending on performance. Electrolyzer performance, emission factors, and growth rates are all assumed to be valid since they are derived from compilations employed by reputable sources. Assumptions regarding future evolutions are difficult to validate: these include future demand of electricity, natural gas, or diesel, as well as the cost reductions associated with various IES components. These are derived through extrapolation or from existing databases like NREL's.

2.4.6. Major sources of uncertainty and limitations of the analysis

Across scenarios, results are most sensitive to electrolyzer capital cost estimates. Expanded deployment of modular technologies like PEM electrolyzers could substantially reduce costs, as seen in the global experience with both solar photovoltaics and lithium-ion battery energy storage. The cost of scenarios will sit close to the best-case results outlined above with initial electrolyzer capital costs of 500 $/kW.

One limitation of this analysis is the assumption made regarding the usability of the M&NP pipeline for this application. It is likely that the M&NP pipeline will have to be adapted or converted to hydrogen use. This entails both time and money, neither of which we consider here. That said, in every case but the transportation scenario δ, the volume of

hydrogen produced is substantially below the M&NP's carrying capacity. While pipeline capacity might not be a constraint, its compatibility with hydrogen could be. A big question facing hydrogen transitions is how and when to construct the requisite pipeline infrastructure, and whether existing infrastructure can be partially or fully adapted to serve this new energy carrier. There is research and experimentation in reusing existing natural gas pipeline infrastructure for hydrogen: construction is underway in Alberta on a project to blend 5% hydrogen by volume into pipeline infrastructure [58] and blending up to 20% hydrogen by volume is possible with minor modifications [59]. Further blending or conversion to 100% hydrogen potentially requires pipeline replacement.

Our simulation method helps estimate the years in which the IES produces enough hydrogen to achieve these levels of blending, which could guide decision-making in future pipeline investment. Starting with one turbine in 2025 and across all natural gas scenarios, the 5% blending target is achieved in the early 2030s, while the 20% blending target is achieved between 2037 and 2042. Starting with 5 turbines accelerates the achievement of blending targets by two to four years. This gives engineers, investors, and regulators a decade to test the M&NP and decide whether refurbishment or replacement are necessary. This result underscores the need, first, for extensive testing of the M&NP to ensure that it can accommodate 20% hydrogen blends. Second, an integrated plan must ensure that any modifications to pipeline infrastructure are carried out within 10 years. Deploying new pipeline infrastructure is challenging and time-consuming, but Canadian experience shows that it could be done expeditiously: the regulatory approval process for the M&NP began in 1995 [60] and it was commissioned in December 1999 [61].

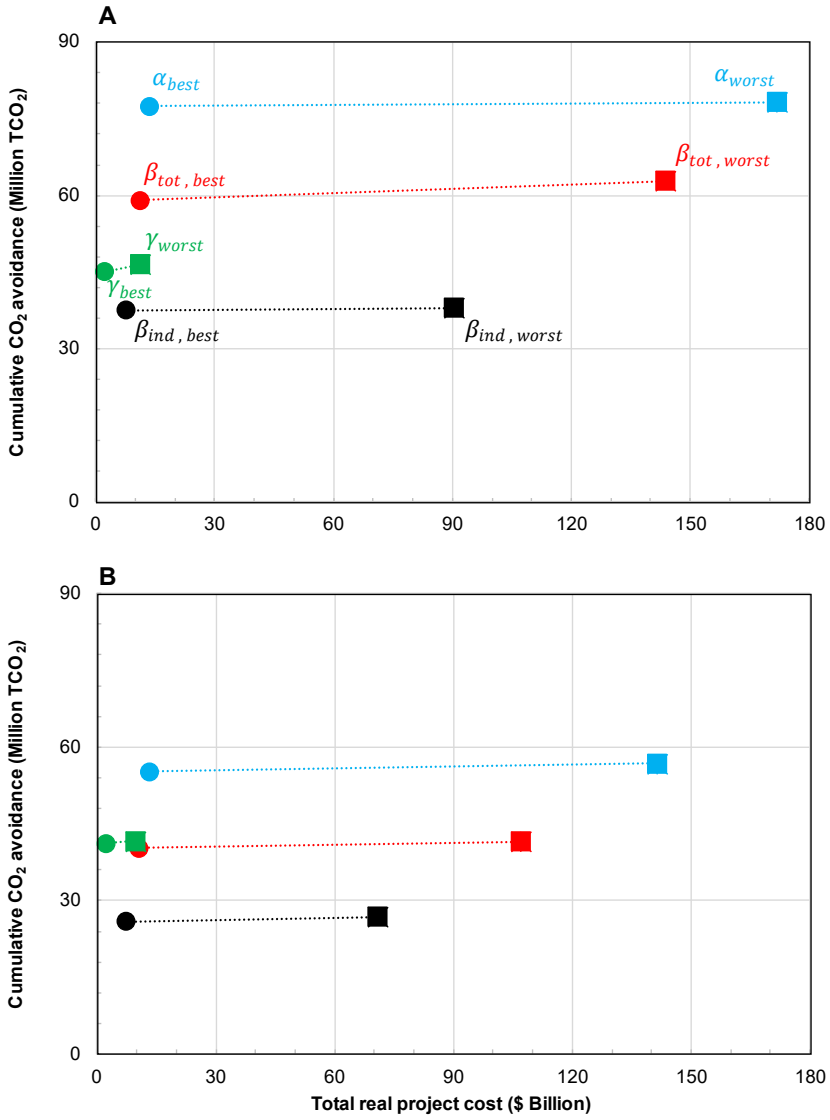

Figure 2.7. Total real project cost (in USD) and cumulative CO_2 avoided over project lifetime for four scenarios under investigation, assuming **A)** 25% and **B)** 36% average annual growth rates. Circles represent the best-case result; squares represent the worst-case result. The large range of uncertainty in electrolyzer capital cost is most responsible for the spread in cost estimates, with scenario γ performing well due to coal's existence in the Maritimes energy mix, the region's reliance on electricity for space heating, and the smaller number of electrolyzers required.

In Figure 2.7, we compare not only the costs of scenarios α, β_{tot}, β_{ind}, and γ across project lifetime, but also their avoided CO_2. Worst-case scenarios always entail greater costs (because higher costs estimates are used as inputs in those model runs), but they also involve greater cumulative CO_2 avoidance. This is because the simulation's end-date is open and depends on both growth rates and component performance. In other words, worst-case scenarios involve slower buildouts, later completion dates, and therefore a larger amount of total carbon emissions that could potentially be avoided, accounting for the positively sloped trendline as we move from best-case to worst-case. An interesting trend develops comparing the 25% and 36% growth rate cases; faster buildouts result in lower total project costs. However, these costs only represent total costs at project completion, so cases with faster growth rates complete the project without as many component replacements as slower growth rate scenarios. For example, with a growth rate of 25% in scenario α, 7 to 79 turbines and 97 to 442 electrolyzers must be replaced in the best and worst cases, respectively. With a 36% growth rate, there are only 0 to 14 turbine replacements and 33 to 282 electrolyzer replacements in the best and worst cases, respectively. This same trend holds true for each scenario and allows for significantly lower costs, despite technology costs decreasing each year.

Scenario γ performs well because it requires a smaller infrastructure buildout while achieving considerable levels of emission avoidance. It is therefore more cost-effective: the cost of CO_2 avoidance in scenario γ ranges from 50 to 240 \$/TCO_2. At the lower end of this range, the costs align with current carbon prices, which are expected to increase to approximately 130 \$/TCO_2 in 2030. Therefore, this scenario aligns with politically feasible costs on carbon pollution that have been legislated in Canada.

2.5. Conclusions and policy implications

Global decarbonization efforts have thus far lagged ambition. Many of the world's nations have pivoted towards a net-zero by 2050 emission target, but there is a risk that public and political support for these targets could wane if they are not grounded in realistic assessments. This research shows the importance of developing assessments that tie energy system upscaling scenarios to emission targets using empirically derived growth and learning rates. Each of the scenarios presented here could contribute to emission reductions, but they only meet Canada's net-zero targets under the best-case assumptions: aggressive growth rates and good technological performance are required.

The scenarios in this research are ambitious: they assume that the amount of hydrogen that is required in the Maritimes is equivalent, in energy terms, to the amount of natural gas they currently consume. However, there are multiple competing technological and political forces that could reduce this amount, chief among which is the extent of end-use electrification of buildings and industry.

Replacing natural gas with green hydrogen would require a substantial expansion in low-carbon electricity generation at a time when the electric power sector is undergoing its own low-carbon transformation. The emission reductions achieved by the green hydrogen scenarios come at a cost premium, even if the need for new pipelines and end-use technologies is ignored. For proponents of hydrogen, urgent investments and reductions in the uncertainty range in electrolyzer capital cost estimates—by demonstrating mass fabrication, cost control, and aggressive technological learning—are of paramount importance. By reducing these costs to 500 $/kW or less, the green hydrogen pathway could achieve production costs that make this option competitive with the hydrogen that is currently produced through steam methane reforming.

Chapter 3. A method for estimating thermal energy loads in Canada's remote and northern communities

3.1. Introduction

Canada's remote and northern communities rely overwhelmingly on fossil-derived liquid fuels to serve their electrical and thermal needs. Currently, for upwards of 350 communities, diesel is the main source of fuel for both power and heat generation. An estimated 682 million litres of diesel fuel were used by these communities in 2020 [62], emitting approximately 1.8 million tons of carbon dioxide (tCO_2) [54].

Governments and communities are pursuing a transition to less polluting fuels, driven not only by concerns regarding climate change and air pollution, but also by the declining cost of climate-friendly alternatives like renewable energy sources. One example of these efforts is the ongoing Clean Energy for Rural and Remote Communities (CERRC) Program, started by Natural Resources Canada (NRCan) in 2017 [51], which provides funding for projects that either increase renewable energy generation or reduce energy consumption [64]. Another is the Off-Diesel Initiative, started in early 2019, which targets a sustainable diesel exit for remote northern communities by 2030 [65].

No one-size-fits-all solution exists for remote and northern communities: their locations (and thus their capacity to deploy various low-carbon energy resources), demographic characteristics, accessibility, energy needs, and preferences differ. Some of the data that must inform each community's transition in the early planning phase is accessible through community and government resources like Statistics Canada and NRCan: the latter has compiled some of this information in Canada's Remote Communities Energy Database (RCED) [66]. However, in other crucial areas such as community thermal loads profiles, little to no data are publicly available. Here, we make

several novel contributions to the literature. First, we develop a method for estimating the thermal load profiles for remote and northern communities. We apply this method to 40 communities that have been selected for their variation across multiple important characteristics. Then, we develop a generalizable model that can help analysts generate first-order estimates of a community's thermal load based on easily retrievable information. Finally, we check these thermal load profiles against the sparse data that do exist to develop estimates of the error between our results and empirical data.

The focus on thermal load profiles is justified for two reasons. First, to our knowledge, no effort has been made to develop hourly thermal load profiles for remote and northern communities, and sparse empirical data exist in the public domain. Second is the importance of thermal energy in the sub-Arctic and Arctic contexts, where heat provision is essential to existence and temperatures can remain below freezing well into late spring. In winter, hourly thermal loads can be up to 23 times greater than hourly electricity loads.

Section 3.2 reviews the literature that exists on this topic. Section 3.3 describes the data and methods that were used in the analysis. Section 3.4 presents results of the thermal load estimation and the generalizable thermal load model, while also discussing the limitations of the proposed method. Section 3.5 offers concluding remarks and suggestions for future work.

3.2. Literature Review

For some remote and northern communities, NRCan's RCED provides information on installed diesel generation capacity or peak and average electrical loads, but this is far

removed from the hourly load profiles that are required for most microgrid investment planning models. Information on thermal loads is unavailable in RCED.

Estimates and empirical datasets of thermal load profiles do not exist for Canada's remote and northern communities. Most efforts to develop thermal load profiles have focused on contexts that are very different from the Arctic. Yao and Steemers developed a method to estimate daily electrical and thermal load profiles for domestic buildings in the United Kingdom, considering both behavioral and physical characteristics [67]. For urbanized, grid-connected settings, there exist many load profile models that focus on both electricity and heat [68], as well as some that focus specifically on heat [69]. More recently, efforts have focused on developing advanced methods for stochastic generation of load profiles for electricity [70] and heat [71, 72] in order to better consider the uncertainty associated with occupant behavior.

More relevant in the Arctic context, Quitoras et al. focused on optimizing an integrated energy system built around the characteristics and load profiles of Sachs Harbour, the northernmost community in the Northwest Territories (NWT) [73]. Water heating loads were estimated by applying a profile from Hendron and Burch [74], and space heating loads were estimated with data from the Arctic Energy Alliance [75] and calculations from Campana et al. [76]. A report released by Hazelton et al., analyzes the potential of renewable energy development in remote communities in Nunavut (NU) [77]. It lists annual volumes of diesel fuel that are consumed to serve electrical and thermal loads and shows that, in almost all communities, more diesel is used to serve thermal loads than electrical loads in this territory.

3.3. Data and Methods

Canada has more than 350 remote and northern communities, and for some it is difficult to retrieve even basic information about the community from sources in the public domain. Therefore, the first step in this research is to select a subset of communities that contains sufficient variation across important attributes to develop a generalizable model for thermal load prediction. Once the communities are selected, community maps (i.e., land planning and zoning maps), government maps, and satellite images are combined with prototypical heating loads for houses and commercial buildings in a comparable climatic region. The resulting thermal loads are adjusted to account for climatic differences. Once thermal load profiles are developed for all 40 communities, statistical models are developed and tested for fit to produce a generalizable model for Canadian remote and northern communities. Figure 3.1 shows a schematic of the process, with the following sections describing each step and applying it to one small community—Aupaluk, Quebéc (QC)—as an example.

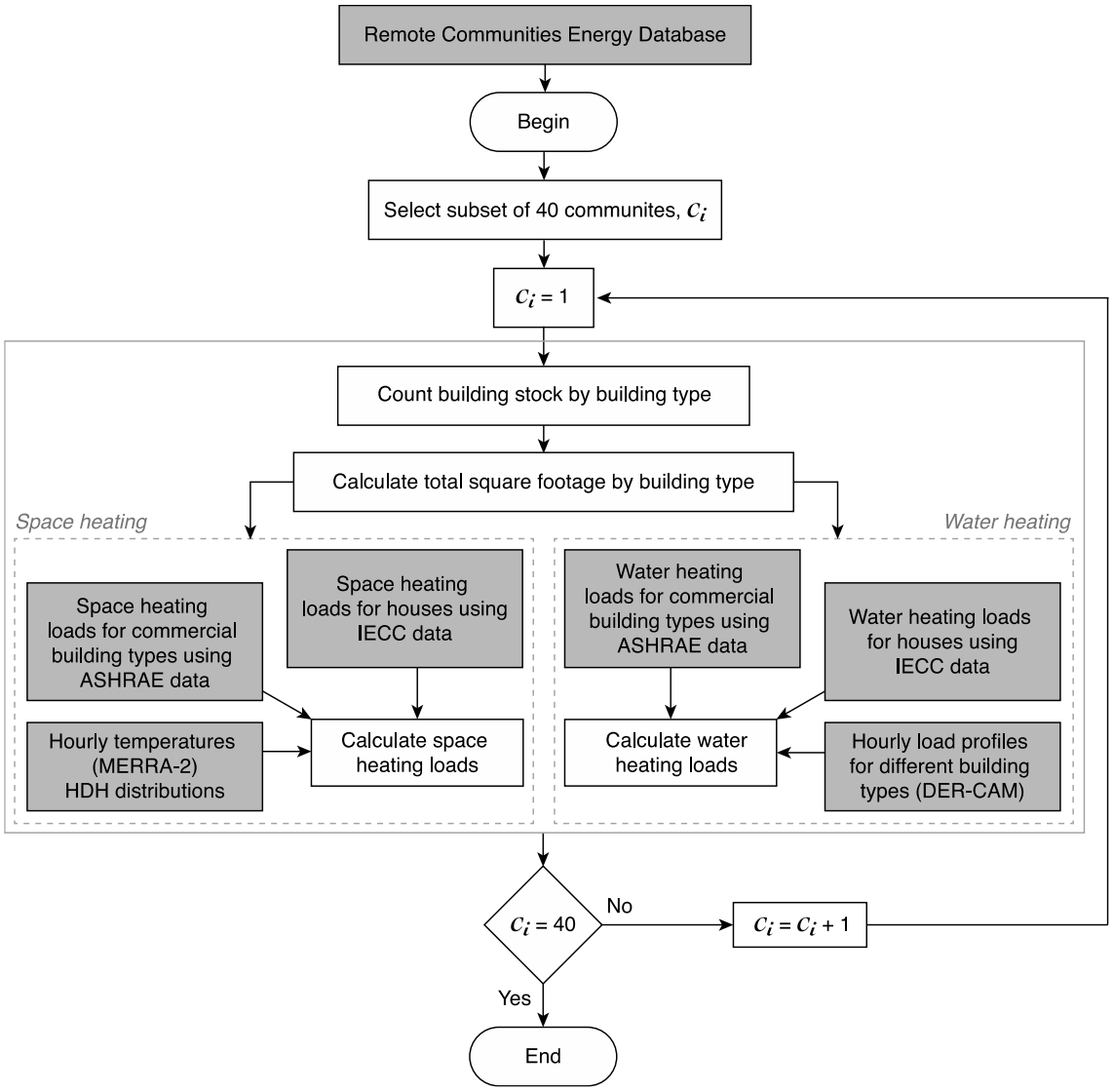

Figure 3.1. Starting with NRCan's Remote Communities Energy Database, an algorithm is devised to estimate the thermal heating loads for a subset of 40 remote and northern communities in Canada. White boxes denote individual steps in the algorithm; shaded boxes denote data inputs from external sources.

3.3.1. Remote and northern community selection

Utilizing both Canada's Remote Communities Energy Database [66] and a database of simulated hourly electric load profiles for all communities that was provided by

NRCan, a subset of 40 communities is selected. The heuristic for the selection is to ensure that the 40 communities are representative of remote and northern communities in Canada across a wide range of reported characteristics. These characteristics included: location (both in terms of province and in terms of latitude); population; renewables penetration; average and peak electric loads; level of access (e.g., road, sea, or air); and whether the community was First Nations, Métis, Inuit, or non-Indigenous. The Off-Diesel Initiative targets Indigenous communities and most of the selected communities are Indigenous, but not all. Table 3.1 lists the selected communities and summarizes some of their characteristics.

Table 3.1. Names and some characteristics of the 40 remote and northern communities investigated. Provincial abbreviations: AB = Alberta; BC = British Columbia; MB = Manitoba; NL = Newfoundland and Labrador; NT = Northwest Territories; NU = Nunavut; ON = Ontario; QC = Québec; and YT = Yukon.

Community name	Alternate name	Province	Pop.	Power source(s)
François		NL	89	Diesel
Beaver Creek		YT	93	Diesel
Wrigley		NT	119	Diesel
Tsiigehtchic	Arctic Red River	NT	172	Diesel
Xeni Gwet'in	Nemiah Valley	BC	197	Diesel and solar
Resolute Bay		NU	198	Diesel
Aupaluk		QC	209	Diesel
Old Crow		YT	221	Diesel
Peawanuck		ON	288	Diesel
Tadoule Lake		MB	311	Diesel
Kwadacha	Fort Ware	BC	332	Diesel and biomass
Makkovik		NL	377	Diesel
Port Hope Simpson		NL	412	Diesel
Umiujaq		QC	442	Diesel
Ramea		NL	447	Diesel and wind

Community name	Alternate name	Province	Pop.	Power source(s)
Whatì		NT	470	Diesel
Brochet		MB	489	Diesel
Fort Good Hope		NT	516	Diesel
Kingfisher Lake		ON	535	Diesel
Old Masset		BC	555	Diesel
Port Clements		BC	555	Diesel
Keewaywin		ON	577	Diesel
Fort Mcpherson	Tetlit Zheh	NT	700	Diesel
Kangiqsujuaq		QC	750	Diesel
Watson Lake		YT	790	Diesel
Masset		BC	793	Diesel
Fort Chipewyan		AB	853	Diesel
Arctic Bay	Ikpiarjuk	NU	868	Diesel
Weagamow Lake	North Caribou	ON	880	Diesel
Natuashish		NL	936	Diesel
Kangiqsualujjuaq		QC	942	Diesel
Naujaat	Repulse Bay	NU	1,082	Diesel
Kitchenuhmaykoosib	Big Trout Lake First Nation	ON	1,156	Diesel
Fort Simpson	Łíídlı̨ı̨ Kų́ę́	NT	1,202	Diesel
Shamattawa		MB	1,443	Diesel
Mittimatalik	Pond Inlet	NU	1,617	Diesel
Inukjuak	Port Harrison	QC	1,757	Diesel
Kuujjuaq	Fort Chimo	QC	2,754	Diesel
Rankin Inlet	Kangiqliniq	NU	2,842	Diesel
Iqaluit		NU	7,740	Diesel

3.3.2. Thermal loads for a similar climatic region

To estimate thermal loads in the absence of empirical data or models, a location is chosen that is both climatically similar to the Canadian North and has been extensively analyzed for the purpose of generating prototypical building energy load profiles. The U.S. Department of Energy's (DOE) Office of Energy Efficiency and Renewable Energy maintains the Building Energy Codes Program [78], which employs the Department's Commercial Reference Building Models to create reference commercial buildings that comply with both standards set by the American Society for Heating, Refrigeration, and

Air Conditioning (ASHRAE) and the International Energy Conservation Code (IECC). The DOE also has prototypical residential energy load profiles for houses that comply with IECC standards. Detailed electrical and thermal load profiles are developed for each of these prototypical buildings using DOE's EnergyPlus model for each of 19 distinct climate zones that are relevant to the U.S. context. This research employs load profile data from Zone 8, which is taken to represent the sub-Arctic/Arctic climate, with Fairbanks, Alaska as its representative city. This enables us to estimate thermal loads for prototypical buildings, and we collect data for monthly space heating loads, monthly water heating loads, and annual energy use per square foot.

3.3.3. Database of building stock in each community

Adapting the collected thermal load data to Canadian remote and northern communities requires counting each community's building stock. This is done by employing maps, including those used for community planning, land-use designation and zoning, government surveying (at all levels), as well as aerial photography and satellite imagery from Google Earth, Google Maps, and Map Carta. Each building in each of the 40 communities was manually counted and categorized into one of the ten categories included in EnergyPlus: small offices, schools, hospitals, outpatient, small hotels or inns, warehouses, restaurants, retail, apartments, and houses. In addition to manual counts, the square footage of buildings was determined using measurement tools built into geospatial platforms like Google Earth. If large numbers of a building type exist within a community, a reference building within the community is selected and assigned a size factor of 1. Every building is then visually assigned a size factor in relation to the

reference building. Once the building counts within each category are complete, the overall square footage of each building category is estimated.

This procedure was followed across all categories except houses, which are the most numerous building type. To estimate the total square footage for houses in each community, five houses were selected that seemed to be representative of the house sizes that exist: this approach was deemed appropriate because communities appeared to have few variations in house designs or sizes, and thus it was possible to estimate the square footage of only a handful of reference houses and apply those estimates to the community's housing stock writ large.

3.3.4. Developing hourly thermal load profiles

Values of annual energy use per square foot, taken from the prototype building datasets, are used to estimate the annual amount of energy required to meet the thermal loads of each building category. Thermal loads for space heating and water heating are calculated separately. Monthly space heating load data from EnergyPlus are converted to hourly loads for each community using heating degree hours (HDH) as a proxy for heating requirements. HDH are calculated by taking hourly temperature data [79, 80] and subtracting each hour's temperature by 18.3 °C. This procedure enables us to create a distribution of hourly heating demand across each month, and the monthly energy use can be applied to these distributions to create hourly loads.

Water heating loads are significantly smaller than space heating loads, and this component is handled differently. Here, monthly water heating load data from EnergyPlus are divided by the number of days in each month to estimate daily water heating loads. This assumes that daily water heating loads are equal within a month,

though they differ across months. Daily water heating loads are converted to hourly loads using a distribution developed by Lawrence Berkeley National Laboratory's DER-CAM microgrid investment planning model for each building type [81]. These building-specific hourly loads are available for all building types except houses, which are not included in DER-CAM. We therefore apply the hourly load distribution that DER-CAM uses for apartment buildings, which are included in that model, since both building types are residential and theoretically involve similar energy use patterns.

3.3.5. The example of Aupaluk, QC

Figure 3.2 shows the maps that were used to classify and count buildings in Aupaluk, QC.

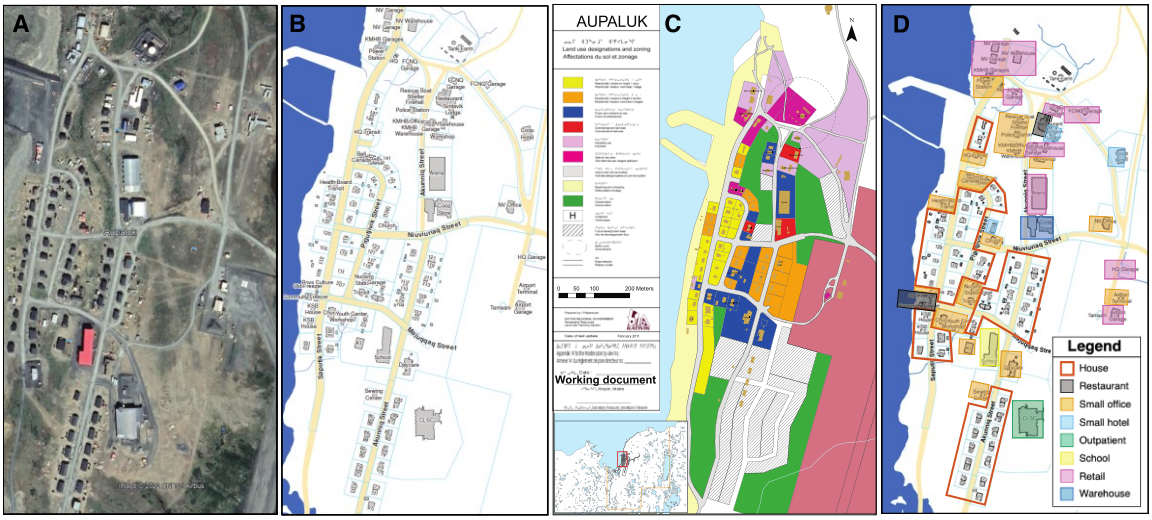

Figure 3.2. Counting buildings in Aupaluk, QC with **A)** Google Earth [82], **B)** the community basemap of Aupaluk (2021) [83], and **C)** the land use and zoning map of Aupaluk (2011). **D)** Counts can help classify individual buildings in the Aupaluk basemap into building types [84].

Counting the buildings in Aupaluk, QC is easy due to the ample amount of information that exists in the public domain. The Kativik regional government's basemap, as well as the community's land-use designation and zoning map are extremely helpful, even though the latter dates from 2011. Employing these, alongside aerial photographs from Overflight Stock [85], meant that multiple sources exist to cross-validate the building stock estimate. Aerial photos also helped confirm which buildings had multiple floors, so the square footage estimates could be made more accurate. Unfortunately, many other communities had fewer sources of information, and some had no basemaps or land use maps, meaning that the counts relied on satellite imagery and judgments by the research team.

3.3.6. Building a statistical model for all remaining communities

Once thermal load profiles are generated for each for the 40 communities, a generalizable model is developed to estimate both the annual and monthly thermal loads of a remote and northern community using a sparse number of retrievable predictor variables. This was done using ordinary least squares (OLS) regression, performed in the R programming language (version 4.1.0). In each case, the dependent variable is the thermal load, and the independent variables include population, heating degree days, electrical load characteristics (e.g., peak, average, and the difference between peak winter and peak summer), and location (e.g., latitude, longitude, and province, recoded as a categorical variable). Multiple models were run starting with a model that included all the above independent variables. Variables that proved statistically insignificant were removed one at a time, with the goal being a parsimonious model that nonetheless

exhibited a good fit. The decision to select a model was based on adjusted R squared values, BIC, AIC, and p-value as discussed more in section 3.4.3.

3.4 Results and Discussion

3.4.1. Thermal load profiles

The results of the investigation emphasize the importance of considering thermal load profiles when exploring diesel exit strategies for remote and northern communities in Canada, since the thermal loads are larger than the electrical loads for more than half the year (October through April).

Each community's thermal load profile can be split into two components, space heating and water heating. The former is significantly larger across communities and seasonal; the latter is relatively constant throughout the year. Figure 3.3 shows both space and water heating load profiles for six communities that vary by population, with panel A representing the thermal load profiles of François, NL (population of 89) and panel F representing those of the north's largest community, Iqaluit, NU (population of 7,740). The estimated annual thermal loads range from approximately 2 GWh for François to 85 GWh for Iqaluit. The remaining four communities have populations (and thermal loads) that lie between those two extremes. This trend generally holds: the larger the population, the larger the annual thermal load. Table 3.2 reports additional characteristics and thermal load information for all 40 communities.

There exists a small number of outlier communities—Watson Lake, YT; Shamattawa, MB; Kangiqsualujjuaq, QC; and Masset, BC—that defy this trend. This occurs when a community's physical building stock does not reflect what might be expected given its reported population. This could be due to it having a particularly

itinerant population, or if it is arranged in a way that demands fewer or more numerous buildings than would be expected for a community of its size. For example, the community of Watson Lake has more buildings than communities like Masset and Fort Chipewyan, which have similar populations. Meanwhile, the community of Shamattawa consists of fewer buildings than Pond Inlet and Fort Simpson, which have similar populations. One of several limitations associated with this method is that the counting process ignores the occupation patterns of a building, though up-to-date land use and zoning maps are very helpful in this regard. Other limitations are discussed in Section 3.4.4 below. Hourly thermal load profiles for these 40 communities are included in the supporting information (SI): https://doi.org/10.5281/zenodo.6948879.

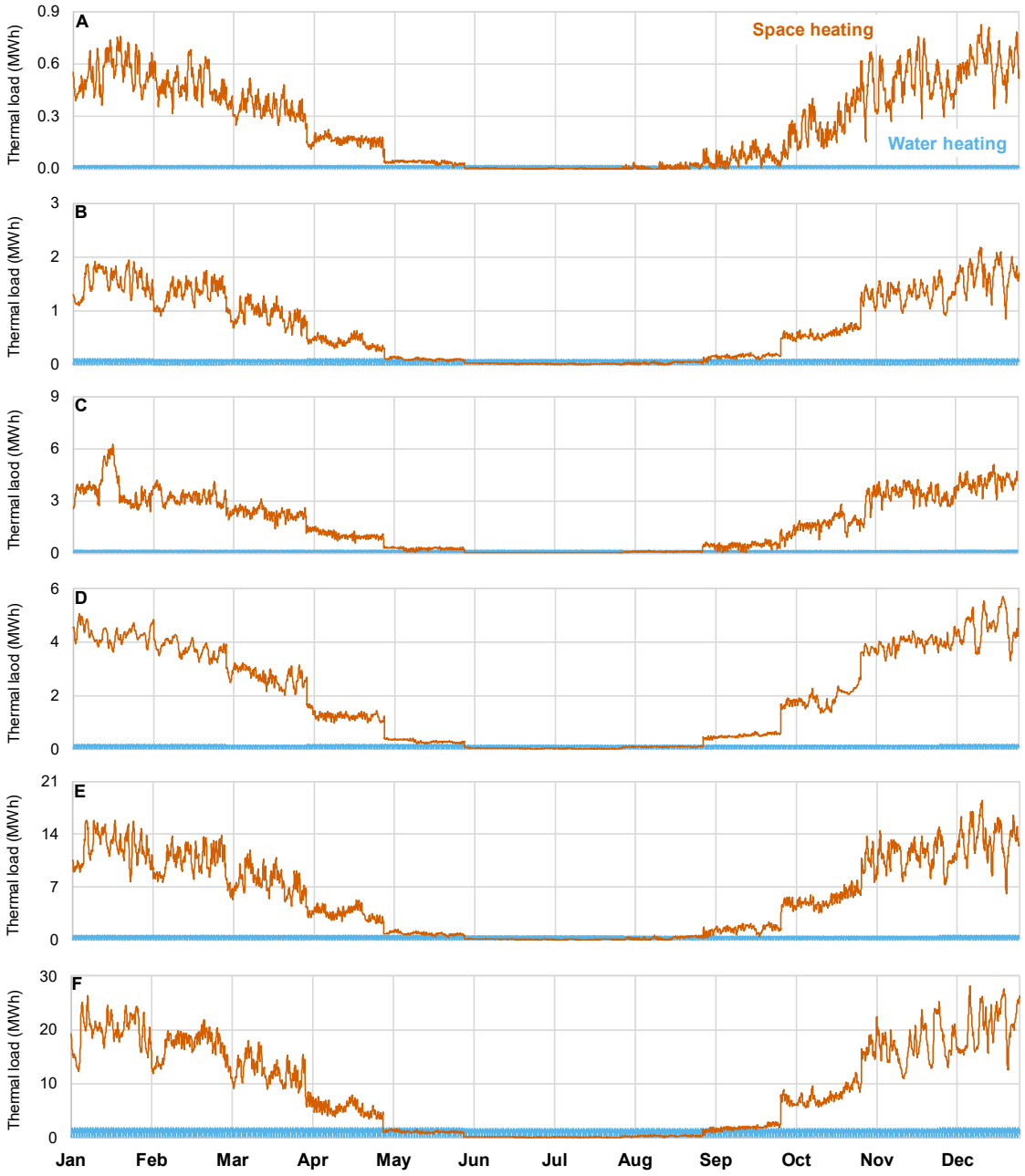

Figure 3.3. Space heating (orange) and water heating (blue) thermal load profiles for six communities that vary by population: **A)** François, NL (population = 89); **B)** Aupaluk, QC (population = 209); **C)** Old Masset, BC (population = 555); **D)** Arctic Bay, NU (population = 868); **E)** Kuujjuaq, QC (population = 2,754); and **F)** Iqaluit, NU (population = 7,740).

Table 3.2. Key thermal load data points (average, peak, and annual) for each of the 40 communities. Hourly thermal load profiles can be found in the SI: https://doi.org/10.5281/zenodo.6948879.

Community name	Pop.	HDH	Temp. range (°C)	Avg. heating load (kWh)	Peak heating load (kWh)	Annual heating load (MWh)
François, NL	89	4,741	-14 – 23	260	840	2,290
Beaver Creek, YT	93	8,399	-41 – 22	610	1,870	5,340
Wrigley, NT	119	9,013	-41 – 26	390	1,280	3,430
Tsiigehtchic, NT	172	9,487	-47 – 28	350	1,140	3,040
Xeni Gwet'in, BC	197	6,408	-34 – 27	230	940	2,000
Resolute Bay, NU	198	11,627	-40 – 12	650	1,870	5,690
Aupaluk, QC	209	9,070	-37 – 22	730	2,250	6,400
Old Crow, YT	221	9,633	-42 – 23	850	2,600	7,460
Peawanuck, ON	288	8,500	-39 – 29	460	1,480	4,060
Tadoule Lake, MB	311	9,691	-46 – 26	710	2,300	6,180
Kwadacha, BC	332	8,224	-42 – 23	700	2,410	6,130
Makkovik, NL	377	7,394	-30 – 23	830	2,950	7,240
Port Hope Simps., NL	412	6,628	-31 – 28	1,500	6,160	13,130
Umiujaq, QC	442	8,164	-33 – 21	1,540	4,840	13,510
Ramea, NL	447	4,658	-12 – 22	1,500	4,670	13,100
Whatì, NT	470	9,508	-49 – 26	930	3,150	8,170
Brochet, MB	489	8,946	-47 – 27	890	3,070	7,760
Fort Good Hope, NT	516	9,337	-49 – 28	1,260	4,330	11,060
Kingfisher Lake, ON	535	7,442	-40 – 31	740	2,310	6,440
Old Masset, BC	555	3,676	-9 – 22	1,740	6,350	15,250
Port Clements, BC	555	3,695	-9 – 22	1,230	4,480	10,790
Keewaywin, ON	577	7,211	-39 – 32	420	1,430	3,650
Fort Mcpherson, NT	700	9,369	-40 – 27	1,350	4,180	11,790
Kangiqsujuaq, QC	750	9,450	-38 – 18	1,910	5,690	16,700
Watson Lake, YT	790	7,863	-39 – 25	3,710	12,130	32,520
Masset, BC	793	3,667	-9 – 21	2,620	9,580	22,920
Fort Chipewyan, AB	853	7,871	-41 – 27	2,020	6,830	17,650
Arctic Bay, NU	868	11,928	-42 – 16	2,020	5,850	17,700
Weagamow Lake, ON	880	7,281	-39 – 31	1,290	4,230	11,290
Natuashish, NL	936	7,829	-31 – 24	1,560	5,280	13,630
Kangiqsualujjuaq, QC	942	8,760	-36 – 22	4,140	13,050	36,290
Naujaat, NU	1,082	11,139	-44 – 21	1,860	5,730	16,330
Kitchenuhmaykoosib, ON	1,156	7,705	-40 – 32	1,660	5,190	14,520
Fort Simpson, NT	1,202	8,596	-41 – 28	2,900	9,800	25,420

Community name	Pop.	HDH	Temp. range (°C)	Avg. heating load (kWh)	Peak heating load (kWh)	Annual heating load (MWh)
Shamattawa, MB	1,443	8,503	-42 – 29	1,150	3,650	10,050
Mittimatalik, NU	1,617	12,113	-47 – 13	2,960	8,690	25,880
Inukjuak, QC	1,757	8,560	-35 – 21	3,680	13,240	32,190
Kuujjuaq, QC	2,754	8,930	-38 – 25	5,810	18,880	50,850
Rankin Inlet, NU	2,842	10,441	-45 – 21	5,250	16,500	46,010
Iqaluit, NU	7,740	10,218	-45 – 19	9,660	29,510	84,580

3.4.2. Comparing thermal loads to electrical loads

Comparing communities' thermal load profiles to their electrical load profiles is crucial to determining how effective a new energy system would be in the transition to a low-carbon community. Figure 3.4 compares electrical and thermal load profiles for both Aupaluk, QC and Kuujjuaq, QC. While the electrical load data are from 2015 and these loads might have changed since, the thermal loads are still substantially higher from October to April.

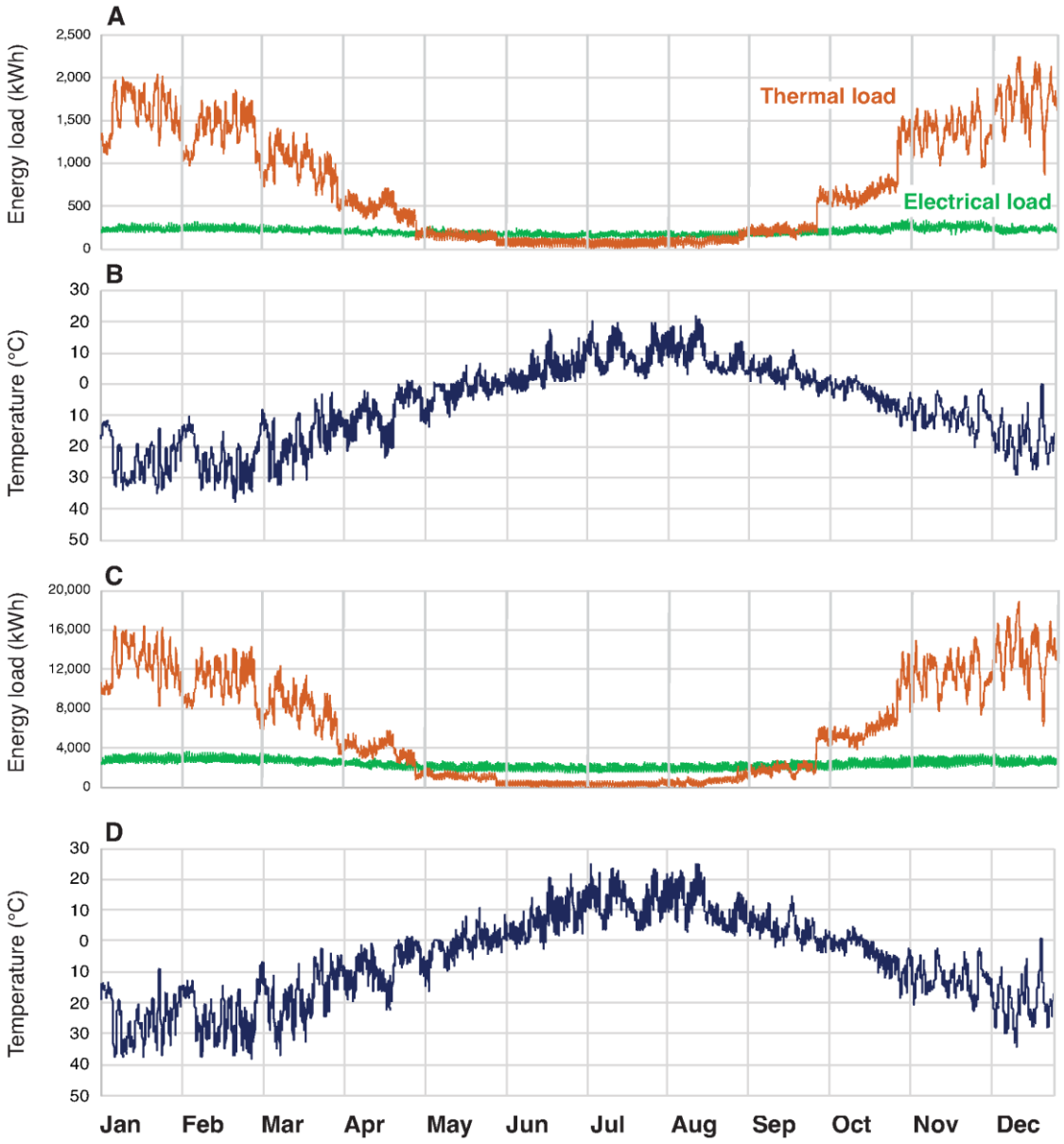

Figure 3.4. Thermal loads exceed electrical loads during the October to April period in both **A)** Aupaluk, QC and **C)** Kuujjuaq, QC. This result holds across communities, emphasizing the importance of diesel exit strategies that center the provision of low-carbon heat. **B)** and **D)** show the hourly temperatures for Aupaluk, QC and Kuujjuaq, QC, respectively.

Figure 3.5 summarizes the ratio of average thermal loads to average electrical loads, as well as the ratio of maximum thermal loads to maximum electrical loads across all 40 communities. The ratio of the annual average of thermal loads to electrical loads ranges from one to seven, with a mean of 3. When considering hourly loads, the maximum ratio of thermal to electrical loads ranges from seven to 23.

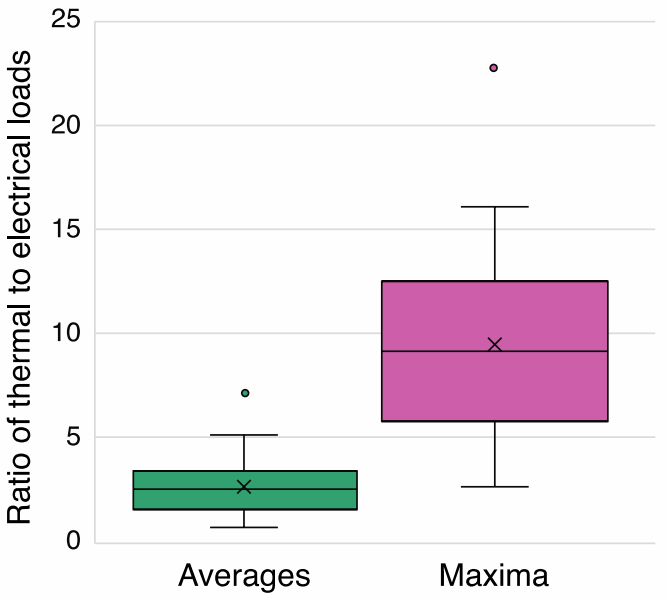

Figure 3.5. Boxplot comparing the ratio of average and maximum thermal loads to electrical loads across all 40 communities under investigation.

3.4.3. Predicting annual and monthly heating loads based on sparse information

Using the characteristics of these 40 communities as independent variables, and the annual heating load as a dependent variable, an OLS regression model was developed and employed to estimate the annual thermal loads for other remote communities using sparse but publicly available data. Multiple models were constructed and tested for fit, exhibiting broadly similar results. The best performing model required three variables as

inputs: population, number of heating degree days, and location. Population emerges as by far the most statistically significant predictor of annual thermal load, and a plot of annual heating load vs. population is presented in Figure 3.6. The best-fitting model is summarized in Table 3.3 below; diagnostic results for other models that were tested for fit are included in the SI: https://doi.org/10.5281/zenodo.6948879.

Table 3.3. The best-fitting model for predicting annual thermal loads for remote and northern communities requires sparse data inputs: population, heating degree days, and location.

	Estimate	**Std. Error**	**P-value**
(Intercept)	5082075.8	4365638.6	0.252
Province	1079519.5	512272.5	0.042**
Population	11498.8	847.6	1.01E-15***
Heating degree days	-630.7	568.2	0.274
Adjusted R-squared: 0.835; AIC: 1375; BIC: 1383			
Significance codes: *** 0.001; ** 0.01; * 0.05			

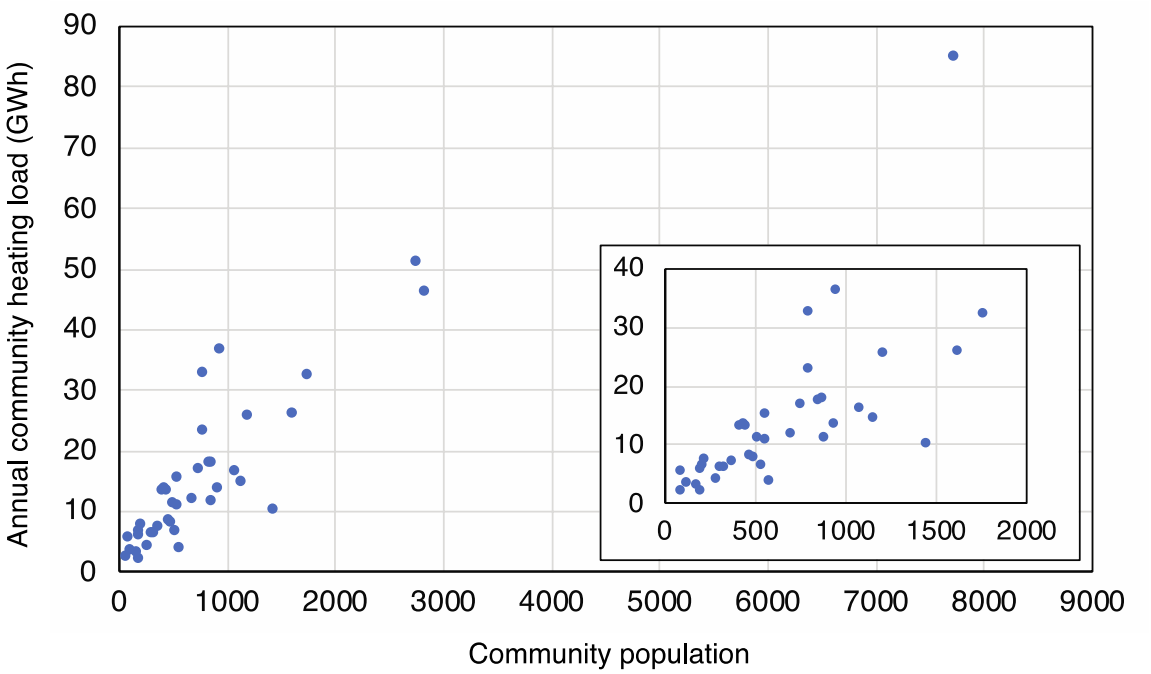

Figure 3.6. A clear trend can be seen between annual thermal load and population: population emerges as the most important variable in predicting annual thermal loads in the regression model.

In addition to annual thermal load prediction, twelve similar models are developed to estimate monthly thermal loads for a community, using monthly heating loads as the dependent variable in each case and population, location, and number of heating degree days as the independent variables. These models yielded adjusted R-squared values of 0.808 at their worst (in December) and 0.918 at their best (in July). Summary diagnostics for the monthly heating load models are also included in the SI: https://doi.org/10.5281/zenodo.6948879.

3.4.4. Validation and limitations of the method

Annual estimated thermal loads are compared to actual annual thermal loads for the few communities where such data exist. We found two sources that report thermal load

data for a fraction of the communities. One source is a report by Hazelton et al., that reports diesel fuel consumption for both heat and electricity across communities in Nunavut [77]. These include six of the communities investigated here. To attempt to validate results, we convert the diesel fuel consumption numbers that are reported for these six communities to MWh of thermal energy, assuming a diesel furnace efficiency of 80% and an energy content of 10 kWh per litre of diesel. (This assumption for diesel furnace efficiency is yet another source of uncertainty.) In 2014, most of the heating in Nunavut was provided by heating oil, while some came from captured residual heat [86]. The second source is the Arctic Energy Alliance, which reports annual thermal loads per source for communities across the Northwest Territories [87]. Six of the reported communities overlap with the communities analyzed in this paper. To calculate the annual thermal loads, we consider only sources that serve thermal loads like heating oil, firewood, wood pellets, propane, and waste heat recovery: these are summed. Table 3.4 lists the results of this comparison: our method overestimates the thermal loads in seven of the twelve communities, but underestimates the thermal loads in the remaining five.

Table 3.4. Comparing thermal load estimates generated with this method to thermal load requirements derived from reported diesel fuel consumption for heating purposes.

Community	Estimated annual thermal load (MWh)	Reported annual thermal load (MWh)	% Error
Rankin Inlet, NU	46,011	44,784	2.7
Pond Inlet, NU	25,882	20,640	25.4
Naujaat, NU	16,331	11,792	38.5
Ikpiarjuk, NU	17,693	10,712	65.2
Iqaluit, NU	84,579	179,568	-52.9
Resolute Bay, NU	5,694	15,216	-62.6
Fort Good Hope, NT	11,063	10,486	5.5

Community	Estimated annual thermal load (MWh)	Reported annual thermal load (MWh)	% Error
Wrigley, NT	3,429	2,424	41.5
Tsiigehtchic, NT	3,044	3,603	-15.5
Whatì, NT	8,174	6,731	21.4
Fort McPherson, NT	11,789	17,544	-32.8
Fort Simpson, NT	25,423	27,558	-7.7

The method adopted in this analysis suffers from multiple limitations. These include lack of sufficient empirical data for validation; limited information on community building stock, limited information on the age, standard, and state of repair of existing building stock; lack of information regarding the behavior of residents in those communities, especially with regard to residential occupant behavior and energy choices. Beyond these limitations, the method itself relies on one set of reference buildings that were developed for the American context, and for a climatic region that approximates Canadian remote and northern communities but might not faithfully represent them. Nonetheless, these reference buildings are widely used in research, building code development, and policy making.

There is also the potential for errors in all labor-intensive modelling and simulation research, including human errors in counting building stock and the potential for misclassification of buildings. This is especially true for communities outside Alberta, Québec, Nunavut, and Yukon, where little to no community mapping or aerial photography exist. In those cases, reliance on satellite imagery was of key importance, but some satellite imagery on Google Earth, Google Maps, and Map Carta is dated.

The slim availability of empirical data with which we could compare our results is a major limiting factor, since it reduces the opportunity for method and model validation.

3.5. Conclusions

This research represents a first attempt to develop simulated thermal loads for Canada's remote and northern communities. It is hampered by paucity of data on thermal energy consumption, building stock performance, occupant behavior, and even official maps. However, the research makes a novel contribution to efforts to develop feasible and sustainable pathways for a low-carbon transition in the challenging northern context. With simulated average annual thermal loads being as much as seven times higher than simulated annual average electrical loads, and with thermal loads sometimes rising to 23 times the electrical load in some hours, it is essential to consider thermal requirements in any investment planning strategy that seeks a sustainable diesel exit. When combined with NRCan's simulated electric load profiles, this research could enable the development of a large-scale optimization model that outlines the decision space for remote and northern communities as they transition to net-zero. For example, which cost targets must low-carbon generation technologies meet to be cost-competitive with diesel? What options for heating exist, and how high a premium do they incur? Finally, which community microgrid configurations are more climate-friendly, more sustainable, and more equitable than the current diesel-dominated paradigm. Since this paradigm is bound to change soon, it is important to make decisions regarding the northern transition imminently, despite the lack of empirical data.

To our knowledge, the preceding results comprise the best estimates of hourly thermal loads that exist for remote and northern communities. This paper must serve as a starting point for more robust methods of hourly thermal load estimation. This includes the development of new databases of prototypical buildings that are more relevant to the Canadian context than the DOE's; surveys of occupant behavior and energy use; and, of

course, gathering empirical data on thermal energy consumption across many communities. Future work should prioritize the implementation of artificial intelligence or machine learning methods for building counts, building classification, and square footage estimation. Recent efforts have focused on implementing and improving machine learning methods for classification of buildings [88, 89]. This would help generate more robust estimates of community thermal loads.

Chapter 4. Optimizing hydrogen microgrids to facilitate diesel exit and meet the energy needs of remote and northern communities

4.1. Introduction

As jurisdictions worldwide move towards legally enshrined net-zero emission targets, remote and isolated communities face a peculiar set of challenges that make it especially difficult to achieve that goal. In addition to their common reliance on liquid and gaseous fuels for which they often pay a premium, these communities must sometimes contend with limited resources and deep-rooted inequities that could delay or threaten their efforts to secure a sustainable future. Canada has approximately 350 remote and northern communities that together consumed more than 680 million liters of diesel in 2020, two-thirds of which was devoted to serving their heating needs while the remaining third was used to produce electricity [62]. Although their overall contribution to the nation's greenhouse gas (GHG) emissions is small [54], it is imperative to transition these communities to low-carbon, sustainable energy systems over the coming decades. Doing so would reduce the climate, air pollution, and albedo impacts of emissions from diesel combustion, helping the country achieve its net-zero emission targets [2]. Depending on the low-carbon alternatives that are chosen, it could also yield a more equitable, secure, and resilient energy system, given the volatility in diesel costs and the challenge of transporting it to the north.

Communities and governments in Canada are investigating the techno-economic viability of diesel exit strategies for remote and northern communities that rely on fossil-derived liquid fuels to serve their electrical and thermal needs. At the federal level, Natural Resources Canada (NRCan) has initiated the Clean Energy for Rural and Remote Communities (CERRC) Program [63] and the Off-Diesel Initiative [65]. In addition, one

of its science and technology research arms—CanmetENERGY Ottawa—is developing tools that could inform communities as they invest in renewable energy resources [90]: these tools simulate community electrical loads and evaluate the portion that could be met with wind and solar power.

Here, we seek to fill two gaps in the analytical literature on the energy transition in remote communities. First, we focus on the role that hydrogen technologies might play in ensuring that the future microgrids deployed in these communities provide reliable, low-carbon energy. Very few existing models envision what a hydrogen-backed microgrid might look like: most optimize investments in variable renewable energy resources and electrochemical energy storage [91, 92]. Commercial microgrid investment planning software envisions the deployment of hydrogen fuel cells for stationary power generation [81, 93], overlooking the versatility of the technology by ignoring electrolytic cells for hydrogen production and hydrogen furnaces for heat provision. More recently, two research efforts have sought to expand on the role that hydrogen might play to complement renewable electricity generation [94, 95], but they focus on specific communities as case studies and refrain from making broader conclusions regarding hydrogen's feasibility.

Second, when it comes to remote and northern communities, no existing models consider both electrical and thermal loads across a broad range of communities, because sparse data on either exists in the public domain. This research develops a new microgrid investment planning model that optimizes the deployment of wind and hydrogen resources to meet the electrical and thermal needs of 40 remote and northern communities that were selected because they span a wide range of locations, populations,

wind resource, accessibility, and renewable energy resources. The model compares diesel-backed and hydrogen-backed microgrids by determining the installed capacity of generators in each scenario, as well as their capital and operating costs. It also explains how a reversible fuel cell (RFC) would need to operate to accomplish the dual goals of complementing intermittent renewables and producing enough hydrogen to serve thermal energy needs in these sub-Arctic and Arctic locations.

4.2. Data and Methods

4.2.1. Northern communities

The 40 communities investigated here are selected because they vary in major attributes, providing a representative snapshot of the hundreds of remote and northern communities in Canada. They vary based on population, province, wind power resource, level of access, and indigenous identity. Figure 4.1 pinpoints these communities; for more details, please consult the Supporting Information (SI): https://doi.org/10.5281/zenodo.6959514 or the Remote Communities Energy Database [66].

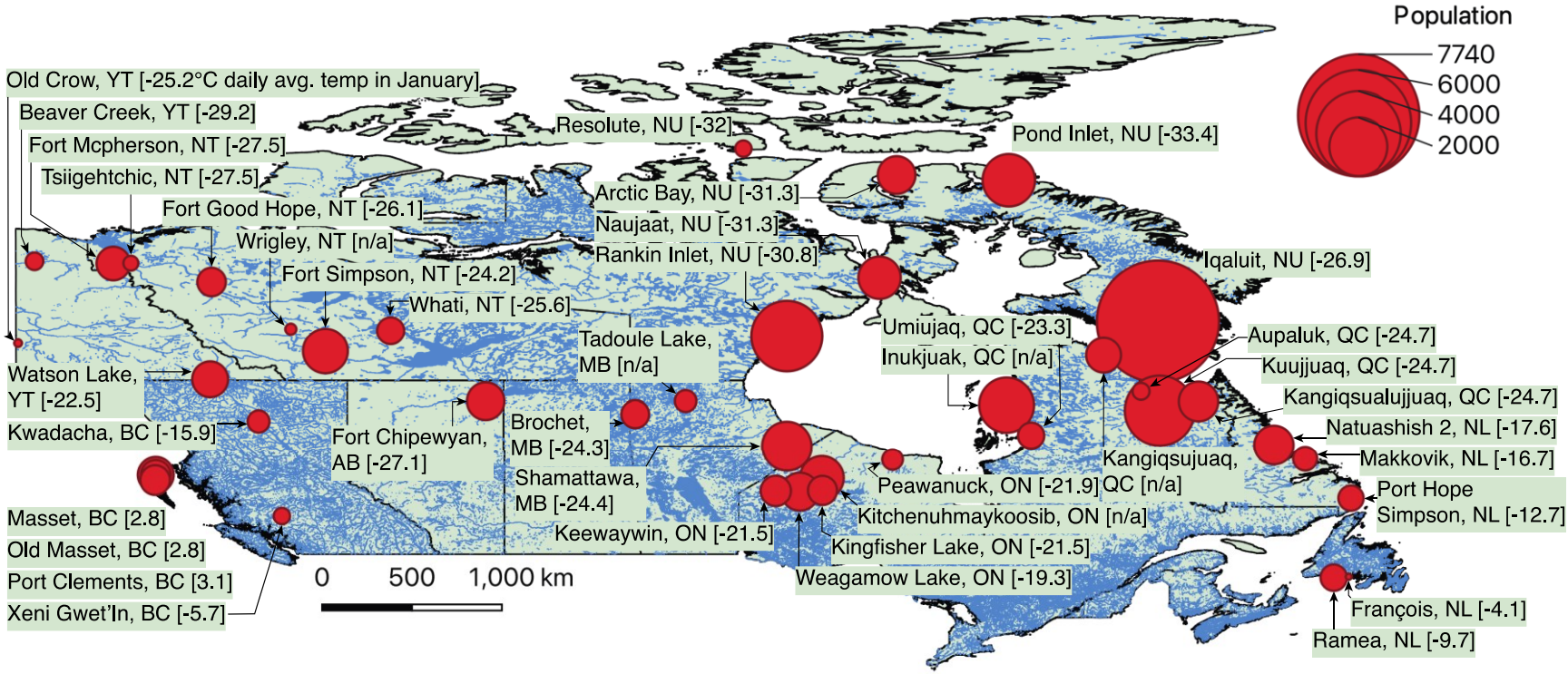

Figure 4.1. Name, location, population, and daily average temperature in January (°C) for the 40 communities investigated. Temperature data are sourced from the most proximate weather station's 1981-2010 climate normals, as reported by Environment and Climate Change Canada [96]. Provincial abbreviations: AB = Alberta; BC = British Columbia; MB = Manitoba; NL = Newfoundland and Labrador; NT = Northwest Territories; NU = Nunavut; ON = Ontario; QC = Québec; and YT = Yukon. Blue represents bodies of water.

4.2.2. Load profile and model development

Simulated, hourly electrical load profiles for these communities that span an entire year were provided to the research team by NRCan. Thermal loads were estimated for each community using the method outlined in Chapter 3. Using these simulated electrical and thermal loads, two optimization models are run for each community. The first invests in sufficient diesel generator and furnace capacity to serve both electrical and thermal energy loads; the second invests in wind power, RFCs, and hydrogen furnace capacity. Because the RFCs are required to both complement the wind energy resource and electrolyze sufficient water to produce hydrogen that serves thermal energy requirements, the installed wind capacity in this renewable microgrid is overbuilt to serve both electrical and thermal loads. The input data that are used to evaluate cost and performance for all models can be found in Table B.1 in Appendix B.

The model considers hourly load and generation data over the course of two summer weeks (14 days) that represent the lowest combined demand of electricity and heat throughout the year, and over the course of two winter weeks (14 days) that represent the highest combined demand. This helps represent the microgrid's performance over the course of the year. All models employed the solver coinbonmin and were run on Jupyter Servers provided by Saturn Cloud. The diesel-backed microgrid model was run with Saturn's 2XLarge server, which has 8 cores and 64 GB RAM. The hydrogen-backed microgrid model was run with Saturn's 8XLarge server with 32 cores and 256 GB RAM.

4.2.3. Diesel-backed microgrid optimization model

The diesel-backed microgrid optimization model considers multiple diesel generator (genset) sizes, since this technology is offered in discrete size options. The possible genset sizes, denoted by GS, are 100 kW, 500 kW, 1,000 kW, and 2,000 kW. Only one furnace size is considered, denoted by DFS and rated at 17.58 kW. This furnace size approximates the heating capacity required for a single-family home. This optimization model has an objective function of minimizing the capital and operating costs:

$$\min(cc + oc) \tag{4.1}$$

where cc are the capital costs and oc are the operating costs. cc considers both diesel genset and diesel furnace costs, cc_{gs}^{G} and cc_{dfs}^{DF}, respectively. These are calculated based on the specific capital expenditures of the technology, CAP, and electrical capacity, ce. Annualized values are generated using a discount rate, r, of 5%, as shown in equations (4.2) and (4.3). Each technology has a lifespan, denoted by L^G for the diesel generator and L^{DF} for the diesel furnace.

$$cc_{gs}^{G} = CAP_{gs}^{G} * ce_{gs}^{G} * \frac{r(1+r)^{L^G}}{(1+r)^{L^G} - 1} \qquad \forall gs \tag{4.2}$$

$$\mathrm{cc}_{\mathrm{dfs}}^{\mathrm{DF}} = \mathrm{CAP}_{\mathrm{dfs}}^{\mathrm{DF}} * \mathrm{ce}_{\mathrm{dfs}}^{\mathrm{DF}} * \frac{\mathrm{r}(1+\mathrm{r})^{\mathrm{L^{DF}}}}{(1+\mathrm{r})^{\mathrm{L^{DF}}} - 1} \qquad \forall\ \mathrm{dfs} \tag{4.3}$$

The two technologies' capital costs are summed to arrive at total capital costs, as shown in equation (4.4) below:

$$cc = \sum_{gs=1}^{GS} cc_{gs}^{G} + \sum_{dfs=1}^{DFS} cc_{dfs}^{DF} \tag{4.4}$$

Operating costs are calculated using equations (4.5) through (4.7). In addition to fixed operating costs, this also includes the fuel usage variables, f^G and f^{DF}, which are multiplied by the cost of diesel, OP^D.

$$oc_{gs}^{G} = OP_{gs}^{G} * ce_{gs}^{G} \qquad \forall gs \tag{4.5}$$

$$oc_{gs}^{G} = OP_{gs}^{G} * ce_{gs}^{G} \qquad \forall gss \tag{4.6}$$

$$oc = \sum_{gs=1}^{GS} oc_{gs}^{G} + \sum_{dfs=1}^{DFS} oc_{dfs}^{DF} + [(f^G + f^{DF}) * OP^D] \tag{4.7}$$

The model invests in enough diesel genset capacity to meet or exceed the electrical load, L_t, for each time step, t, while remaining below the maximum allotted genset capacity, Ke_{gs}^{G}, which is set to an arbitrarily high value. Equation (4.8) defines the installed electrical capacity for each size of genset by multiplying the number of gensets, ne_{gs}^{G}, by their unit capacity, Ue_{gs}^{G}. Equation (4.9) ensures that the sum of the electrical outputs of each generator size, $e_{t,gs}^{G}$, exceeds or meets the electrical demand. Equation (4.10) forces the electrical capacity of each genset to be lower than its maximum given capacity. Equation (4.11) ensures that the capacity is at least equal to the electrical output of each size. Equation (4.12) calculates the annual amount of fuel used assuming diesel energy content of 0.1 L/kWh, D_E, and an efficiency, Eta^G, of 38% [77]. τ is used to convert the calculated four-week value to an annual estimate and is set to 13. This assumes that every four-week period of the year consumes the same amount of fuel.

$$ce_{gs}^{G} = ne_{gs}^{G} * Ue_{gs}^{G} \qquad \forall gs \tag{4.8}$$

$$\sum_{gs=1}^{GS} e_{t,gs}^{G} \geq L_t \qquad \forall t \tag{4.9}$$

$$ce_{gs}^{G} \leq Ke_{gs}^{G} \qquad \forall gs \tag{4.10}$$

$$ce_{gs}^{G} \geq e_{t,gs}^{G} \qquad \forall t, gs \tag{4.11}$$

$$F^{G} = \sum_{t=0,gs=1}^{T,GS} e_{t,gs}^{G} * \frac{D_E}{Eta^{G}} * \tau \tag{4.12}$$

Similarly, the model will invest in sufficient diesel furnace capacity to meet or exceed the thermal load, LT_t. The thermal capacity of the furnace, ct_{dfs}^{DF}, is defined in equation (4.13) by the number of furnaces, nt_{dfs}^{DF}, and unit capacity, Ut_{dfs}^{DF}, for each furnace size. Equation (4.14) sets the thermal output, $t_{t,dfs}^{DF}$, to match the thermal load. Equations (4.15) and (4.16) ensure that the thermal capacity is at or below the maximum capacity, Kt_{dfs}^{DF}, and greater than or equal to the thermal output, respectively. Equation (4.17) calculates the annual fuel usage assuming diesel energy content of 0.1 L/kWh, D_T, and an efficiency, Eta^{DF}, of 80%. τ is used in the same way as above to estimate the annual amount of fuel consumed.

$$ct_{dfs}^{DF} = nt_{dfs}^{DF} * Ut_{dfs}^{DF} \qquad \forall dfs \tag{4.13}$$

$$\sum_{dfs=1}^{DFS} t_{t,dfs}^{DF} = LT_t \qquad \forall t \tag{4.14}$$

$$ct_{dfs}^{DF} \leq Kt_{dfs}^{DF} \qquad \forall dfs \tag{4.15}$$

$$ct_{dfs}^{DF} \geq t_{t,dfs}^{DF} \qquad \forall t, dfs \tag{4.16}$$

$$F^{DF} = \sum_{t=0,dfs=1}^{T,DFS} t_{t,dfs}^{DF} * \frac{D_T}{Eta^{DF}} * \tau \tag{4.17}$$

4.2.4. Hydrogen-backed microgrid optimization model

The hydrogen-backed microgrid optimization model includes multiple sizes of wind turbines, WS, RFCs, RS, and hydrogen furnaces, HFS. We consider three wind turbine sizes that are small and therefore appropriate for these communities: 500 kW, 800 kW, and 1,500 kW. We consider three RFC sizes: 1,000 kW, 20,000 kW, and 100,000 kW and one hydrogen furnace sized at 17.58 kW. This model also minimizes the total cost of the system by minimizing the sum of capital and operating costs:

$$\min(cc + oc) \tag{4.18}$$

Here, cc and oc are split up into three components. For capital costs, equation (4.19) shows each of the three components. The capital costs of the wind turbines, RFCs, and hydrogen furnaces are calculated in equations (4.20), (4.21), and (4.22), respectively.

$$cc = \sum_{ws=1}^{WS} cc_{ws}^{W} + \sum_{rs=1}^{RS} cc_{rs}^{R} + \sum_{hfs=1}^{HFS} cc_{hfs}^{HF} \tag{4.19}$$

$$cc_{ws}^{W} = CAP_{ws}^{W} * ce_{ws}^{W} * \frac{r(1+r)^{L^W}}{(1+r)^{L^W} - 1} \qquad \forall ws \tag{4.20}$$

$$cc_{rs}^{R} = CAP_{rs}^{R} * ce_{rs}^{R} * \frac{r(1+r)^{L^R}}{(1+r)^{L^R} - 1} \qquad \forall rs \tag{4.21}$$

$$cc_{hfs}^{HF} = CAP_{hfs}^{HF} * ce_{hfs}^{HF} * \frac{r(1+r)^{L^{HF}}}{(1+r)^{L^{HF}} - 1} \qquad \forall hfs \tag{4.22}$$

Operating costs are calculated similarly, as show in the four equations below:

$$oc = \sum_{ws=1}^{WS} oc_{ws}^{W} + \sum_{rs=1}^{RS} oc_{rs}^{R} + \sum_{hfs=1}^{HFS} oc_{hfs}^{HF} \tag{4.23}$$

$$oc_{ws}^{W} = OP_{ws}^{W} * ce_{ws}^{W} \qquad \forall ws \tag{4.24}$$

$$oc_{rs}^{R} = OP_{rs}^{R} * ce_{rs}^{R} \qquad \forall rs \tag{4.25}$$

$$oc_{hfs}^{HF} = OP_{hfs}^{HF} * ce_{hfs}^{HF} \qquad \forall hfs \tag{4.26}$$

Next is to define how the model invests in wind energy capacity. Equation (4.27) defines the electrical capacity of the wind turbines. Equation (4.28) ensures that the total electrical output, $e_{t,ws}^{W}$, is less than or equal to the maximum potential output, W_{ws}, multiplied by the number of turbines built. Equation (4.29) forces the electrical capacity to be at most equal to the maximum capacity. Equation (4.30) ensures that the electrical capacity is at least equal to the electrical output.

$$ce_{ws}^{W} = ne_{ws}^{W} * Ue_{ws}^{W} \qquad \forall ws \tag{4.27}$$

$$e_{t,ws}^{W} \leq W_{t,ws} * ne_{ws}^{W} \qquad \forall t, ws \tag{4.28}$$

$$ce_{ws}^{W} \leq Ke_{ws}^{W} \qquad \forall ws \tag{4.29}$$

$$ce_{ws}^{W} \geq e_{t,ws}^{W} \qquad \forall t, ws \tag{4.30}$$

The RFC portion of the model is more complicated due to the reversible operation of the electrochemical cell and consists of eleven equations. The first three equations develop the logic for RFC operation. Equation (4.31) determines whether there is a power excess or deficit with the variable, pl_t. Equations (4.32) and (4.33) serve to force y_t to be binary. If there is excess power at any given time, y_t will be equal to 1; if there is a deficit, it will equal 0. The variable M is a very large number (i.e., 1E+8). The installed capacity of the RFC is defined by equation (4.34), equation (4.35), which makes sure its total capacity can meet the excess or deficit in power, and equation (4.36), which makes sure that it is below the maximum allotted capacity.

$$pl_t = \sum_{ws=1}^{WS} e_{t,ws}^{W} - L_t \qquad \forall t \tag{4.31}$$

$$pl_t \leq M * y_t \qquad \forall t \tag{4.32}$$

$$pl_t \geq M * (1 - y_t) \qquad \forall t \tag{4.33}$$

$$ce_{rs}^{R} = ne_{rs}^{R} * Ut_{rs}^{R} \qquad \forall rs \tag{4.34}$$

$$\sum_{rs=1}^{RS} ce_{rs}^{R} \geq pl_t \qquad \forall t \tag{4.35}$$

$$ce^{R} \leq Ke_{rs}^{R} \qquad \forall rs \tag{4.36}$$

With the above logic, it is possible to develop an operational duty cycle for the RFC to determine when it is operating in fuel cell (power generation) mode, when in

electrolysis (hydrogen production) mode, and how much electric power or hydrogen it is producing as a result. Calculating the state of the RFC, SoR_t, is split across three equations, culminating in equation (4.39), which calculates the state of the RFC. This requires one equation for electricity and another for heat. Equation (4.37) addresses the electrical component: in any time period, if pl_t is positive, meaning that there is an excess of power, then the first term is calculated to determine how much hydrogen is created with the excess electricity. H_E is the conversion factor of electrical energy to hydrogen (0.03 kgH_2/kWh). If pl_t is negative, meaning there is a power deficit, then hydrogen must be converted to electricity, and the first term goes to zero while the second term is calculated. E_H is the conversion rate of hydrogen to electricity (0.023 kgH_2/kWh).

Equation (4.38) addresses the thermal component. Since hydrogen is the only option for meeting the thermal load, it must be consumed whenever heat is needed. Here, H_T is the conversion rate of hydrogen to thermal energy (0.03 kgH_2/kWh) and Eta^{HF} is the efficiency of the hydrogen furnace, which is assumed to be 80%. Equation (4.39) is a step function based on time. When t > 0, the previous time step's SoR value is added to the values calculated in equations (4.37) and (4.38) to determine a net level of hydrogen inventory. When t = 0, the value of SoR is initialized to equal the amount of hydrogen that is required to meet the thermal load during the two-week summer period, SLT.

$$\alpha = [(pl_t * H_E) * y_t] + [(pl_t * E_H) * (1 - y_t)] \tag{4.37}$$

$$\beta = \left[\frac{LT_t * H_T}{Eta^{HF}}\right] \tag{4.38}$$

$$SoR_t = \begin{cases} SoR_{t-1} + \alpha - \beta & t > 0 \\ \left[\frac{\sum_{t=1}^{SLT} LT_t}{Eta^{HF}}\right] + \alpha - \beta & t = 0 \end{cases} \tag{4.39}$$

Equation (4.40) ensures that the SoR ends the run at the same value with which it began. This ensures that the hydrogen storage logic is sound: the last value of the two-week winter period should equal the first value of the two-week summer period under consideration. Equation (4.41) forces the SoR to be at or above the minimum allowed value, R_{min}, which is 0. In other words, the inventory of stored hydrogen cannot be negative, because that implies that the loads have not been met.

$$SoR_{671} \geq \frac{\sum_{slt=1}^{SLT} LT_t}{33} \qquad \forall t \tag{4.40}$$

$$SoR_t \geq R_{min} \qquad \forall t \tag{4.41}$$

The last four equations in the model comprise the investment in hydrogen furnace capacity. Equation (4.42) defines the thermal capacity of the hydrogen furnaces. Equation (4.43) sets the thermal output to meet the thermal load. Equation (4.44) keeps the thermal capacity at or below the set value, and equation (4.45) ensures that the thermal capacity is greater than or equal to the thermal output.

$$ct_{hfs}^{HF} = nt_{hfs}^{HF} * Ut_{hfs}^{HF} \qquad \forall hfs \tag{4.42}$$

$$\sum_{hfs=1}^{HFS} t_{t,hfs}^{HF} = LT_t \qquad \forall t \tag{4.43}$$

$$ct_{hfs}^{HF} \leq Kt_{hfs}^{HF} \qquad \forall hfs \tag{4.44}$$

$$ct_{hfs}^{HF} \geq t_{t,hfs}^{HF} \qquad \forall t, hfs \tag{4.45}$$

4.2.5. Wind turbine output

The maximum wind turbine output was estimated by applying correction factors to the 2020 performance data of Enercon's E-66 (1,500 kW), E-48 (800 kW), and E-40 (500 kW) turbines from Renewables Ninja [79, 80]. The correction factors consider these turbines' cut-in and cut-out speeds, as found in the RETScreen software program's database [97]. The power outputs from any wind speed outside of the turbines' operating limits are set to zero.

4.2.6. Calculating emissions

Emissions are calculated once the optimization model runs are completed. An emission factor of 2680.5 g CO_2/L diesel [54] is multiplied by the annual fuel consumption for each technology deployed by the diesel-backed microgrid model. This yields an estimate of annual emissions. For the hydrogen-backed microgrid model, the avoided emissions are equivalent to the emissions produced from the diesel-backed microgrid.

4.2.7. Water consumption

Water consumption is also calculated once the optimization model runs are completed. Two scenarios are considered: one in which the water that is created when the

RFC is running in fuel cell mode are captured (i.e., stored) for future electrolysis to produce hydrogen, and another scenario in which no water is captured (i.e., no water storage).

These scenarios are further broken down into a best and worst case, depending on RFC performance. Equation (4.46) defines the RFC duty, Δ_t^{SoR}, which helps calculate the water consumption in the following equations. Equation (4.47) calculates the summer water consumption, wtr_{nocap}^{s}. W_H is the amount of water, in liters, needed to produce 1 kgH_2. In the worst case, this value is 40.5 LH_2O/kgH_2; in the best case, it's 11 LH_2O/kg H_2 [98]. The next three equations correspond to the capture scenario. Equation (4.48) calculates what the water consumption would be if pure water is used during the conversion and no inefficiencies exist, W_E (9 LH_2O/kgH_2) [98]. This value can also be negative, which corresponds to the pure water produced when converting hydrogen to electricity. This pure water is stored in the water tank, wt_t, the capacity of which is calculated in equation (4.49). This equation ensures that the tank size does not go below zero and adds to or subtracts from the inventory in the water tank during the previous time step. Equation (4.50) calculates the summer water consumption with a capture system, wtr_{cap}^{s}.

$$\Delta_t^{SoR} = \sum_{t=1}^{671} SoR_t - SoR_{t-1} \tag{4.46}$$

$$wtr_{nocap}^{s} = \sum_{t=0}^{335} \begin{cases} \Delta_t^{SoR} * W_H & \Delta_t^{SoR} > 0 \\ 0 & \Delta_t^{SoR} \leq 0 \end{cases} \tag{4.47}$$

$$wtr_t^{pure} = \Delta_t^{SoR} * W_E \qquad \forall t \tag{4.48}$$

$$wt_t = max(wt_{t-1} - wtr_t^{pure}, \quad \mathrm{wt_{t-1}} - 0) \qquad \forall t \tag{4.49}$$

$$wtr_{cap}^{s} = \sum_{t=1}^{335} \begin{cases} \begin{cases} \Delta_t^{SoR} - \dfrac{(wt_{t-1} - wt_t)}{W_E} * W_H & wt_t > 0 \\ \Delta_t^{SoR} * W_H & wt_t = 0 \end{cases} & \Delta_t^{SoR} > 0 \\ \begin{cases} 0 & wt_t > 0 \\ 0 & wt_t = 0 \end{cases} & \Delta_t^{SoR} \leq 0 \end{cases} \tag{4.50}$$

The winter consumption values are calculated in a similar manner with the following two equations:

$$wtr_{nocap}^{w} = \sum_{t=336}^{671} \begin{cases} \Delta_t^{SoR} * W_H & \Delta_t^{SoR} > 0 \\ 0 & \Delta_t^{SoR} \leq 0 \end{cases} \tag{4.51}$$

$$wtr_{cap}^{w} = \sum_{t=336}^{671} \begin{cases} \begin{cases} \Delta_t^{SoR} - \dfrac{(wt_{t-1} - wt_t)}{W_E} * W_H & wt_t > 0 \\ \Delta_t^{SoR} * W_H & wt_t = 0 \end{cases} & \Delta_t^{SoR} > 0 \\ \begin{cases} 0 & wt_t > 0 \\ 0 & wt_t = 0 \end{cases} & \Delta_t^{SoR} \leq 0 \end{cases} \tag{4.52}$$

The annual estimates of water consumption can be calculated using equations (4.53) and (4.54).

$$wtr_{nocap}^{a} = \left(wtr_{nocap}^{s} + wtr_{nocap}^{w}\right) * \tau \quad (4.53)$$

$$wtr_{cap}^{a} = \left(wtr_{cap}^{s} + wtr_{cap}^{w}\right) * \tau \quad (4.54)$$

The water tank size is determined by taking the max wt_t value. Optimizing the size of water storage is beyond the scope of this model, as are any energy needs to maintain the water.

4.2.8. Estimating microgrid costs

Most of the costs are calculated by the optimization model, but some are calculated once the runs are complete, including the annual costs, the cost of CO_2 avoidance, the lifetime (25-year) costs, and best-case costs. The annual costs are simply the sum of the CAPEX and OPEX values. The cost of CO_2 avoidance is the total annual cost divided by the amount of avoided CO_2. The 25-year costs are reported in the SI: 25 years is taken to be the project lifetime, and this cost incorporates replacement costs for components that retire before 25 years. The lifetimes of technologies are set at 25 years for wind turbines and diesel gensets, 10 years for RFCs, and 20 years for both hydrogen and diesel furnaces. Both best-case and worst-case scenarios are considered for the hydrogen-backed microgrid, and the full range of calculated costs is provided in the SI. For the diesel-backed microgrids, we only consider one capital cost for diesel generators and one for diesel furnaces, since both technologies are mature and we expect no further cost declines due to learning economies. Diesel prices are taken to be 2.0865 USD/L, which is Petro-Canada's rack price for Ultra Low Sulfur diesel in Hay River, Northwest Territories, as reported on June 7, 2022 [99]. Costs for both systems are reported in the SI: https://doi.org/10.5281/zenodo.6959514.

4.3. Results and Discussion

4.3.1. Installed capacities of different technologies

A hydrogen-backed microgrid requires an overbuilt system to power the electrolytic cells that will generate hydrogen to serve the community's thermal needs. The ratio of wind power installed capacity to diesel generator installed capacity, which we refer to as the electric generator overbuild ratio (EGOR), ranges from 7 to 185. Ten of the communities (25%) require an EGOR of 13 or less. Twenty-two of the communities (55%) require an EGOR greater than 25. That said, diesel generators only serve electric capacity, whereas the wind turbines would serve both electric and thermal loads. Table 4.1 lists all 40 communities, which are ranked in ascending order by population, and their installed capacities for the hydrogen-backed microgrid and the diesel-backed microgrid. This data is also available in the SI: https://doi.org/10.5281/zenodo.6959514.

Table 4.1. Installed capacities of wind, RFC, and hydrogen furnaces in the hydrogen-backed microgrids, and of diesel generators and furnaces in the diesel-backed microgrids.

		Hydrogen-backed microgrid (kW)			Diesel-backed microgrid (kW)	
No.	**Community name**	**Wind**	**RFC**	**Furnace**	**Genset**	**Furnace**
1	Francois, NL	1,800	1,000	840	200	840
2	Beaver Creek, YT	55,500	5,000	1,830	300	1,830
3	Wrigley, NT	6,000	2,000	1,280	200	1,280
4	Tsiigehtchic, NT	6,800	2,000	1,140	200	1,140
5	Xeni Gwet'in, BC	7,400	1,000	720	400	720
6	Resolute Bay, NU	12,000	3,000	1,880	800	1,880
7	Aupaluk, QC	4,800	2,000	2,250	400	2,250
8	Old Crow, YT	9,200	3,000	2,600	400	2,600
9	Peawanuck, ON	4,000	2,000	1,500	500	1,490
10	Tadoule Lake, MB	5,200	2,000	2,300	400	2,300
11	Kwadacha, BC	53,300	5,000	2,250	500	2,250

No.	Community name	Hydrogen-backed microgrid (kW)			Diesel-backed microgrid (kW)	
		Wind	RFC	Furnace	Genset	Furnace
12	Makkovik, NL	6,400	2,000	2,830	800	2,830
13	Port Hope Simp., NL	23,700	6,000	6,170	600	6,170
14	Umiujaq, QC	8,200	4,000	4,710	500	4,710
15	Ramea, NL	8,500	5,000	4,680	700	4,680
16	Whati, NT	14,400	3,000	3,160	300	3,160
17	Brochet, MB	19,700	4,000	3,080	600	3,080
18	Fort Good Hope, NT	23,400	5,000	4,340	500	4,340
19	Kingfisher Lake, ON	14,100	3,000	2,320	500	2,320
20	Old Masset, BC	13,600	6,000	5,190	700	5,190
21	Port Clements, BC	13,500	4,000	3,760	700	3,760
22	Keewaywin, ON	12,000	2,000	1,440	800	1,440
23	Fort Mcpherson, NT	27,100	7,000	4,180	600	4,180
24	Kangiqsujuaq, QC	11,700	7,000	5,700	800	5,700
25	Watson Lake, YT	106,900	20,000	12,130	2,400	12,130
26	Masset, BC	31,400	20,000	9,600	4,300	9,600
27	Fort Chipewyan, AB	82,900	20,000	6,840	2,100	6,840
28	Arctic Bay, NU	31,600	8,000	5,850	600	5,850
29	Weagamow Lake, ON	26,400	5,000	4,150	800	4,150
30	Natuashish, NL	10,300	5,000	5,310	1,500	5,290
31	Kangiqsualujjuaq, QC	19,700	20,000	13,060	800	13,060
32	Naujaat, NU	12,700	7,000	5,750	700	5,750
33	Kitchenuhmay., ON	35,200	6,000	5,200	1,100	5,200
34	Fort Simpson,	91,000	20,000	9,810	1,200	9,810
35	Shamattawa, MB	29,600	4,000	3,660	1,100	3,660
36	Pond Inlet, NU	45,300	20,000	8,700	1,100	8,700
37	Inukjuak, QC	22,400	10,000	13,260	1,700	13,260
38	Kuujjuaq, QC	33,200	20,000	18,900	3,300	18,900
39	Rankin Inlet, NU	36,800	20,000	16,510	3,000	16,510
40	Iqaluit, NU	85,600	40,000	29,520	9,400	29,520

Across all 40 communities, the diesel-backed microgrids require the installation of approximately 1.2 MW_e of diesel generator capacity on average, whereas the hydrogen-backed microgrids require the installation of approximately 27 MW_e of wind power capacity on average. In addition to the wind turbines, communities must install 8 MW of electrolyzer capacity on average. In both diesel-backed and hydrogen-backed configurations, the average installed capacity of furnaces across all 40 communities is 6 MWe. The overbuild across all 40 communities is summarized in Figure 4.2.

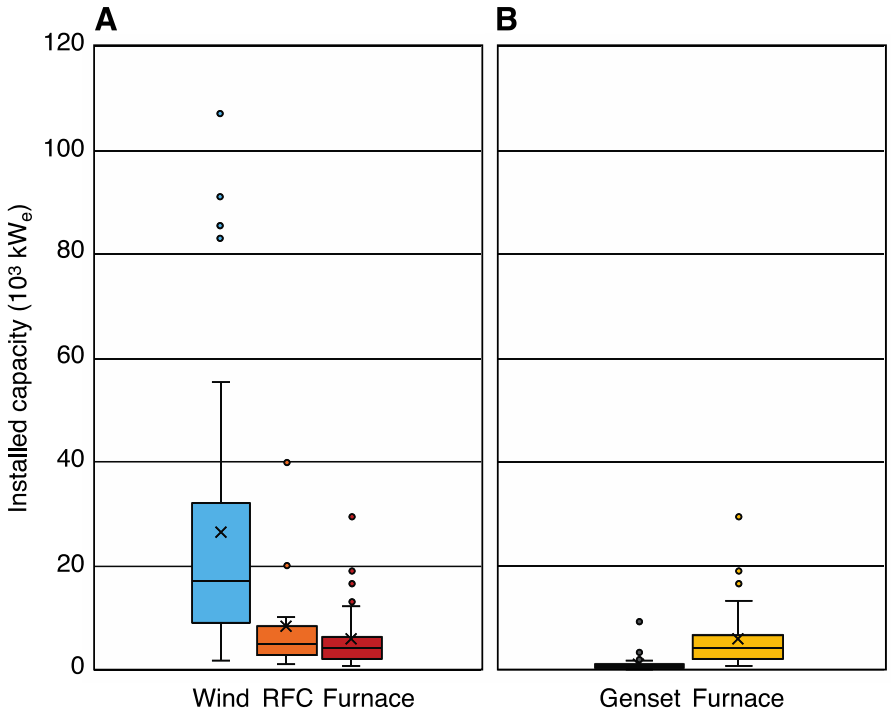

Figure 4.2. A) Hydrogen-backed microgrids require extensive overbuilding compared to **B)** diesel-backed microgrids: columns represent the interquartile range; X marks denote the means, and black lines embedded in the bars denote the medians.

Two factors are responsible for large EGOR values. The first, as expected, is population: larger communities require greater amounts of electric and thermal energy

production to serve their needs. The second factor is the quality of the wind resource. There are relatively small communities that nonetheless require very large capacity installation to overcome their poor wind resource. The most striking example is the community of Watson Lake, YT: despite having a population of 790, building a hydrogen-backed microgrid in Watson Lake requires approximately 107 MW_e of wind turbines. The city of Iqaluit, NU, despite a population that is ten times larger (7,740), requires approximately 86 MWe of wind turbines.

4.3.2. Characterizing RFC operation in a hydrogen-backed microgrid

Operationally, the demand for electricity in these communities is met with the overbuilt wind power capacity, though there remain periods of variability and intermittency associated with that resource, including prolonged wind droughts, that require the RFCs to cease operations in electrolysis mode and to begin operating as fuel cells instead, providing stationary power generation to ensure that the community's electric load is reliably met. Figure 4.3 presents the load curve for the largest community of Iqaluit, NU, the smallest community of François, NL, and the community of Watson Lake, YT, which experiences poor wind resource. A characteristic of winter is the excellent wind resource across most communities (except those, like Watson Lake, which experience wind droughts), which highlights the promise of deploying wind energy for decarbonization in Canada's remote and northern communities. The wind resource in the summer is poorer than it is in winter, but the systems are overbuilt to provide electrical power during that season, and to generate and store enough hydrogen in preparation for winter.

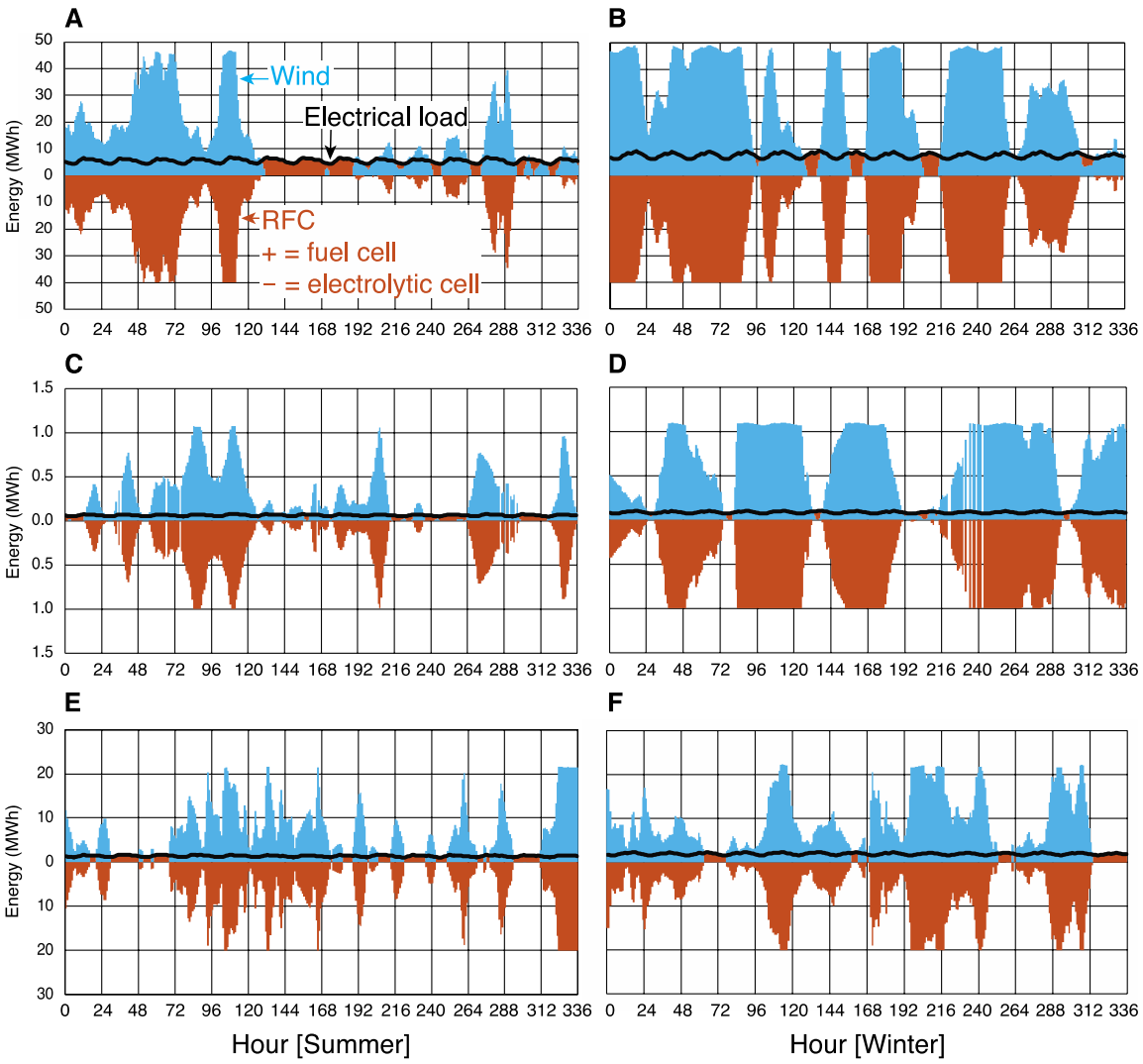

Figure 4.3. Microgrid operations during summer hours (left panels) and winter hours (right panels) for **A** and **B)** the largest community of Iqaluit, NU, **C** and **D)** the smallest community of François, NL, and **E** and **F)** the community of Watson Lake, YT, which has a particularly poor wind resource that necessitates a large EGOR. RFC operation is positive when it is running in fuel cell (power generation) mode and negative when it is running in electrolytic (hydrogen production) mode.

The hydrogen-backed microgrids envisioned in this analysis hinge not only on the commercial availability of polymer electrolyte membrane (PEM) reversible fuel cells, but also on their long-term durability and reliability. RFCs are technologically proven, but they are not widely deployed in commercial settings. It is thus important to expand on the extent to which these RFCs operate in either fuel cell (power generation) or electrolytic (hydrogen generation) mode. Figure 4.4 reports the percentage of time that the RFCs operate in electrolytic mode in each community. Given the stark difference in thermal loads between winter and summer, we present average results for winter, summer, and the entire four-week period under investigation.

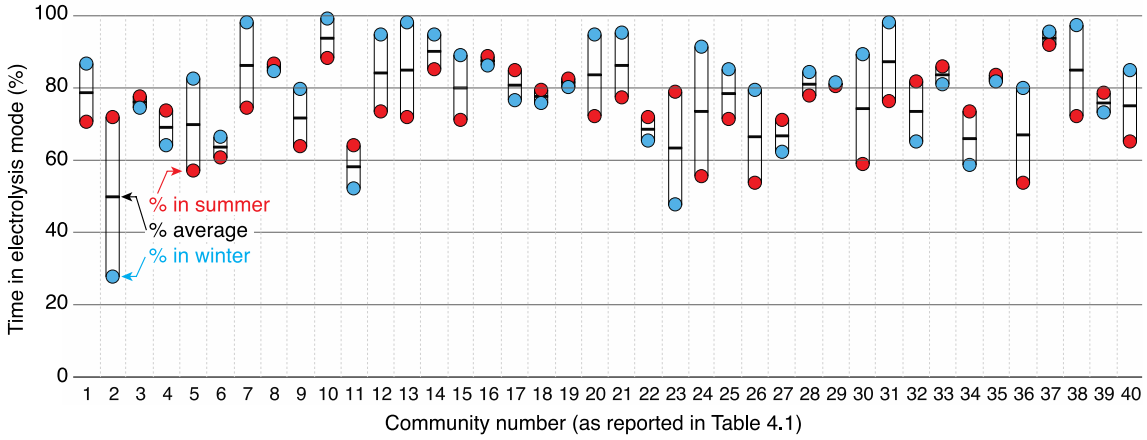

Figure 4.4. A hydrogen-backed microgrid that deploys RFCs would see these systems operate variably and intermittently to produce both electricity that sustains reliable grid operations and hydrogen that provides thermal energy. The percentage of time that RFCs operate in electrolysis mode is reported for winter (blue circle), summer (red circle), and annually (black line). The percentage of time that the RFCs operate in fuel cell mode is simply one minus the value on the y-axis. Community numbers correspond to those in Table 4.1.

4.3.3. Resource requirements of a hydrogen-backed microgrid

Large thermal loads entail not just an overbuilt hydrogen-backed microgrid, but also one that is operated with sufficient foresight to generate and store over the summer months enough hydrogen to meet thermal demand in the cold winters of Canada's North. This requires sufficient amounts of hydrogen storage, and it is crucial to estimate the size of the hydrogen storage infrastructure that might be required to meet winter demand. In addition, electrolysis requires purified water: in remote, resource-constrained locations like the North, it might be wise to capture and store any water that the RFC generates when it operates in fuel cell (power generation) mode, and then to use that pure water when the RFC operates in electrolysis (hydrogen production) mode. This will reduce the resource intensity of the hydrogen-backed microgrid and the costs of water purification, ensuring that the system is more sustainable than it would be otherwise. Figure 4.5 reports the size of the hydrogen storage infrastructure that would be required in each community, as well as the amount of water that each microgrid would consume. Both values are reported annually, though the hydrogen storage tanks would comprise a one-off capital investment as opposed to an annual expense.

Capturing water produced during the power generation process for future electrolysis is a prudent strategy: depending on the community, this reduces annual water consumption by anywhere from 2% to 73%, with an average reduction in annual water consumption of 23%. Of course, deploying this strategy hinges on practical considerations, like whether there is space and sufficient resources to deploy water storage infrastructure. In particular, keeping the water liquid during the cold winter months will require insulated water tanks, water heating, or both.

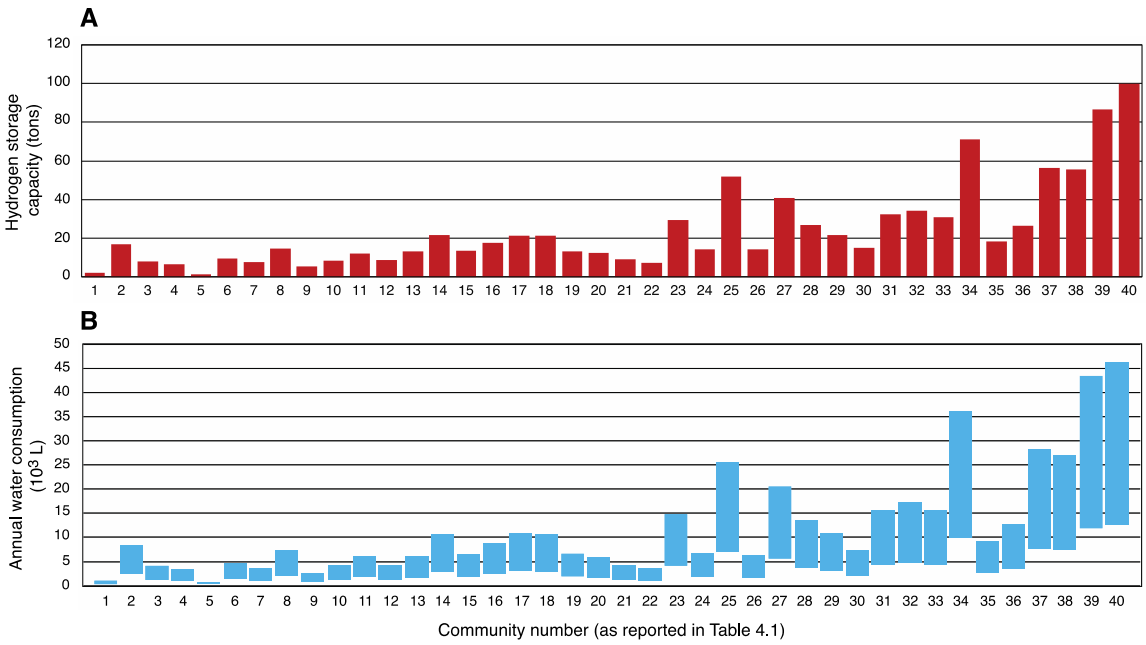

Figure 4.5. To ensure that the hydrogen-backed microgrid can operate successfully in each of the 40 communities under investigation, **A)** Hydrogen storage capacity (in tons) and **B)** annual water consumption (in millions of liters) required is shown. Annual water consumption varies between a lower bound an upper bound, depending on the efficiency of the water electrolysis process, as discussed in section 4.2.7. Community numbers correspond to those in Table 4.1. Exact values can be found in the SI: https://doi.org/10.5281/zenodo.6959514.

4.3.4. Cost, avoided emissions, and feasibility in the current policy context

Given the additional installed capacity and operational complexity associated with a hydrogen-backed microgrid, the cost of this system would have to be equal to or lower than the cost of the diesel-backed microgrid for investors to be tempted to make the switch. Model results demonstrate that the costs of the hydrogen-backed microgrids are lower than the costs of the diesel-backed microgrids across communities; this is driven by

the high diesel fuel costs over 25 years of operation. Using conservative cost estimates, hydrogen microgrids for 31 of the 40 communities are less costly than their diesel counterparts. When using optimistic costs, this number jumps to 38. Figure 4.6 shows the cost comparisons of both systems using conservative costs over a 25-year period.

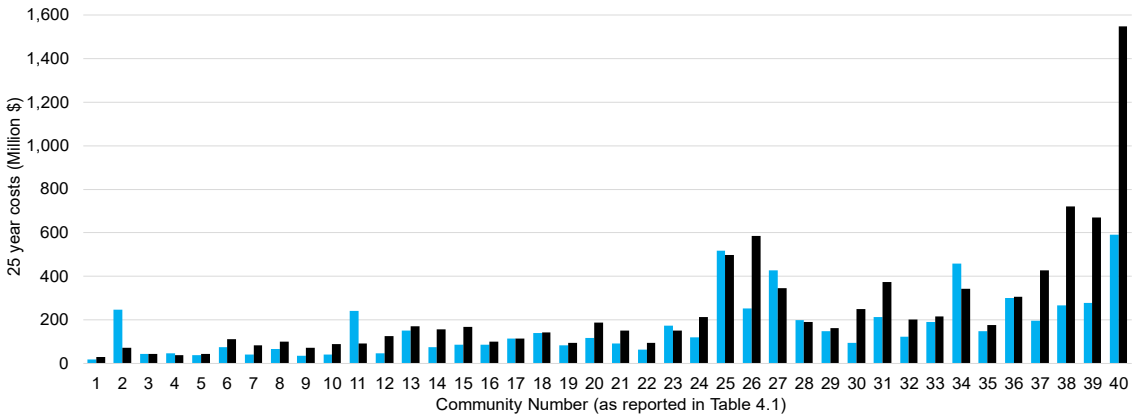

Figure 4.6. 25-year cost comparison between hydrogen microgrids (blue) and diesel microgrids (black). The hydrogen microgrid costs reported in this figure use "conservative" costs. Community numbers correspond to those in Table 4.1. Exact costs for all communities can be found in the SI: https://doi.org/10.5281/zenodo.6959514.

Hydrogen-backed microgrids might be cost-competitive with diesel-backed microgrids, but their deployment is not equally feasible across communities: in fact, for smaller communities with a poor wind resource, the cost of a hydrogen system would be especially high and deployment especially unlikely. To aid communities, investors, and policy makers in determining where near-term deployment of hydrogen-backed microgrids is feasible, Figure 4.7 shows both the cost of electricity and the cost of avoided CO_2 emissions under the best-case scenario.

The federal carbon price in Canada is set to increase to 170 CAD/tCO_2 in 2030, which is equivalent to approximately 130 USD/tCO_2 at current exchange rates [56]; the

cost of avoided carbon emissions from all but one of these 40 communities is higher than this value. Natuashish, NL is the only community with a cost of avoided emissions that is lower than this, sitting just below 170 CAD/tCO_2. A first cluster (Figure 4.7B) of communities yields a cost of avoided emissions that is at or only marginally higher than this value: for 5 of the 40 communities, hydrogen-backed microgrids would become feasible by the time the cost of carbon hits 200 CAD/tCO_2. A second cluster (Figure 4.7C) includes 25 communities where hydrogen-backed microgrids would become feasible if carbon prices increase to between 200 and 500 CAD/tCO_2. This is emblematic of a world where deep decarbonization becomes a policy and political imperative and aggressive emission reduction is achieved. Beyond 500 CAD/tCO_2 is a third cluster of ten communities where alternatives to hydrogen or wind would likely be required to effect a low-carbon transition, unless carbon prices increase dramatically to >500 CAD/tCO_2.

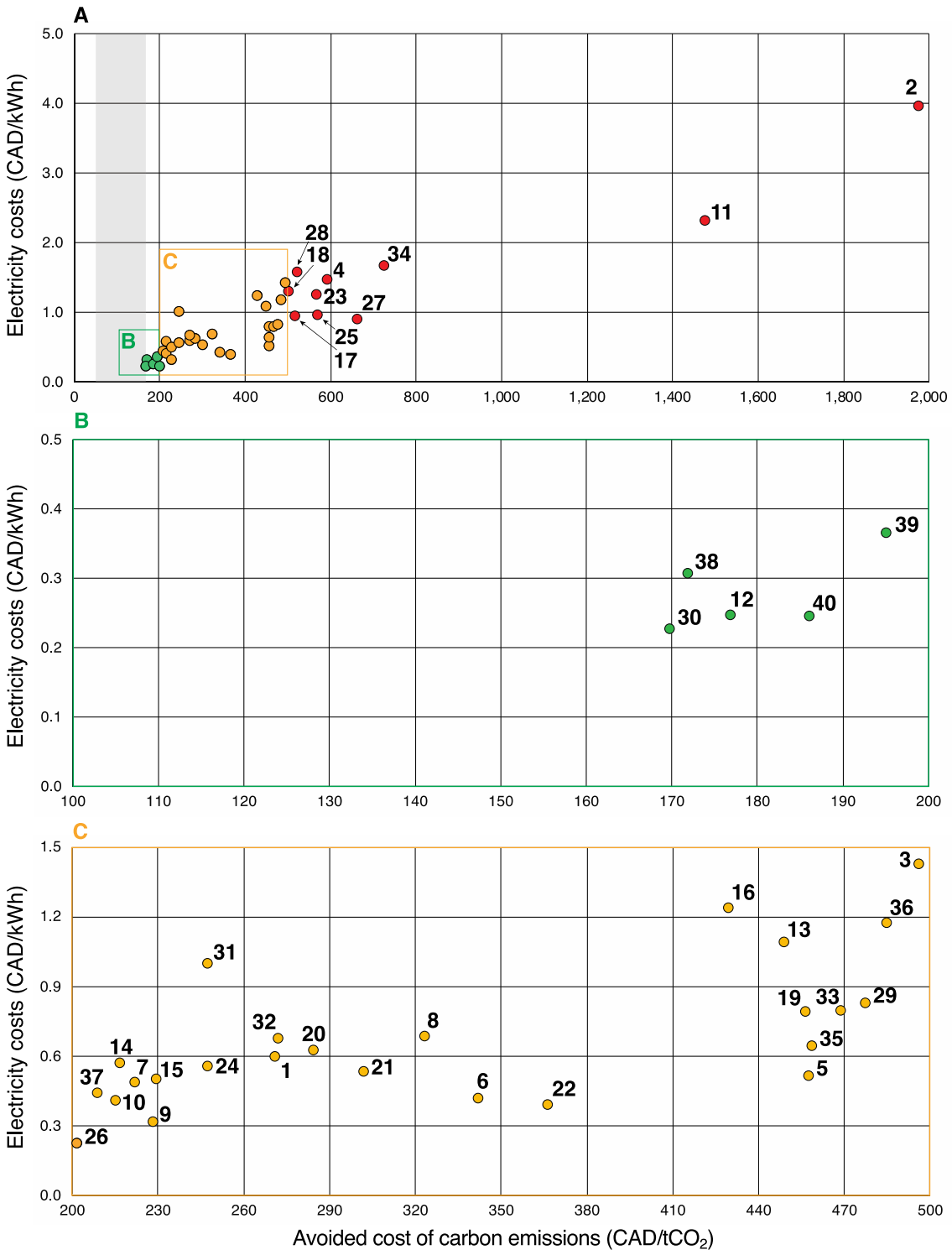

Figure 4.7. A) Cost of delivered electricity and cost of avoided emissions if hydrogen-backed microgrids are deployed across all 40 communities. Best-case data inputs are employed: these values can be found in Appendix B. **B)** In five communities, the cost of

avoided emissions from a hydrogen-backed microgrid would be smaller than 200 CAD/tCO_2, which is close to the value that the federal carbon price is expected to reach in 2030. **C)** In another 25 communities, the cost of avoided emissions is smaller than 500 CAD/tCO_2, a higher carbon price that represents a world that moves aggressively to limit the emission of carbon pollution. The grey vertical band represents the federal carbon price, which sits at 50 CAD/tCO_2 in 2022 and will increase to 170 CAD/tCO_2 in 2030. Community numbers correspond to those in Table 4.1.

4.3.5. Limitations of the analysis

Limitations associated with the estimated thermal loads are discussed above in section 3.4.4. The analysis focused intentionally on wind plus hydrogen. It did not consider a full suite of technologies, like solar, biofuels, or energy storage, that are also potentially viable or preferable for deployment. Moreover, it considered several—but not every—component size possible for each technology. It also ignored the question of thermal management of fuel cells, and the viability of instantaneous switching between fuel cell and electrolysis modes: this operation has been demonstrated in laboratories but not at such large scales. Finally, it assumes that the water required to produce hydrogen is available, which is an assumption in need of validation.

4.4. Conclusions

Any transition to a net-zero emission energy system in remote and northern communities must focus on the central question of diesel exit. This issue is exacerbated by the age of current diesel systems. Some communities have decades-old systems—on average, community energy systems were built or refurbished in 2003, making them

twenty years old. Current initiatives have focused on developing microgrids that are dominated by renewables plus energy storage, or by more climate-friendly liquid fuels like biodiesel. The key is to serve both electrical and thermal loads, with the latter being almost always greater than the former across remote and northern communities during the winter months. Small modular nuclear reactors (SMRs) could reliably provide a combination of electricity and heat to communities without the need for overbuilding the energy system on account of poor wind resources [100]. They could also power electrolysis to produce hydrogen if desired. Future work should compare the systems investigated in this paper to other potential low-carbon transition pathways.

Here, we develop a mixed integer linear program that optimizes the deployment of wind power and reversible fuel cells to meet the electrical and thermal loads of 40 communities in Canada that demonstrate wide variation in attributes like location, population, wind resource, and accessibility. We compare these hydrogen-backed microgrids, which are necessarily overbuilt to produce hydrogen that meets thermal energy requirements, with diesel-backed microgrids analogous to those that currently dominate these communities. Three conclusions stand out:

Extent of infrastructure overbuild: the thermal loads in these remote and northern communities are so large that the hydrogen-backed systems are substantially overbuilt to meet both electrical and thermal load requirements. This yields an electric generator overbuild ratio of between 7 and 185 when comparing the hydrogen-backed microgrids to the diesel ones.

Resource requirements: the amount of hydrogen storage that is required to meet the thermal energy needs of these communities is large (average = 24 tons, maximum =

100 tons), but well within the limits of today's tank-based storage systems. As for water consumption, we find that capturing the water that is produced when the RFC is running in fuel cell mode is prudent, reducing annual water consumption levels by an average of 23% across communities. In locations like these where water extraction and purification are likely to prove difficult and expensive, water capture makes for a cheaper and more sustainable energy system.

Cost and avoided emissions: The hydrogen-backed microgrids envisioned in this research are not only feasible with today's technology, but a small number (5 of 40) are also cost-effective at or slightly above 170 CAD/tCO_2, which is the value that the federal carbon price is set to reach in 2030. The cost of avoided carbon emissions in most communities (30 of 40) is below 500 CAD/tCO_2. While 500 CAD/tCO_2 is beyond the level that is considered realistic in today's political and policy discourse, it is consistent with carbon prices in a world that is aggressively pursuing deep decarbonization this century and are thus in line with Canada's legislative target to achieve net-zero emissions by 2050.

The same can be said of electricity costs: the 5 communities where this solution appears to be feasible from the perspective of avoided costs of carbon emissions also witness costs of electricity delivery that range from 0.2 CAD/kWh to 0.4 CAD/kWh. This is in line with the high residential electricity prices paid by citizens of Yukon (0.19 CAD/kWh), Nunavut (0.38 CAD/kWh), and the Northwest Territories (0.38 CAD/kWh) [101]. Electricity costs for 29 of the 40 communities are below 1 CAD/kWh. The proposed technology is clearly not a solution for every community, and different low-

carbon energy systems must be devised for communities that are so large—or where the wind resource is so poor—that the system proves cost-ineffective.

To our knowledge, this research comprises the first effort to envision a hydrogen-backed microgrid system for a large sample of remote and northern communities, employing community-specific, simulated load profiles and considering both electrical and thermal loads. Among its limitations are the fact that the load profiles used are simulated, that it does not consider water purification and storage costs, and that it only considers one (typical) cost of diesel, rather than employing a probabilistic assessment or sensitivity analysis of diesel fuel costs. Future work is geared towards further developing the model to address these shortcomings, and to experimentally characterize RFC behavior and performance when electrochemical modules are forced to operate under such variable, intermittent, and reversible load signals.

Chapter 5. Conclusions and future work

The research presented here comprises a multiscale analysis of the role that hydrogen could play in the transition to net-zero emissions in two niche applications that are promising candidates for near-term demonstration. In a large-scale assessment, we investigate what the buildout of an integrated energy system with offshore wind and water electrolysis might look like. We find that supplanting natural gas needs in the Atlantic Maritimes with wind-powered hydrogen production is possible by 2050, but only if aggressive growth rates and good technological performance are assumed. For hydrogen produced by this integrated energy system to be cost competitive with steam methane reforming, component costs, especially those of electrolyzers, must be lower than 500 $/kW, which has not been demonstrated yet at commercial scale. In the small-scale assessment, an optimization model is developed that envisions how 40 remote and northern communities in Canada might deploy hydrogen-backed microgrids: microgrids that build wind turbines, reversible fuel cells, and hydrogen furnaces to ensure a zero- or low-carbon energy system that satisfies both their electrical and thermal requirements. We compare these hydrogen-backed microgrids to the current diesel option and find that they are cheaper, given the price of diesel. Moreover, for five of the 40 communities, the cost of avoided emissions is only slightly higher than 170 CAD/tCO_2, the federal carbon price in 2030. At a carbon price of 500 CAD/tCO_2, the hydrogen option becomes feasible for the majority (30 of 40) of communities.

Chapter 2 makes several contributions to the literature. First, it shows just how long a time is required for substantial buildouts of infrastructure to be achieved, even if it is modular infrastructure. Once techno-economic assessments are grounded in empirically derived growth and learning rates, the 2050 target becomes difficult to

realize, and this highlights the urgency of the decarbonization challenge. Second, it shows the role that upscaling electrolyzer manufacturing could play in achieving cost-parity with steam methane reforming: electrolyzer capital costs must fall four- or five-fold for green hydrogen production to be economically competitive, and this integrated energy system assumes that the electricity would not need to be purchased, which might incur a substantial additional cost.

Chapter 3 fills a gap in the literature by generating first-order estimates of hourly thermal loads for remote and northern communities, and by developing a model for estimating the thermal loads of communities based on commonly available data like population and location.

Chapter 4 comprises the first effort to envision what hydrogen-backed microgrids might look like in terms of installed component capacities, how they might operate in practice, and what they might cost. It also quantifies the resource requirements in terms of hydrogen storage and water consumption, and divides communities into three clusters based on their readiness for hydrogen deployment. Communities that are more ready constitute excellent candidates for demonstration and further research.

Simplifications have been made where data are unavailable. Future work must devote resources to eliminating the need for such simplifications, either by acquiring proprietary data or by developing a research program for acquiring new data. Future work can also integrate policy levers into the simulation and optimization models to determine how key government incentives or legislation could accelerate or retard the prospects of a hydrogen transition in the two sectors under investigation.

References

1. The Paris Agreement. Government of Canada; [updated 2016 Jan 06; accessed 2022 Jul 29]. https://www.canada.ca/en/environment-climate-change/services/climate-change/paris-agreement.html.
2. Bill C-12: An Act respecting transparency and accountability in Canada's efforts to achieve net-zero greenhouse gas emissions by the year 2050. Second Session, Forty-third Parliament; 2021 Jun 29 [accessed 2021 Jul 3]. https://www.parl.ca/LegisInfo/en/bill/43-2/c-12.
3. International Energy Agency. The Future of Hydrogen: Seizing today's opportunities. 2019 Jun [accessed 2022 Jul 29]. https://iea.blob.core.windows.net/assets/9e3a3493-b9a6-4b7d-b499-7ca48e357561/The_Future_of_Hydrogen.pdf.
4. European Commission. COM(2018) 773 final: A Clean Planet for all: A European strategic long-term vision for a prosperous, modern, competitive and climate neutral economy. Brussels (Belgium); 2018 Nov 28 [accessed 2021 Jul 3]. https://eur-lex.europa.eu/legal-content/EN/TXT/?uri=CELEX%3A52018DC0773.
5. Climate Change Act 2008 c. 27. Government of the UK; 2008 Nov 26 [updated 2019; accessed 2021 Jul 3]. https://www.legislation.gov.uk/ukpga/2008/27/contents.
6. Fact Sheet: President Biden's Leaders Summit on Climate. Washington (D.C): The White House; 2021 Apr 23 [accessed 2021 Aug 10]. https://www.whitehouse.gov/briefing-room/statements-releases/2021/04/23/fact-sheet-president-bidens-leaders-summit-on-climate/.

7. The National Academies of Sciences, Engineering, and Medicine. Negative Emissions Technologies and Reliable Sequestration: A Research Agenda. Washington (D.C): The National Academies Press; 2009. https://nap.nationalacademies.org/read/25259.
8. Nova Scotia Power. Promoting a Green Nova Scotia, Together: 2020 Integrated Resource Plan Summary. Halifax (NS); 2020 Nov 27. https://irp.nspower.ca/files/key-documents/E3_NS-Power_2020_IRP_Report_final_Nov-27-2020.pdf.
9. Jones R. Rejuvenated Lepreau to operate uninterrupted through next two winters. CBC News; 2020 Nov 10 [accessed 2021 Aug 9]. https://www.cbc.ca/news/canada/new-brunswick/lepreau-rejuvenated-nuclear-plant-1.5795991.
10. Jupia Consultants, Inc. Natural gas supply and demand report New Brunswick and Nova Scotia 2015-2025. Saint John (NB): Atlantica Centre for Energy; 2015. http://www.atlanticaenergy.org/uploads/file/natural_gas_supply_demand_report.pdf.
11. Canada Energy Regulator. Canada's Energy Future 2020. 2020 Dec 2 [accessed 2021 Aug 9]. https://www.cer-rec.gc.ca/en/data-analysis/canada-energy-future/2020/.
12. Hessing M, Howlett M, Summerville T. The Socioeconomic Context: Canadian Resource Industries and the Postwar Canadian Political Economy. In Hessing M, Howlett M, Summerville, Canadian Natural Resource and Environmental Policy, 2nd ed. Vancouver (BC): UBC Press; 2014.

13. Fertel C, Bahn O, Vaillancourt K, Waaub J. Canadian energy and climate policies: A SWOT analysis in search of federal/provincial coherence. Energ Pol. 2013 Dec; Vol.63: p. 1139-1150. https://doi.org/10.1016/j.enpol.2013.09.057.
14. Bird S, Lachapelle E, Gattinger M. Polarization over Energy and Climate in Canada: Survey Results. University of Ottawa, Ottawa (ON): 2019 Dec 10. https://www.uottawa.ca/positive-energy/sites/www.uottawa.ca.positive-energy/files/polarization_survey_final.pdf.
15. Natural Resources Canada. Hydrogen Strategy for Canada: Seizing the Opportunities for Hydrogen. A Call to Action. Ottawa (ON): Government of Canada; 2020 Dec. https://www.nrcan.gc.ca/sites/nrcan/files/environment/hydrogen/NRCan_Hydrogen-Strategy-Canada-na-en-v3.pdf.
16. Ministry of Energy. Natural Gas Vision and Strategy. Edmonton (AB): Government of Alberta; 2020 Oct [accessed 2021 Aug 10]. https://open.alberta.ca/dataset/988ed6c1-1f17-40b4-ac15-ce5460ba19e2/resource/a7846ac0-a43b-465a-99a5-a5db172286ae/download/energy-getting-alberta-back-to-work-natural-gas-vision-and-strategy-2020.pdf.
17. Ministère de l'Environnement et de la Lutte contre les changements climatiques. Plan pour une économie verte 2030: Politique-cadre d'électrification et de lutte contre les changements climatiques. Québec (QC): Gouvernement du Québec; 2020. https://cdn-contenu.quebec.ca/cdn-

contenu/adm/min/environnement/publications-adm/plan-economie-verte/plan-economie-verte-2030.pdf?1605540555.

18. Zen and the Art of Clean Energy Solutions. A Feasibility Study of Hydrogen Production, Storage, Distribution, and Use in the Maritimes. Halifax (NS): OERA; 2020 Oct. https://oera.ca/sites/default/files/2020-11/A%20Feasibility%20Study%20of%20Hydrogen%20Production%20Storage%20Distribution%20and%20Use%20in%20the%20Maritimes.pdf.
19. CleanBC. B.C. Hydrogen Strategy: A sustainable pathway for B.C.'s energy transition. Victoria (BC): Government of British Columbia; 2021. https://www2.gov.bc.ca/assets/gov/farming-natural-resources-and-industry/electricity-alternative-energy/electricity/bc-hydro-review/bc_hydrogen_strategy_final.pdf.
20. Government of Ontario. Ontario Low-Carbon Hydrogen Strategy: A Path Forward. Toronto (ON): Government of Ontario; 2022. https://www.ontario.ca/files/2022-04/energy-ontarios-low-carbon-hydrogen-strategy-en-2022-04-11.pdf.
21. Market Snapshot: The end of natural gas production in the Maritimes increases reliance on imports. Canada Energy Regulator; 2019 Feb 27 [accessed 2021 Aug 9]. https://www.cer-rec.gc.ca/en/data-analysis/energy-markets/market-snapshots/2019/market-snapshot-end-natural-gas-production-in-maritimes-increases-reliance-imports.html.
22. International Energy Agency. Offshore Wind Outlook 2019. Paris (France); 2019 Nov. https://iea.blob.core.windows.net/assets/495ab264-4ddf-4b68-b9c0-514295ff40a7/Offshore_Wind_Outlook_2019.pdf.

23. The Associated Press. Fishermen Back Compensation Plan For Wind Farm Proposal. WBUR; 2019 Feb 24 [accessed 2021 Aug 9]. https://www.wbur.org/bostonomix/2019/02/24/vineyard-wind-fishermen-proposal-approved.
24. Mukano R. Hokkaido wind farms get tailwind as tides shift for fisheries. Nikkei Asia; 2020 Aug 10 [accessed 2021 Aug 9]. https://asia.nikkei.com/Business/Energy/Hokkaido-wind-farms-get-tailwind-as-tides-shift-for-fisheries.
25. Fast S, Mabee W, Baxter J, Christidis T, Drive L, Hill S, McMurtry JJ, Tomkow M. Lessons learned from Ontario wind energy disputes. Nat Energy. 2016 Jan 25; Vol. 1. https://doi.org/10.1038/nenergy.2015.28.
26. Grant T. Nova Scotia looking for ways to attract offshore wind industry. CBC News; 2021 Jan 15. https://www.cbc.ca/news/canada/nova-scotia/nova-scotia-government-renewable-energy-offshore-wind-1.5872787.
27. Mike M. 'Hydrogen alliance' formed as Canada, Germany sign agreement on exports. CBC News; 2022 Aug 23 [accessed 2022 Sep 12]. https://www.cbc.ca/news/canada/newfoundland-labrador/canada-germany-hydrogen-partnership-nl-1.6559787.
28. P.E.I. makes moves toward hydrogen future. CBC News; 2009 May 20 [accessed 2022 Sep 12]. https://www.cbc.ca/news/canada/prince-edward-island/p-e-i-makes-moves-towards-hydrogen-future-1.844785.
29. Dong C, Huang G, Cheng G. Offshore wind can power Canada. Energy. 2021 Dec 1 [accessed 2022 Sep 12]; Vol. 236. https://doi.org/10.1016/j.energy.2021.121422.

30. Eamer JBR, Shaw J, King EL, Mackillop K. The inner shelf geology of Atlantic Canada compared with the North Sea and Atlantic United States: Insights for Canadian offshore wind energy. Cont Shelf Res. 2021 Jan 15 [accessed 2022 Sep 12]; Vol. 213. https://doi.org/10.1016/j.csr.2020.104297.

31. Gbadamosi SL, Nwulu NI, Sun Y. Multi-objective optimisation for composite generation and transmission expansion planning considering offshore wind power and feed-in tariffs. IET Renew Power Gen. 2018 Sep 20 [accessed 2022 Sep 12]; Vol. 12(14): p. 663 – 671. https://doi.org/10.1049/iet-rpg.2018.5531.

32. Ederer N. The price of rapid offshore wind expansion in the UK: Implications of a profitability assessment. Renew Energy. 2016 Jul [accessed 2022 Sep 12]; Vol. 92: p. 357 – 365. https://doi.org/10.1016/j.renene.2016.02.007.

33. Gaertner E, Rinker J, Sethuraman L, Zahle F, Anderson B, Barter G, Abbas N, Meng F, Bortolotti P, Skrzypinski W, et al. Definition of the IEA Wind 15-Megawatt Offshore Reference Wind Turbine. Golden (CO): National Renewable Energy Laboratory; 2020 Mar. https://www.nrel.gov/docs/fy20osti/75698.pdf.

34. Office of Energy Efficiency and Renewable Energy. 2018 Offshore Wind Technologies Market Report. Oak Ridge (TN): U.S. Department of Energy; 2019 Jul 30. https://www.energy.gov/eere/wind/downloads/2018-offshore-wind-market-report.

35. Schlensog C, Rubio O. Green Hydrogen: A Rising Star in the Energy Landscape. Siemens Energy; 2020 Dec 9.

36. Block Island Wind Farm. Power Technology; 2016 Dec 30 [accessed 2021 Aug 9]. https://www.power-technology.com/projects/block-island-wind-farm/.

37. NCEP GFS 0.25 Degree Global Forecast Grids Historical Archive. Research Data Archive at the National Center for Atmospheric Research, Computational and Information Systems Laboratory. National Centers for Environmental Prediction/National Weather Service/NOAA/US Department of Commerce; 2015 Jan 15 – 2020 Dec 16. [accessed 2020 Dec 18]. https://doi.org/10.5065/D65D8PWK.

38. National Renewable Energy Laboratory. Electricity Annual Technology Baseline, 2020. Golden (CO): U.S. Department of Energy; 2020.

39. Hou P, Zhu J, Ma K, Yang G, Hu W, Chen Z. A review of offshore wind farm layout optimization and electrical system design methods. J Mod Power Syst Cle. 2019 Sept; Vol. 7: p. 975-986. https://doi.org/10.1007/s40565-019-0550-5.

40. Hydrogen Council. Path to hydrogen competitiveness: A cost perspective. 2020 Jan 20 [accessed 2021 Aug 9]. https://hydrogencouncil.com/wp-content/uploads/2020/01/Path-to-Hydrogen-Competitiveness_Full-Study-1.pdf.

41. Felgenhauer M, Hamacher T. State-of-the-art of commercial electrolyzers and on-site hydrogen generation for logistic vehicles in South Caroline. Int J Hydrogen Energy. 2015 Feb 9; Vol. 40: p. 2084-2090. https://doi.org/10.1016/j.ijhydene.2014.12.043.

42. Amos WA. Costs of Storing and Transporting Hydrogen. Golden (CO): National Renewable Energy Laboratory; 1998 Nov. https://www.nrel.gov/docs/fy99osti/25106.pdf.

43. Wipke K, Sprik S, Kurtz J, Ramsden T, Ainscough C, Saur G. National Fuel Cell Electric Vehicle Learning Demonstration Final Report. Golden (CO): National

Renewable Energy Laboratory; 2012 Jul. https://www.nrel.gov/docs/fy12osti/54860.pdf.

44. CNSC Staff Presentation. Point Lepreau Nuclear Generating Station 2022 Licence Renewal: Commission Hearing Part 2. Canadian Nuclear Safety Commission; 2022 Jun 16. https://www.nuclearsafety.gc.ca/eng/the-commission/hearings/cmd/pdf/CMD22/CMD22-H2-C.pdf
45. SaskPower, Énergie NB Power, Bruce Power, Ontario Power Generation. Feasibility of Small Modular Reactor Deployment and Deployment in Canada. 2021 Mar.
46. Canadian Freight Analysis Framework. Ottawa (ON): Statistics Canada; 2011 – 2017 [updated 2020 May 14; accessed 2021 Jul 7]. https://www150.statcan.gc.ca/n1/pub/50-503-x/50-503-x2018001-eng.htm.
47. U.S. Department of Energy. Average Fuel Economy by Major Vehicle Category. 2020 Feb. https://afdc.energy.gov/data/10310.
48. Table 25-10-0055-01 Supply and disposition of natural gas, monthly (data in thousands) (x 1,000). Statistics Canada; 2016 Jan – 2021 Dec [accessed 2022 Jun 1]. https://doi.org/10.25318/2510005501-eng.
49. Kotowicz J, Wecel D, Jurczyk M. Analysis of component operation in power-to-gas-to-power installations. Appl Energy. 2018 Apr 15 [accessed 2021 Feb 24]: Vol. 216; p. 45-59. https://doi.org/10.1016/j.apenergy.2018.02.050.
50. Northwest Power and Conservation Council. Seventh Power Plan. 2016 Feb 25 [accessed 2021 Feb 24]. https://www.nwcouncil.org/reports/seventh-power-plan/.

51. Environmental Protection Agency. Renewable Energy Fact Sheet: Wind Turbines. 2013 Aug [accessed 2021 Feb 24]. https://www.epa.gov/sites/default/files/2019-08/documents/wind_turbines_fact_sheet_p100il8k.pdf.

52. How Long Do Wind Turbines Last? Can Their Lifetime Be Extended?. TWI; [accessed 2021 Jun 30]. https://www.twi-global.com/technical-knowledge/faqs/how-long-do-wind-turbines-last.

53. U.S. Department of Energy. Fuel Cells Fact Sheet. 2015 Nov [accessed 2021 Feb 24]. https://www.energy.gov/sites/prod/files/2015/11/f27/fcto_fuel_cells_fact_sheet.pdf.

54. Canada's Official Greenhouse Gas Inventory. Ottawa (ON): Government of Canada; [updated 2022 Apr 13; accessed 2022 Apr 20]. https://data.ec.gc.ca/data/substances/monitor/canada-s-official-greenhouse-gas-inventory/?lang=en.

55. Rosenfeld MJ. Cold Weather Can Play Havoc on Natural Gas Systems. Pipe Gas J. 2015 Jan; Vol. 242(1). https://pgjonline.com/magazine/2015/january-2015-vol-242-no-1/features/cold-weather-can-play-havoc-on-natural-gas-systems.

56. Daily Exchange Rates Lookup. Bank of Canada; 2022 Aug 4 [accessed 2022 Aug 5]. https://www.bankofcanada.ca/rates/exchange/daily-exchange-rates-lookup/?lookupPage=lookup_daily_exchange_rates_2017.php&startRange=2017-01-01&series%5B%5D=FXUSDCAD&lookupPage=lookup_daily_exchange_rates_2017.php&startRange=2017-01-01&rangeType=range&rangeValue=&dFrom=2022-08-04&dTo=2022-08-04&submit_button=Submit

57. Environment and Climate Change Canada. National Inventory Report 1990 – 2019: Greenhouse Gas Sources and Sinks in Canada. Gatineau (QC); 2021. https://publications.gc.ca/collections/collection_2021/eccc/En81-4-2019-1-eng.pdf.

58. Hydrogen Blending Project. Government of Alberta; [accessed 2021 Aug 9]. https://majorprojects.alberta.ca/details/Hydrogen-Blending-Project/4169.

59. Melaina MW, Antonia O, Penev M. Blending Hydrogen into Natural Gas Pipeline Networks: A Review of Key Issues. Golden (CO): National Renewable Energy Laboratory; 2013 Mar. https://www.nrel.gov/docs/fy13osti/51995.pdf.

60. National Energy Board. Reasons for Decision – Maritimes & Northeast Pipeline Management Ltd. MH-3-98. Detailed Route Hearings. Calgary (AB); 1998 Oct. https://publications.gc.ca/collections/Collection/NE22-1-1998-8E.pdf.

61. Pipeline Profiles: Maritimes & Northeast. Canada Energy Regulator; 2020 Jun [accessed 2021 Aug 9]. https://www.cer-rec.gc.ca/en/data-analysis/facilities-we-regulate/pipeline-profiles/natural-gas/pipeline-profiles-maritimes-northeast.html?=undefined&wbdisable=true.

62. Pembina Institute. Diesel Reduction Progress in Remote Communities: Research summary. 2020 Jul 6 [accessed 2022 Feb 1]. https://www.pembina.org/pub/diesel-reduction-progress-remote-communities.

63. Clean Energy for Rural and Remote Communities Program. Natural Resources Canada; [updated 2022 Apr 26; accessed 2022 Jul 15]. https://www.nrcan.gc.ca/reducingdiesel.

64. Clean Energy for Rural and Remote Communities funded projects. Natural Resources Canada; [updated 2022 Apr 26; accessed 2022 Jul 15].

https://www.nrcan.gc.ca/reducingdiesel/clean-energy-for-rural-and-remote-communities-funded-projects/22524.

65. Canada Launches Off-Diesel Initiative for Remote Indigenous Communities. Natural Resources Canada; 2019 Feb 13 [accessed 2022 Feb 1]. https://www.canada.ca/en/natural-resources-canada/news/2019/02/canada-launches-off-diesel-initiative-for-remote-indigenous-communities.html.

66. The Atlas of Canada – Remote Communities Energy Database. Natural Resources Canada; [updated 2018 Aug 3; accessed 2022 Feb 1]. https://atlas.gc.ca/rced-bdece/en/index.html.

67. Yao R, Steemers K. A method of formulating energy load profile for domestic buildings in the UK. Energy Build. 2005 Jun [accessed 2022 Jul 13]; Vol. 37(6): p. 663 – 671. https://doi.org/10.1016/j.enbuild.2004.09.007.

68. Proedrou E. A Comprehensive Review of Residential Electricity Load Profile Models. IEEE Access. 2021 Jan 8 [accessed 2022 Jul 26]; Vol. 9: p. 12114-12133. https://doi.org/10.1109/ACCESS.2021.3050074.

69. Fischer D, Wolf T, Scherer J, Wille-Haussmann B. A stochastic bottom-up model for space heating and domestic hot water load profiles for German households. Energy Build. 2016 Jul 15 [accessed 2022 July 26]: Vol. 125; p. 120-128. https://doi.org/10.1016/j.enbuild.2016.04.069.

70. Bouvenot J, Latour B, Flament B, Siroux M. High resolution stochastic generator of European household specific electricity demand load curves for decentralized power self-production applications. Energy Build. 2020 Dec 15 [accessed 2022 Jul 26]: Vol. 229. https://doi.org/10.1016/j.enbuild.2020.110480.

71. Flett G, Kelly N. Modelling of individual domestic occupancy and energy behaviours using existing datasets and probabilistic modelling methods. Energy Build. 2021 Dec 1 [accessed 2022 Jul 26]: Vol. 252. https://doi.org/10.1016/j.enbuild.2021.111373.

72. Maria ED, Secchi M, Macil D. A Flexible Top-Down Data Driven Stochastic Model for Synthetic Load Profiles Generation. Energies. 2021 Dec 31 [accessed 2022 Jul 26]: Vol. 15(1). https://doi.org/10.3390/en15010269.

73. Quitoras MR, Campana PE, Rowley P, Crawford C. Remote community integrated energy system optimization including building enclosure improvements and quantitative energy trilemma metrics. Appl Energy. 2020 Oct 15 [accessed 2022 Jul 10]: Vol. 276. https://doi.org/10.1016/j.apenergy.2020.115017.

74. Hendron R, Burch J. Development of standardized domestic hot water event schedules for residential buildings. Energy Sustainability 2007; 2007 Jul 27-30; Long Beach (CA). National Renewable Energy Laboratory; 2008 Aug [accessed 2022 Jul 10]. https://www.nrel.gov/docs/fy08osti/40874.pdf.

75. Sachs Harbour: Community Information. Yellowknife (NT): Arctic Energy Alliance; [accessed 2022 Jul 13]. https://aea.nt.ca/communities/sachs-harbour/.

76. Campana PE, Quan SJ, Robbio FI, Lundblad A, Zhang Y, Ma T, Karlsson B, Yan J. Optimization of a residential district with special consideration on energy and water reliability. Appl Energy. 2017 May 15 [accessed 2022 Jul 13]: Vol. 194; p. 751-764. https://doi.org/10.1016/j.apenergy.2016.10.005.

77. Hazelton J, Jordan J, Dedman S, Logan N. Renewable Energy in Nunavut - Scoping Analysis. 2019 Sep [accessed 2022 Jun 15]. http://dx.doi.org/10.13140/RG.2.2.32946.43203.

78. Prototype Building Models. Office of Energy Efficient & Renewable Energy; [accessed 2022 Feb 1]. https://www.energycodes.gov/prototype-building-models.

79. Pfenninger S, Staffel I. Long-term patterns of European PV output using 30 years of validated hourly reanalysis and satellite data. Energy. 2016 Nov 1 [accessed 2022 Jan 27]: Vol. 114; p. 1251 – 1265. https://dx.doi.org/10.1016/j.energy.2016.08.060.

80. Staffel I, Pfenninger S. Using Bias-Corrected Reanalysis to Simulate Current and Future Wind Power Output. Energy. 2016 Nov [accessed 2022 Jan 27]: Vol. 114; p. 1224 – 1239. https://dx.doi.org/10.1016/j.energy.2016.08.068.

81. Deforest N, Cardoso G, Brouhard T, &USDOE. Distributed Energy Resources Customer Adoption Model (DER-CAM) version 2.5.1. Berkeley (CA): Grid integration group: Energy technologies area: DER-CAM. Berkeley National Laboratory (LBL); October 2018 [accessed 2021 Feb 1]. doi:10.11578/dc.20181016.2.9. https://gridintegration.lbl.gov/der-cam.

82. Google earth pro version 7.3.4.8642. Aupaluk (QC); 2021 Jul 6 [accessed 2021 Oct 14]. 59° 18’ 10.86” N, 69° 36’ 09.39” W, Eye alt 801 meters. CNES / Airbus 2022. https://www.google.com/earth/versions/.

83. Aupaluk Community Basemap. Kativik Regional Government; 2021 Jan 1 [accessed 2021 Oct 14]. https://www.krg.ca/en-CA/map/community-maps.

84. Aupaluk land use designations and zoning. Kativik Regional Government; 2011 Feb [accessed 2021 Oct 14]. https://www.krg.ca/en-CA/map/community-maps.

85. Aupaluk. Overflight Stock; [accessed 2021 Oct 14]. https://www.overflightstock.com/?search=Aupaluk&gallery=a58e27a0-7b4f-4993-b40a-477ffd23cb92&media_type=.

86. Standing Senate Committee on Energy, the Environment and Natural Resources. Powering Canada's Territories. Ottawa (ON): Second Session, Forty-first Parliament; 2015 Jun 15 [accessed 2021 Sep 20]. https://publications.gc.ca/collections/collection_2015/sen/yc26-0/YC26-0-412-14-eng.pdf.

87. Communities. Arctic Energy Alliance; [accessed 2022 Sep 1]. https://aea.nt.ca/communities/.

88. Meng C, Liu E, Neiswanger W, Song J, Burke M, Lobell D, Ermon S. IS-Count: Large-Scale Object Counting from Satellite Images with Covariate-Based Importance Sampling. Proceedings of the 36th AAAI Conference on Artificial Intelligence. 2022 Jun 28 [accessed 2022 Sep 12]. https://doi.org/10.1609/aaai.v36i11.21462.

89. Yan X, Ai T, Yang M, Yin H. A graph convolutional neural network for classification of building patterns using spatial vector data. ISPRS J Photogramm Remote Sens. 2019 Apr [accessed 2022 Sep 2]; Vol. 150: p. 259 – 273. https://doi.org/10.1016/j.isprsjprs.2019.02.010.

90. Renewable energy for the North. Ottawa (ON): CanmetENERGY; 2021 Apr 7 [accessed 2021 Sep 20]. https://www.nrcan.gc.ca/energy/offices-

labs/canmet/ottawa-research-centre/northern-and-remote-energy/renewable-energy-for-the-north/23559.

91. Hanna R, Ghonima M, Kleissl J, Tynan G, Victor DG. Evaluating business models for microgrids: Interactions of technology and policy. Energ Pol. 2017 Apr [accessed 2021 Sep 8]; Vol. 103: p. 47 – 61. https://doi.org/10.1016/j.enpol.2017.01.010.

92. Jung J, Villaran M. Optimal planning and design of hybrid renewable energy systems for microgrids. Renew Sustain Energy Rev. 2017 Aug [accessed 2022 Aug 2]; Vol. 75: p. 180 – 191. https://doi.org/10.1016/j.rser.2016.10.061.

93. Optimize the value of your hybrid power system-from utility-scale and distributed generation to standalone microgrids. Boulder (CO): UL Solutions; [accessed 2022 Aug 2]. https://www.homerenergy.com/.

94. Li B, Li J. Sizing and operation of a pure renewable energy based electric system through hydrogen. Energy Reports. 2022 Apr [accessed 2022 Aug 2]; Vol. 8(1): p. 1391 – 1403. https://doi.org/10.1016/j.egyr.2021.11.276.

95. Maheri A, Unsal I, Mahian O. Multiobjective optimisation of hybrid wind-PV-battery-fuel cell-electrolyser-diesel systems: An integrated configuration-size formulation approach. Energy. 2022 Feb 15 [accessed 2022 Aug 2]; Vol. 241. https://doi.org/10.1016/j.energy.2021.122825.

96. Canadian Climate Normals. Ottawa (ON): Government of Canada; [updated 2022 May 25; accessed 2022 Aug 2]. https://climate.weather.gc.ca/climate_normals/index_e.html.

97. Natural Resources Canada. RETScreen Expert version 8.1.2.13. 2021 [accessed 2022 Feb 1]. https://www.nrcan.gc.ca/maps-tools-and-publications/tools/modelling-tools/retscreen/7465.

98. Lampert D, Cai H, Wang Z, Wu M, Han J, Dunn J, Sullivan J, Elgowainy A, Wang M, Keisman J. Development of a Life Cycle Inventory of Water Consumption Associated with the Production of Transportation Fuels. Argonne (IL): Argonne National Laboratory; 2015 Oct [accessed 2022 Jul 1]. https://publications.anl.gov/anlpubs/2015/10/121551.pdf.

99. Our Petro-Canada rack pricing. Petro-Canada; 2022 Jun 7 [accessed 2022 Jun 7]. https://www.petro-canada.ca/en/business/rack-prices#intra-day.

100. Canadian Small Modular Reactor Roadmap Steering Committee. A Call to Action: A Canadian Roadmap for Small Modular Reactors. Ottawa (ON); 2018 Nov [accessed 2022 Sep 12]. https://smrroadmap.ca/wp-content/uploads/2018/11/SMRroadmap_EN_nov6_Web-1.pdf?x64773.

101. Urban R. Electricity Prices in Canada 2021. Energyhub.org; 2020 Feb 14 [updated 2021 Mar 11; accessed 2022 Aug 3]. https://www.energyhub.org/electricity-prices/.

102. Archer CL, Mirzaeisefat S, Lee S. Quantifying the sensitivity of wind farm performance to array layout options using large-eddy simulation. Geophys Res Lett. 2013 Aug 29 [accessed 2021 Jan 26]; Vol. 40(18): p. 4963 – 4970. https://doi.org/10.1002/grl.50911.

103. HALIFAX CLIMATE. Climate-Data.org; [accessed 2021 Jan 26]. https://en.climate-data.org/north-america/canada/nova-scotia/halifax-129/.

104. World Meteorological Organization. Guide to Instruments and Methods of Observation Volume I – Measuerment of Meteorological Variables. Geneva (Switzerland); 2018. Annex. The Effective Roughness Length; p. 210-211. https://library.wmo.int/index.php?id=12407&lvl=notice_display#.YuLlmnbMKbg.

105. Kilpatrick R. Effect of Cold Climate on Wind Energy Production in Canada. Ottawa (ON): Natural Resources Canada's CanmetENERGY; 2017 May [accessed 2021 Feb 1]. https://www.nrcan.gc.ca/sites/www.nrcan.gc.ca/files/canmetenergy/pdf/Effect-of-Cold-Climate-on%20Wind-Energy-Production-in-Canada_access.pdf.

106. Earth Atmosphere Model. National Aeronautics and Space Administration; [accessed 2021 Jun 24]. https://www.grc.nasa.gov/www/k-12/airplane/atmosmet.html.

107. Government of Canada. Electricity and Gas Inspection Regulations (SOR/86-131). 2018 Nov 23 [accessed 2021 Apr 20]. https://laws.justice.gc.ca/eng/regulations/SOR-86-131/page-1.html#h-891035.

108. Isothermal Properties for Hydrogen. National Institute of Standards and Technology; 2021 [accessed 2021 Apr 20]. https://webbook.nist.gov/cgi/fluid.cgi?T=15&PLow=0&PHigh=1&PInc=.101325&Applet=on&Digits=5&ID=C1333740&Action=Load&Type=IsoTherm&TUnit=C&PUnit=MPa&DUnit=kg%2Fm3&HUnit=kJ%2Fkg&WUnit=m%2Fs&VisUnit=Pa*s&STUnit=N%2Fm&RefState=DEF.

109. U.S. Department of Energy. Alternative Fuels Data Center Fuel Properties Comparison. 2021 Jan [accessed 2022 Apr 1]. https://afdc.energy.gov/files/u/publication/fuel_comparison_chart.pdf.

110. Compressed Natural Gas (CNG). Unitrove; [accessed 2021 Jun 20]. https://www.unitrove.com/engineering/gas-technology/compressed-natural-gas.

111. The Climate Registry. 2020 Default Emission Factors. Los Angeles (CA): 2020 Apr [accessed 2021 Jul 28]. https://www.theclimateregistry.org/wp-content/uploads/2020/04/The-Climate-Registry-2020-Default-Emission-Factor-Document.pdf.

112. U.S. Energy Information Administration. Table 8.1. Average Operating Heat Rate for Selected Energy Sources. [accessed 2021 Jul 25]. https://www.eia.gov/electricity/annual/html/epa_08_01.html.

113. Wiltsee G. Lessons Learned from Existing Biomass Power Plants. Golden (CO): National Renewable Energy Laboratory; 2000 Feb [accessed 2021 Jul 25]. https://www.nrel.gov/docs/fy00osti/26946.pdf.

114. Environment and Climate Change Canada. Technical Update to Environment and Climate Change Canada's Social Cost of Greenhouse Gas Estimates. Gatineau (QC); 2016 Mar [accessed 2021 Feb 24]. https://publications.gc.ca/collections/collection_2016/eccc/En14-202-2016-eng.pdf.

115. Wilson C, Grubler A, Bento N, Healey S, De Stercke S, Zimm C. Granular technologies to accelerate decarbonization. Science. 2020 Apr 3 [accessed 2021 Feb 24]; Vol. 368(6486): p. 36-39. https://doi.org/10.1126/science.aaz8060.

116. Palisade. @Risk for Risk Analysis Version 8.2. [accessed 2022 May 1]. https://www.palisade.com/risk/.

117. Map. Maritimes & Northeast Pipeline; [accessed 2021 Jul 5]. https://mnpp.com/canada/map.

118. Table 12-10-0011-01 International merchandise trade for all countries and by Principal Trading Partners, monthly (x 1,000,000). Statistics Canada; 2021 Jan – 2022 Dec [accessed 2022 Jul 6]. https://doi.org/10.25318/1210001101-eng.

119. Oil-fired furnaces. Natural Resources Canada; [updated 2021 May 10; accessed 2022 Jun 10]. https://www.nrcan.gc.ca/energy-efficiency/energy-efficiency-regulations/guide-canadas-energy-efficiency-regulations/oil-fired-furnaces/6887.

120. Lazard. Lazard's Levelized Cost of Hydrogen Analysis – Version 2.0. 2021 Oct [accessed 2022 Feb 1]. https://www.lazard.com/media/451922/lazards-levelized-cost-of-hydrogen-analysis-version-20-vf.pdf.

121. DOE Technical Targets for Hydrogen Production from Electrolysis. Office of Energy Efficiency & Renewable Energy; [accessed 2022 Feb 1]. https://www.energy.gov/eere/fuelcells/doe-technical-targets-hydrogen-production-electrolysis.

122. National Renewable Energy Laboratory. Electricity Annual Technology Baseline, 2021. Golden (CO): U.S. Department of Energy; 2021. https://atb.nrel.gov/electricity/2021/data.

Appendix A. Supporting information for Chapter 2

A.1. Data inputs for simulating wind turbine performance

The model used for simulating the performance data discussed within this paper was compiled and run using MATLAB code developed by the authors. Table A.1 below contains the specific inputs used to obtain this report's dataset. Some of the inputs are pre-defined based on the type and location of the wind turbines, while others are set by the authors.

Table A.1. List of variables used in the model for simulating wind turbine performance.

Description	Variable	Value	Reference
Annual project growth rate	G	25%, 30%, 36%	[22]
Area swept by blades	A	45,239 m^2	
Array losses	L_{array}	0%, 5%, 10%	[102]
Auxiliary loads	L_{aux}	5%, 10%	Authors
Average monthly temperatures			[103]
January	T_{jan}	-4.9 °C	
February	T_{feb}	-5.0 °C	
March	T_{mar}	-1.1 °C	
April	T_{apr}	4.0 °C	
May	T_{may}	9.3 °C	
June	T_{jun}	14.4 °C	
July	T_{jul}	17.9 °C	
August	T_{aug}	18 °C	
September	T_{sep}	14.2 °C	
October	T_{oct}	9.1 °C	
November	T_{nov}	3.9 °C	
December	T_{dec}	-2.2 °C	
Blade radius	R	120 m	[33]
Cut-in speed	C_{in}		[33]
Cut-out speed	C_{out}		[33]

Description	Variable	Value	Reference
Hub height	h_{hub}	150 m	[33]
Natural gas consumption			[48]
Number of starting turbines	$TN_i(i = 1)$	1, 5	Authors
Start year	i_{start}	2025	Authors
Surface roughness	z	0.005 m	[104]
Total summer climate losses	L_s	0.0559 GWh / (Installed MW)	[105]
Total turbines	TN_{max}		Authors
Total winter climate losses	L_w	0.2436 GWh / (Installed MW)	[105]
Wind data			[37]

Employing these inputs, the model simulates electrical output from the turbine array, the number of electrolyzers needed, the amount of hydrogen produced, and the amount of liquid or gaseous fuel consumption in the Maritimes that could be substituted for each month from start to end (this is omitted for scenario γ). The simulation is run for 36 cases. Table A.2 below lists these 36 cases, each of which is run monthly from the start (2025) to the end year. The end year depends on the scenario and allows the IES to scale up to the size required to achieve its objective. These are run for each of the five scenarios.

Table A.2. Model runs represent a range of deployment ambition and technical performance.

Case number	No. of starting turbines	Growth rate (%)	Auxiliary losses (%)	Array losses (%)
1	1	25	5	0
2	1	25	5	5
3	1	25	5	10
4	1	25	10	0
5	1	25	10	5
6	1	25	10	10

Case number	No. of starting turbines	Growth rate (%)	Auxiliary losses (%)	Array losses (%)
7	1	30	5	0
8	1	30	5	5
9	1	30	5	10
10	1	30	10	0
11	1	30	10	5
12	1	30	10	10
13	1	36	5	0
14	1	36	5	5
15	1	36	5	10
16	1	36	10	0
17	1	36	10	5
18	1	36	10	10
19	5	25	5	0
20	5	25	5	5
21	5	25	5	10
22	5	25	10	0
23	5	25	10	5
24	5	25	10	10
25	5	30	5	0
26	5	30	5	5
27	5	30	5	10
28	5	30	10	0
29	5	30	10	5
30	5	30	10	10
31	5	36	5	0
32	5	36	5	5
33	5	36	5	10
34	5	36	10	0
35	5	36	10	5
36	5	36	10	10

A.2. Model schematics

Table A.3. Five scenarios are investigated in this research effort.

Scenario	Description
α	IES meets **monthly** energy demand served by natural gas. Monthly demand is the most granular data available. U.S. market absorbs excess hydrogen.
β_{tot}	IES meets **total annual** energy demand served by natural gas. This entails investments in storage and compression capacity.
β_{ind}	IES meets the **industrial sector's annual** energy demand that is served by natural gas. This entails investments in storage and compression capacity.
γ	IES feeds **electricity** into the grid through subsea cables. OSW farm sized to replace fossil generation, including sufficient electrolysis and hydrogen storage to provide the grid with two-weeks' worth of OSW output through fuel cells.
δ	IES meets the **freight transportation sector's annual demand** for hydrogen, but only for freight miles traveled within the region.

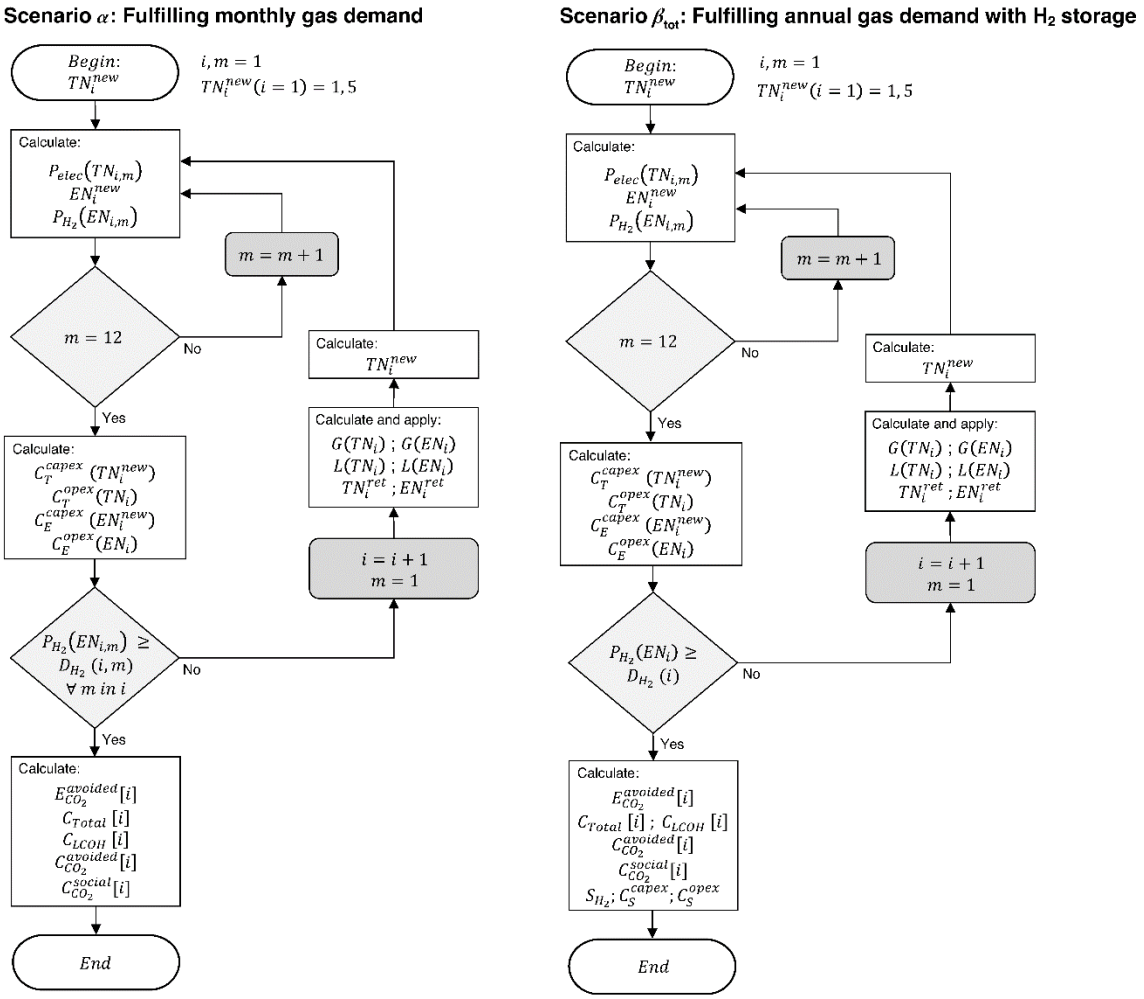

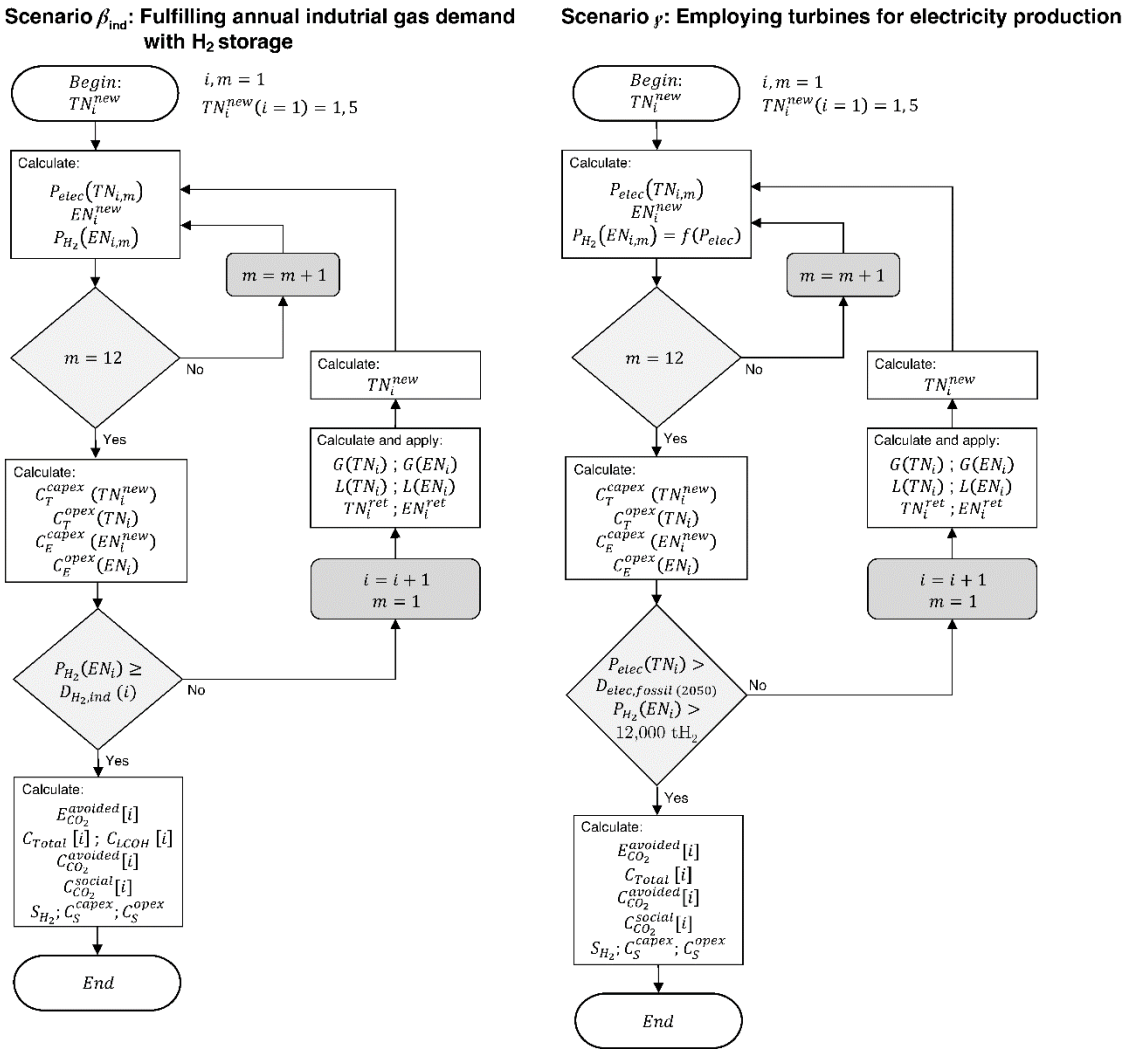

Figure A.1. Schematics outlining how the recursive simulation proceeds in the scenarios under investigation.

A.3. Total number of offshore wind turbines

The total number of offshore wind turbines required to achieve scenario objectives changes depending on the scenario. Each of the five scenarios is run assuming two separate turbine performance profiles, one that simulates maximum (or best) performance and one that simulates minimum (or worst) performance. The maximum performance cases require fewer total turbines due to the higher performance output and vice versa. For scenario α, 388 or 456 turbines are needed to surpass each month's hydrogen demand depending on performance. Scenario β_{tot} requires 310 or 364 to satisfy the annual demand of hydrogen. Scenario β_{ind} requires 209 or 246 turbines to satisfy the annual demand of hydrogen for industry. To replace fossil fueled generation in the Maritimes under the Canada Energy Regulator's "Reference" scenario, scenario γ requires 73 or 86 turbines. Replacing the annual commercial transportation diesel usage in scenario δ requires 12,983 or 15,278 turbines.

A.4. Completion years for each scenario

The table below shows the date range when each scenario could expect to be completed.

Table A.4. Range of completion dates for each scenario, including the cases that begin with 5 starting turbines rather than just 1 starting turbine.

Scenario	Range of completion dates
α	2051 - 2066
β_{tot}	2049 - 2065
β_{ind}	2047 – 2061
γ	2041 – 2052
δ	2070 - 2095

A.5. Wind speed data

The simulated wind speed data used in this investigation come from the National Center for Atmospheric Research's (NCAR) Global Forecast System (GFS) database [37]. Wind speed data are provided at a hub height of 100m, in 6-hour intervals, over the period 2015 to 2020. The wind speed data are for a point on the Scotian shelf—approximately above the Maritimes and Northeast Pipeline (M&NP)—located 44° N and 61° W. We assume that all turbines constituting a wind farm centered on these coordinates would experience similar wind speeds. Using equation (A.1) below, we extrapolate these wind speeds to wind speeds at a hub height of 150 m, which is the hub height of the International Energy Agency's (IEA) 15MW$_e$ offshore reference turbine that is used in this research:

$$V_w^{hub} = V_w^{100m} \times \frac{\ln\left(\frac{h_{hub}}{z}\right)}{\ln\left(\frac{h_{100\,m}}{z}\right)} \tag{A.1}$$

where, V_w^{100m} is the wind speed at 100 m, h_{hub} is the hub height of 150 m, $h_{100\,m}$ is the height at 100 m, and z is the surface roughness. Since these turbines are located offshore, the surface roughness for open sea is typically 0.0002 m [104]. In this model, it is set to a conservative value of 0.005 m to account for rough waters, islands, and shipping boat traffic. The wind speed data from each month over the 6-year span are then converted into the percentages of wind speeds for an average day of each month. Wind speeds range from 0 to 35 m/s.

A.6. Electrical production of array

The turbine used in this research is the International Energy Agency's (IEA) 15 MWe offshore reference turbine [33] and its hub height, h_{hub}, along with the average monthly temperatures, T_m, in Halifax, Nova Scotia [103] are used to estimate the air density at the hub, ρ_{air}^{hub}. This is done by applying the equations below [106]:

$$T_{air}^{hub} = 15.04 - (0.00649 \times h_{hub}) \tag{A.2}$$

$$P_{air}^{hub} = 101290 \times \left(\frac{T_{air}^{hub} + 273.15}{288.08}\right)^{5.256} \tag{A.3}$$

$$\rho_{air}^{hub} = \frac{P_{air}^{hub}}{[286.9 \times (T_m - (0.00649 \times h_{hub}) + 273.15)]} \tag{A.4}$$

Equation (A.2) and Equation (A.3) calculate the temperature, T_{air}^{hub}, and pressure, P_{air}^{hub}, at the hub height, respectively, assuming that sea level is at standard temperature and pressure conditions [107]. Equation (A.4) is the ideal gas law formula and takes the average monthly temperatures into account.

The model takes the wind data, the coefficient of performance table (C_p) of the reference turbine, the density of the air, the area swept by the blades, and the auxiliary loads, and uses these to calculate the net turbine electrical production, P_{elec}^{net}. The raw electrical production, P_{elec}^{raw}, of a single turbine is first calculated using equation (A.5) below:

$$P_{elec}^{raw} = \sum_{C_{in}}^{C_{out}} C_p \times \left(\frac{1}{2}\rho_{air}^{hub} \times A \times {V_w^{hub}}^3\right) \times (w \times 24) \tag{A.5}$$

where C_{out} is the cut-out speed, C_{in} is the cut-in speed, C_p is the coefficient of performance for the turbine at a specific wind speed, ρ_{air}^{hub} is the density of the air at the

hub, A is the area swept by the blades, V_w^{hub} is the velocity of the wind, and w is the percentage of time in a day that a specific wind speed occurs. The raw power output is reduced by the auxiliary loads and average climate losses for both winter and summer climates [105]. The equations used for calculating the net electrical production of a single turbine, P_{elec}^{net}, for both winter and summer climates respectively are:

$$P_{elec}^{net} = [P_{elec}^{raw} \times (1 - L_{aux})] - \frac{(L_w \times 15)}{6} \tag{A.6}$$

$$P_{elec}^{net} = [P_{elec}^{raw} \times (1 - L_{aux})] - \frac{(L_s \times 15)}{6} \tag{A.7}$$

where L_{aux} is the percentage of auxiliary load the turbine experiences, L_w are the losses associated with winter, and L_s are the losses associated with the summer. The climate losses are evenly split into the 6 months they affect with November to April constituting the winter months and May to October constituting the summer months. To calculate the electrical production of the entire array, P_{elec}^{array}, the following equation is used:

$$P_{elec}^{array} = P_{elec}^{net} \times TN_i \times (1 - L_{array}) \tag{A.8}$$

where TN_i is the number of turbines in year i and L_{array} refers to the losses associated with the array arrangement of the turbines. From here, the average monthly power outputs for a single turbine can estimated by multiplying the P_{elec}^{array} value for a given month by the number of days in that month.

Due to the vast size of the Scotian shelf, it is likely that array losses could be minimized: inter-array distances can be increased to achieve minimal array losses of 0% to 10%, unless other social, economic, and political constraints intrude, which is possible. Constraints most often manifest in concerns regarding other marine interests and

aesthetics; our choice of location reduces these. For example, many of the turbines would not be visible from shore.

Ignoring socio-technical constraints, array losses can be minimized by staggering the turbines, specifically by spacing them out parallel to the direction of wind by more than 6.4 times the rotor diameter and spacing them out perpendicular to the direction of the wind by at least 4.3 times the rotor diameter [102].

A.7. Annual project growth rates

To calculate the array electrical production, the value of a single turbine's net power generation in year i is multiplied by the number of turbines in year i. The number of turbines in any given year but the first is determined by the annual project growth rate. The growth rate equation is as follows:

$$TN_{i+1} = (G \times TN_i) \times \left(1 - \frac{TN_i}{TN_{max}}\right) + TN_i \tag{A.9}$$

where TN_{i+1} is the number of turbines in year $i + 1$, G is the growth rate, TN_i is the number of turbines for year i, and TN_{max} is the maximum number of turbines for each scenario, in accordance with section A.3.

A.8. Electrolyzers

The electrolyzers used in this research are based on a commercial offering by Siemens, the Silyzer 300, which has a power demand of 17.5 MW and a production rate of 335 kg of hydrogen per hour [35]. We assume the electrolyzers operate at 80% capacity factors. The number of electrolyzers is calculated monthly and depends on the average hourly array electrical production. This assumes that for any given monthly array electrical production, each hour of that month produces the same amount as the next. While this is not ideal, this helps estimate the number of electrolyzers needed to keep up with the array. The required number needed is calculated using the following equation:

$$EN_{i,m} = \frac{P_{elec}^{array}}{d_m \times 24 \times 17.5 \times 0.8} \tag{A.10}$$

where E is the number of electrolyzers needed per hour on an average day and d_m is the number of days in a particular month, m. This is calculated monthly and the number of electrolyzers needed in any given year is reported based on the month that requires the largest number of electrolyzers to process array power into hydrogen. (This month is usually December.) This ensures sufficient annual electrolysis capacity. The average daily hydrogen output of each of these electrolyzers can then be estimated as follows:

$$P_{H_2}^{kg} = EN_{i,12} \times (355 \times 24) \times 0.8 \tag{A.11}$$

Using the specific volume at standard temperature and pressure [108], the average daily volumetric output of hydrogen can then be calculated:

$$P_{H_2}^{m^3} = P_{H_2}^{kg} \times 11.736 \tag{A.12}$$

To calculate the volume of hydrogen that would provide the same amount of energy per volume of natural gas or diesel, the ratios of the lower heating values (LHV) are used [109]. For scenario δ, this is done by taking the LHV of hydrogen and dividing it by the LHV of diesel. The LHV of hydrogen and diesel are 10,224 kJ/m^3 and 35,811,696 kJ/m^3, respectively so the following equation looks like:

$$D_{supp} = P_{H_2}^{m^3} \times \frac{10{,}224}{35{,}811{,}696} \tag{A.13}$$

For all other scenarios, the LHV ratio of hydrogen to natural gas is used. Due to natural gas having a variety of compositions, the density was assumed to be 0.7 kg/m^3, which is typical and fits within the range of densities for natural gas [110] and leads to a LHV of 32,825 kJ/m^3. The equation used is:

$$NG_{supp} = P_{H_2}^{m^3} \times \frac{10{,}224}{32{,}825} \tag{A.14}$$

A.9. Estimating avoided emissions

In scenarios α, β_{tot}, and β_{ind}, the emissions avoided by the hydrogen option are found by taking the amount of natural gas that is substituted with hydrogen and multiplying that by the emission factor of natural gas in the Maritimes, which is 1921 gCO_2/m^3 NG [54]. The resulting value represents the total amount of CO_2 that would be avoided by substituting natural gas with this hydrogen regardless of when the hydrogen is used (i.e., it might be stored or exported). This is done for each month from the start year to the end year and is reported per year.

In scenario γ, we estimate the annual emissions from fossil fuel generators in the Maritimes up to 2065. We use data from the Canada Energy Regulator's (CER) Reference scenario [11] to compile projections of the amount of electricity that is generated by each source up to 2050. Beyond 2050, we assume that the electricity generation mix remains the same in the absence of further federal projections. The Reference scenario assumes that the share of carbon-intensive electric power generation declines over time, but this decline is not as aggressive as it is in CER's Evolving scenario. The Reference scenario thus represents a hypothetical Canada that does not aggressively pursue its net-zero targets, but muddles through to lower carbon intensities as technology improves and the cost of low-carbon generation falls further.

The goal of the offshore wind farm in scenario γ is to replace the maximum share of electric power generation that comes from fossil fuel resources in the time period under investigation. We consider coal/coke, natural gas, oil, and biomass to be carbon-intensive resources. Each source's emission factor and heat content are taken from both The Climate Registry [111] and Canada's annual Greenhouse Gas Inventory [54], and

generator heat rates are extracted from the U.S. Energy Information Administration (EIA) and the National Renewable Energy Laboratory (NREL) [112, 113]. The estimated amount of CO_2 emitted annually from each source, EM_s, is found using the equation below:

$$EM_s = \frac{Elec_s \times \frac{HR_s}{HC_s} \times EF_s}{1000} \tag{A.15}$$

where $Elec_s$ is the annual amount of electricity generated from that source in a year, HR_s is the generator heat rate, HC_s is the heat content of the fuel, and EF_s is the emission factor for source s. The result corresponds to the maximum amount of emissions that could be avoided from that source in that year. We prioritize the replacement of fossil generators in their expected order of prevalence in 2025, replacing coal first then natural gas, oil, and biomass. The amount of CO_2 avoided, EM_{avoid}, is then calculated using the following equation:

$$E_{CO_2}^{avoided} = \begin{cases} \frac{P_{elec}^{annual} \times \frac{HR_c}{HC_c} \times EF_c}{1000} & P_{elec}^{annual} < Elec_c \\ \frac{(P_{elec}^{annual} - Elec_c) \times \frac{HR_{ng}}{HC_{ng}} \times EF_{ng}}{1000} + EM_c & P_{elec}^{annual} < Elec_c + Elec_{ng} \\ \frac{\left(P_{elec}^{annual} - Elec_c - Elec_{ng}\right) \times \frac{HR_o}{HC_o} \times EF_o}{1000} + EM_c + EM_{ng} & P_{elec}^{annual} < Elec_c + Elec_{ng} + Elec_o \\ \frac{\left(P_{elec}^{annual} - Elec_c - Elec_{ng} - Elec_o\right) \times \frac{HR_b}{HC_b} \times EF_b}{1000} + EM_c + EM_{ng} + EM_o & P_{elec}^{annual} < Elec_s^{annual} \\ EM_s^{total} & P_{elec}^{annual} \geq Elec_s^{annual} \end{cases} \tag{A.16}$$

where P_{elec}^{annual} is the annual amount of electricity produced by the turbine array, EM_s^{total} is the total amount of emissions generated by carbon-intensive sources, $Elec_s^{annual}$ is the annual electricity generated by carbon-intensive sources, and HR, HC, EF, and $elec$ are the heat rate, heat content, emission factor, and generated electricity for coal (c), natural gas (ng), oil (o), and biomass (b). We compare the emissions avoided by our wind farm

with the total amount of CO_2 emitted by the Maritimes using data provided by Environment and Climate Change Canada and stretching from 2014 to 2020. The 2019 values for Nova Scotia, New Brunswick, and Prince Edward Island are added to generate estimates of total emissions from the Maritimes, which are approximately 30 million metric tons of CO_2 [54]. These emissions are expected to decline every year in CER's Reference scenario [11].

For scenario δ, the emission reductions are calculated by converting the amount of generated hydrogen to the diesel equivalent. The amount of diesel that is replaced is then multiplied by the emission factor of diesel, which is 2,680,500 gCO_2/m^3 diesel [54].

A.10. Reporting upper and lower bounds

Instead of reporting results for each of the 36 scenarios in the manuscript, we take the best and worst performing cases as indicative of the upper and lower bounds, respectively. Given the centrality of growth rates to our analysis, we report the upper and lower bounds for each of the three different growth rates. This reduces the number of cases to 8 while faithfully summarizing the full range of results.

Table A.5. Summary of upper and lower bound scenarios for which results are reported in the manuscript

Number of Starting Turbines	Growth Rate (%)	Auxiliary Losses (%)	Array Losses (%)
1	25	5	0
1	25	10	10
1	36	5	0
1	36	10	10
5	25	5	0
5	25	10	10
5	36	5	0
5	36	10	10

A.11. Cost estimation

Nine categories of costs are considered in this techno-economic analysis, as summarized in Table A.6 below. Some costs are relevant only fir some scenarios.

Table A.6. Nine costs are considered in this techno-economic analysis

Cost group	Cost	Relevant scenarios	Reference
Turbine costs	CAPEX	α, β_{tot}, β_{ind}, γ, δ	[38]
	FO&M	α, β_{tot}, β_{ind}, γ, δ	
Electrolyzer costs	CAPEX	α, β_{tot}, β_{ind}, γ, δ	[40, 41, 49]
	FO&M	α, β_{tot}, β_{ind}, γ, δ	
Storage costs	Compressor CAPEX	β_{tot}, β_{ind}, γ, δ	[42]
	Conditioning	β_{tot}, β_{ind}, γ, δ	
	Cavern storage CAPEX	β_{tot}, β_{ind}, γ, δ	
Social cost of carbon		α, β_{tot}, β_{ind}, γ, δ	[114]
Discount rate		α, β_{tot}, β_{ind}, γ, δ	[50]

This model incorporates declining prices for the turbines and electrolyzers to account for technological learning, also known as learning economies. Storage costs remain the same regardless of year: the storage cavern comprises a one-time purchase, though storage might first become necessary at different years in different scenarios. The social cost of carbon is taken to be a step-function, increasing every 5 years. The values of the step function are taken from [114].

These costs all have a lower, middle, and upper value, except for storage costs. In addition, both project growth rate and turbine performance could take a lower, middle, or upper value. The number of starting turbines can only be changed between its low and high value. These changes introduce many different possible scenarios that affect the total cost, cost of H_2, cost of CO_2 abatement, and total emission reductions. The values

listed in Table A.7 below are the range of values for the first year as some values change as the years progress.

Table A.7. Input data used in this analysis

Input	Unit	Lower	Middle	Upper	Reference
Annual project growth rate		25%	30%	36%	[22]
Turbine performance	GWh	71.5		75.7	Model
Turbine CAPEX[a]	USD/kW	$3172.54	$3774.80	$5459.65	[38]
Turbine FO&M[a]	USD/kWyr	$58.26	$68.40	$95.28	
Electrolyzer CAPEX[a]	USD/kW	$500	$2000	$6500	[40, 41, 49]
Electrolyzer FO&M[a]	USD/kWyr	$14.25	$57	$360	[40, 41, 49]
Discount rate	%	3	5	7	[50]
Turbine lifetime	Year	20	25	30	[51, 52]
Electrolyzer lifetime	Year	5	10	15	[35]
Compressor efficiency	kWh/kgH_2	1.6	4.4	18	[43]
PEM fuel cell efficiency	%	50	60	70	[53]

[a] Starting cost in 2025

The turbine costs are in 2018 USD with inflation considered by the authors. The turbine costs decrease every year per the 2020 Annual Technology Baseline (ATB) estimates from the National Renewable Energy Laboratory (NREL) [38].

For this study, we take the costs of offshore wind turbines class 8 through 12 as representative of the type of systems that would be deployed in the Scotian Shelf, given its water depths. The lower bound costs come from the class 8 advanced estimates, the middle costs are from the class 10 moderate estimates, and the upper bound cost come from class 12 conservative estimates.

We develop annual estimates for capital expenditure (CAPEX) and Fixed Operation and Maintenance (FO&M). CAPEX costs include offshore wind overnight capital costs (OCC), construction financing, and grid connection costs. While it may seem unnecessary to include grid connection costs in scenarios all scenarios except for γ, this large array will need auxiliary power, most likely from the bulk grid, to maintain system health during periods of no wind. Grid connection costs could be associated with running an undersea cable to shore, or with providing some form of on-site power if that is deemed feasible and preferrable. Grid connection costs are smaller than OCC, but they are significant (between ~28% and ~40% of OCC, depending on turbine class).

The same cost evolution seen in offshore wind was then implemented on a database of (widely varying) electrolyzer costs [40, 41]. The two technologies sit at a similar technological readiness level: they are technologically ready, commercially available, but not widely deployed yet. While the supply chain has not scaled up to the level that would enable radical deployment, they remain somewhat modular technologies relative to nuclear power or carbon capture technologies. There is evidence that modular technologies experience faster learning rates than non-modular systems [115].

Storage costs are held static due to uncertainty regarding how the cost of building storage caverns might change over time. The few data we found on storage costs are

dated. Storage costs are split into three groups: compressor capital costs, conditioning, and cavern capital costs. Compressor capital costs deal with the initial capital cost of the compressors needed for the storage system: we take these to be ~$1,300/kW. Conditioning costs refer to the costs associated with compressing and cooling the hydrogen and are taken to be ~$0.02/kg$H_2$. Cavern capital costs refer to the cost of building the physical underground cavern required to store hydrogen, as well as the balance of the storage system, apart from compression and conditioning. These costs are taken to be approximately $9/kg$H_2$. For scenarios β_{ind} and δ, the rates of hydrogen generated is significantly higher, so the costs are adjusted accordingly. For β_{ind}, the compressor costs and conditioning costs are ~$800/kW and ~$0.01/kgH_2, respectively. For δ, the compressor costs and conditioning costs are ~$500/kW and ~$0.01/kgH_2, respectively. All these values assume a rate of hydrogen production of the same order of magnitude as that in our scenarios, as outlined in [42].

A.12. Retirements and replacement

In the recursive simulation, turbines and electrolyzers are replaced once they reach the end of their useful lives. We take 25 years to be our best estimate of the lifetime of an offshore wind turbine; for the electrolyzers, this estimate is 10 years (~100,000 hours). Lower and upper bounds are developed for both, assuming that the lifetime of both turbines and electrolyzers could be extended or shortened by 5 years. When calculating costs, we consider both the addition of new turbines to meet the stipulated growth rate and the number of replacements needed to replace retired assets.

A.13. Hydrogen storage

For the four cases that involve hydrogen storage, scenarios β_{tot}, β_{ind}, γ, and δ, an underground cavern storage system is employed. The overall cost of this system is split into three separate costs: compressor capital costs, compression costs, and cavern capital costs. In scenarios β_{tot} and β_{ind}, the amount of hydrogen storage is determined by finding the excess of hydrogen produced each year after project completion. The purchase of storage does not actually occur on this year, but on the first year where there is a month that produces excess hydrogen. In scenarios γ and δ, the hydrogen storage is purchased at the beginning of the project. In both cases, storage cost is static due to uncertainty regarding how the cost of building storage caverns might change over time. The calculation of storage cavern capacity is different in each scenario. The storage capacity is estimated by calculating the minimum amount required to meet annual demand and adding the amount needed for two-weeks' worth of storage. The two-weeks' worth of storage is also different for each of the scenarios. The table below lists each of the scenarios and their required storage size.

Table A.8. Storage size requirements for each scenario

Scenario	Two-weeks of storage (Tonnes)	Total storage (Tonnes)
α	0	0
β_{tot}	12,100	22,300
β_{ind}	9,100	27,800-28,000[a]
γ	6,400 - 9,000[b]	6,400 - 9,000[b]
δ	695,000	695,000

[a] Depends on turbine performance.
[b] Depends on fuel cell efficiency. Efficiencies used range from 50-70%

The additional storage constitutes an effort to build resilience into this system, helping address unaccounted downtime for up to two weeks (e.g., due to a wind drought). This value is also rounded up to the nearest 100 tH_2 to ensure there is adequate storage capacity. The cost of storage is calculated using (now admittedly dated) cost estimates provided by Amos at NREL [42].

In scenario γ, storage capacity is sized to accommodate sufficient hydrogen to meet two-weeks' worth of OSW output. Again, this is intended to provide some measure of resource adequacy and resilience in case of extended wind droughts. For context, the longest wind drought in the Scotian Shelf data we collected from NCAR lasted approximately 5 days. 6,400 to 9,000 metric tons of hydrogen storage are needed, depending on fuel cell efficiency. This number is also rounded up to the nearest 100 tH_2 to be conservative.

A.14. Uncertainty analysis

To determine the uncertainty of project or production costs to the various cost components under investigation, a Monte Carlo simulation is performed using Palisade's @Risk software version 8.2 [116]. The Monte Carlo simulations were each run with 10,000 samples and cumulative ascending distributions were created for each of the following results: total real project costs; hydrogen (or electricity) costs in 2025; and hydrogen (or electricity) costs at project completion. This simulation varied all the variables listed above in Table A.7. Below are all three distributions for each scenario.

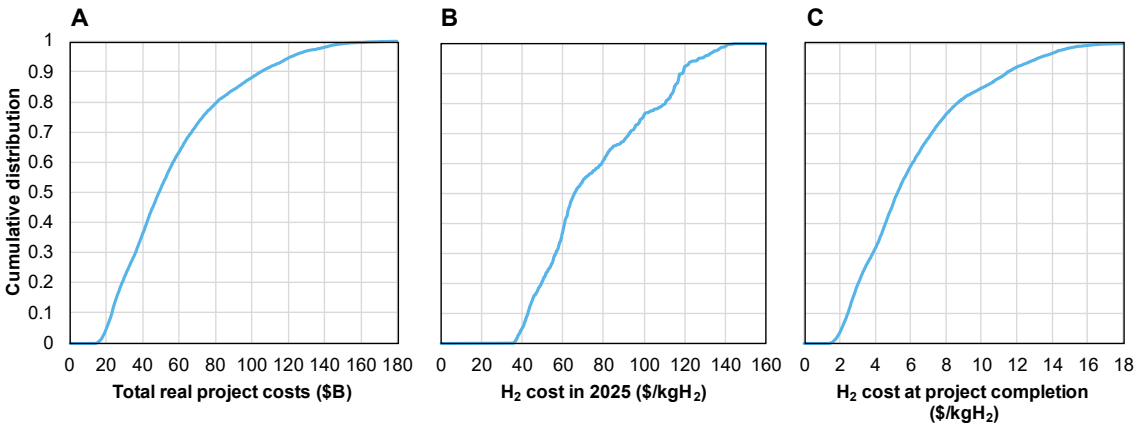

Figure A.2. Scenario α cumulative distributions of the **A)** total real cost of the project, **B)** hydrogen production costs in 2025 (the initial year in the simulation), and **C)** hydrogen production costs at project completion.

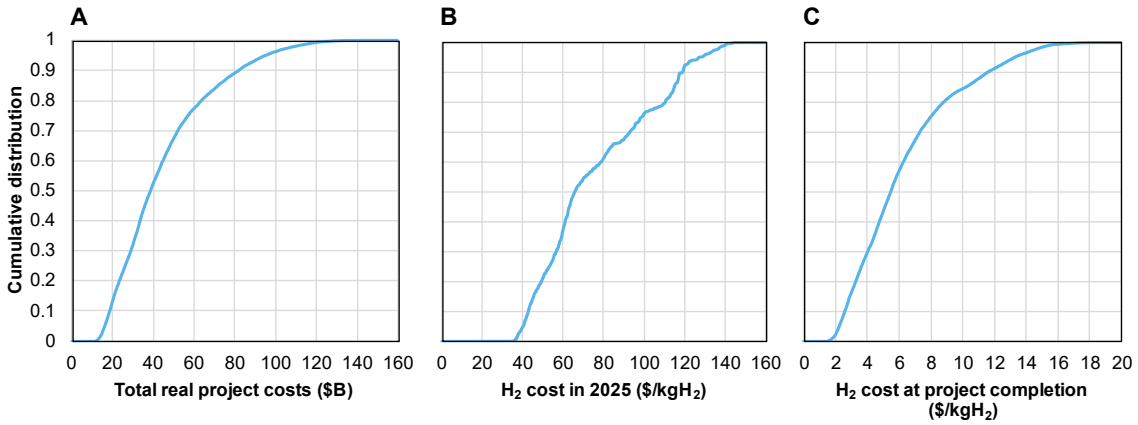

Figure A.3. Scenario β_{tot} cumulative distributions of the **A)** total real cost of the project, **B)** hydrogen production costs in 2025 (the initial year in the simulation), and **C)** hydrogen production costs at project completion.

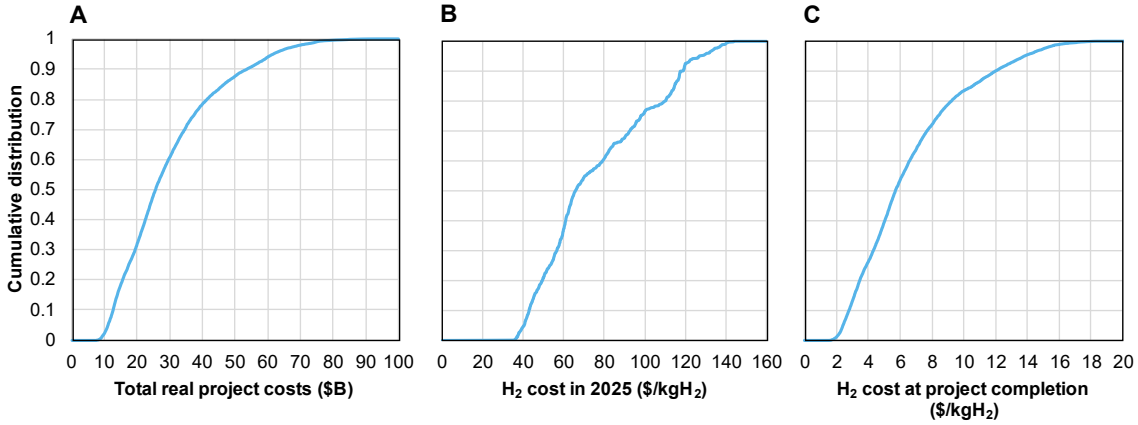

Figure A.4. Scenario β_{ind} cumulative distributions of the **A)** total real cost of the project, **B)** hydrogen production costs in 2025 (the initial year in the simulation), and **C)** hydrogen production costs at project completion.

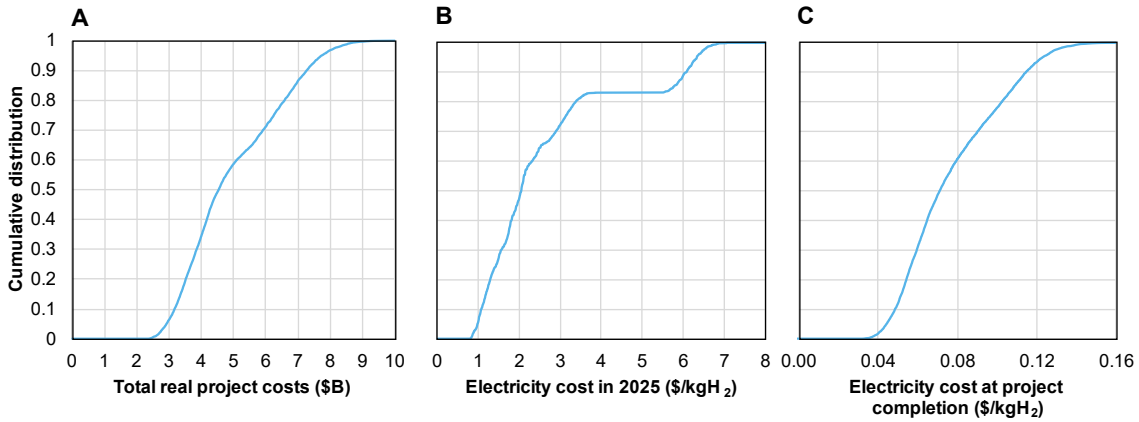

Figure A.5. Scenario γ cumulative distributions of the **A)** total real cost of the project, **B)** electric power production costs in 2025 (the initial year in the simulation), and **C)** the electric power production costs at project completion.

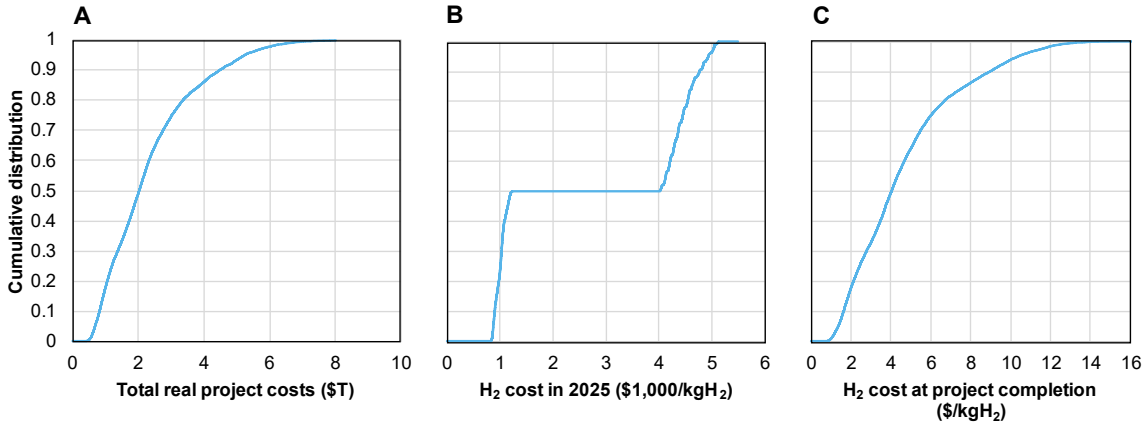

Figure A.6. Scenario δ cumulative distributions of the **A)** total real cost of the project, **B)** hydrogen production costs in 2025 (the initial year in the simulation), and **C)** hydrogen production costs at project completion.

A.15. Monthly capacity factors

To assess monthly variations in the utilization of system components, monthly capacity factors are calculated for both turbine and electrolyzer arrays using the following two equations, respectively.

$$CF_t = \frac{P_{elec}^{array}}{\left(\frac{TN_i \times 15 \times 24 \times d_m}{10\text{^}6}\right)} \tag{A.17}$$

$$CF_e = \frac{\left(\frac{P_{H_2}^{kg}}{24}\right)}{335 \times NE_i} \tag{A.18}$$

A.16. Natural gas consumption in the Maritimes

The natural gas consumption data for α, β_{tot}, and β_{ind} were obtained from Statistics Canada [48]. Consumption data from January 2016 to December 2021 was collected for Nova Scotia and New Brunswick (PEI is excluded since there is no natural gas consumption). These monthly datasets include a breakdown of industrial, commercial, and residential use. Exploratory data analysis showed wide variation between the Statistics Canada data and the data compiled by the Canada Energy Regulator (CER). Personal communication with the former helped the research team isolate line items in Statistics Canada's databases that, when summed, generate an estimate of natural gas consumption that is close to CER's data.

In order to estimate 2050 loads, the annual consumption of 2016 to 2021 was plotted and a linear trend was developed to forecast 2050 annual consumption. 2050 monthly values were also estimated by creating an average percentage distribution of the consumptions for each month within a year. Every year after 2050 is assumed to have the same consumption. In scenario α, the system is overbuilt so that even in the worst case, the minimum hydrogen production exceeds the estimated monthly demand. In scenarios β_{tot} and β_{ind}, where storage is utilized, there is no need for the turbine array to be overbuilt because storage exists to satisfy demand. An additional two-weeks' worth of storage is added to these values and would enhance the resilience of the system (or help account for decreases in wind power production or increases in energy demand). Scenarios γ and δ include these safety factors within their storage components. Enough hydrogen is stored to account for two-weeks' worth of electrical or diesel demand. Like the previous scenario, this could help absorb changes in the supply and demand.

A.17. Natural gas pipeline

The presence and coordinates of the Maritimes and Northeast Pipeline (M&NP) dictated our choice of case study location. Having access to a large, relatively new, bidirectional pipeline that extends throughout the Maritimes—from Maine to the Sable Island Bank 200km offshore—means that the current infrastructure to transport gas across the Maritimes already exists as well as the ability to contain the amount of hydrogen produced [117]. While many natural gas distribution pipelines in the Maritimes are made of hydrogen-compatible materials, extensive testing and modification might be required to ensure that hydrogen can be carried safely in these pipelines [18]. The pipeline integrity question is reserved for future work.

A.18. Results from the case with 5 starting turbines

While the manuscript focuses on elaborating the results of cases with 1 starting turbine, results from cases with 5 starting turbines can be found in the tables below.

Table A.9. Cost ranges for hydrogen production scenarios with 5 starting turbines

Scenario	Completion year	Starting H_2 cost ($/kg H_2)	Completion H_2 cost ($/kg H_2)	Total emission reduction (million tonnes)
α	2051 – 2062	36 – 122	1.3 – 18.0	55.1 – 78.2
β_{tot}	2049 – 2061	36 – 122	1.4 – 18.5	40.2 – 62.8
β_{ind}	2047 – 2057	36 – 122	1.6 – 18.9	25.8 – 37.9
δ	2070 – 2090	834 – 1,230	0.8 – 15.3	3,600 – 5,500

Table A.10. Cost ranges for scenario γ with 5 starting turbines

Scenario	Completion Year	Starting electricity cost ($/kWh)	Completion electricity cost ($/kWh)	Total emission reduction (million tonnes)
γ	2041 – 2048	0.8 – 3.0	0.04 – 0.20	42.0 – 53.7

A.19. Scenario δ – Transportation calculations

Scenario δ, which replaces the diesel usage in the Maritimes with hydrogen, is calculated by summing up the total vehicle miles traveled in the Maritimes by freight trucks. The Canadian Freight Analysis Framework (CFAF) from Statistics Canada [46] contains data from 2011 to 2017 containing the number of shipments, total distance traveled, shipment values, etc. for various pairs of routes to, from, and across Canada. For simplicity, it is assumed that the distance per each trip for any route can be found by taking the total distance traveled and dividing it by the number of shipments for that route. The yearly datasets are used to estimate the amount of diesel required for the 2050 target date with a linear trend.

Only the routes that included one of the Maritime's provinces as either an origin or destination were considered. Not every exact origin or destination is listed—some are grouped under a provincial label (e.g., "Rest of Nova Scotia", rather than "Halifax" or "Truro"). For these locations, cities that lead to a distance error of less than 5% (when compared to the distance per trip) were selected. It was also assumed that any routes that had either origin or destination as the same two cities traveled along the same route, but in different directions (e.g., freight from "Halifax to Montreal" is assumed to travel along the same route as freight from "Montreal to Halifax"). Table A.11 below shows all the cities selected to replace "provincially labeled" Canadian locations.

Table A.11. Locations selected to replace "provincially labeled" Canadian locations

Original Location Label	New Location
New Brunswick, NB	Priceville, NB
Newfoundland and Labrador, NL	St. Johns, NL

Original Location Label	New Location
Northwest Territories, NT	Whati, NT
Prince Edward Island, PE	Oyster Bed Bridge, PE
Rest of Alberta, AB	Slave Lake, AB
Rest of British Columbia, BC	Sunnyside, BC
Rest of Manitoba, MB	Brandon, MB
Rest of Nova Scotia, NS	Stewiacke, NS
Rest of Ontario, ON	Peterborough, ON
Rest of Quebec, QC	Trois-Rivières, QC
Rest of Saskatchewan, SK	Waskesiu Lake, SK
Yukon Territories, YT	Mayo, YT

The only location not listed in the table above is Nunavut, Nunavut. This was not included because it is assumed that the total distance driven for these routes is within the Maritimes, with the actual trip from the border to Nunavut requiring either air or sea shipment. The new locations chosen in Table A.11 sometimes had to be modified to reduce the error between our analysis and CFAF data to <5%. Table A.12 lists these exceptions.

Table A.12. Routes selected to replace specific Canadian domestic routes

Original Route	New Route
Whati, NT → Oyster Bed Bridge, PE	Wrigley, NT → Oyster Bed Bridge, PE
Trois-Rivières, QC → Priceville, NB	Beauceville, QC → Priceville, NB
Montreal, QC → Priceville, NB	Montreal, QC → Neguac, NB
Whati, NT → Priceville, NB	Whati, NT → Moncton, NB
Peterborough, ON → Priceville, NB	Peterborough, ON → Moncton, NB
Toronto, ON → Priceville, NB	Toronto, ON → Moncton, NB
Edmonton, AB → Stewiacke, NS	Edmonton, AB → Sherbrooke, NS
Montreal, QC → Stewiacke, NS	Montreal, QC → Sherbrooke, NS
Whati, NT → Stewiacke, NS	Whati, NT → Cape North, NS

Original Route	New Route
Oshawa, ON → Stewiacke, NS	Oshawa, ON → Sherbrooke, NS
Quebec City, QC → Stewiacke, NS	Quebec City, QC → Antigonish, NS
Peterborough, ON → Stewiacke, NS	Peterborough, ON → Sherbrooke, NS
Trois-Rivières, QC → Stewiacke, NS	Trois-Rivières, QC → Sherbrooke, NS
Winnipeg, MB → Stewiacke, NS	Winnipeg, MB → Sydney, NS
Peterborough, ON → Oyster Bed Bridge, PE	Peterborough, ON → Elmira, PE
Trois-Rivières, QC → Oyster Bed Bridge, PE	Trois-Rivières, QC → North Wiltshire, PE
St. Johns, NL → Halifax, NS	Whitebourne, NL→ Halifax, NS
St. Johns, NL → Priceville, NB	Clarenville, NL→ Priceville, NB
St. Johns, NL → Oyster Bed Bridge, NB	Clarenville, NL→ Oyster Bed Bridge, NB

Moreover, some of the routes were international and included origins or destinations within the United States or Mexico. We assume all such shipments travel to the United States, since the amount of trade with the United States (~$900 billion in 2020) is significantly higher than that with Mexico (~$28 billion in 2020) [118]. International routes were plotted as a histogram and split into six bins depending on the length of the shipment's route, as reported in CFAF. This can be seen in Figure A.7 below.

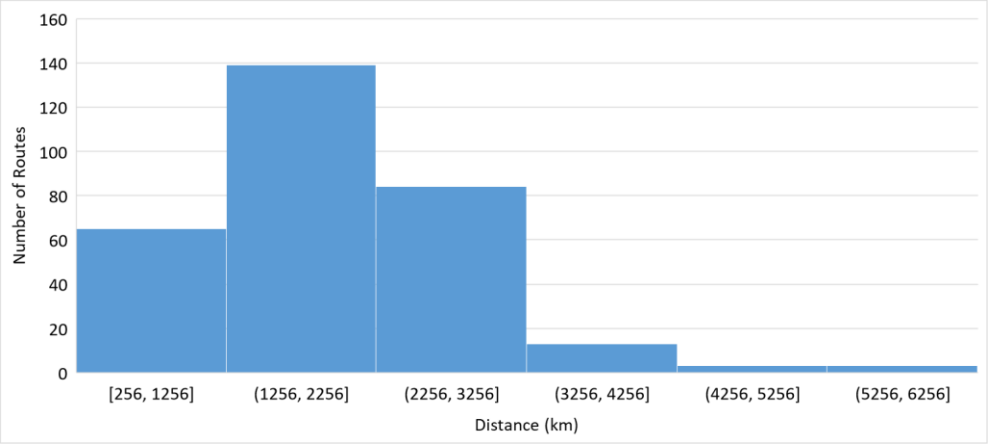

Figure A.7. Histogram of international routes split into 1000 km bins.

Table A.13 shows the specific city locations used to represent each of the route bins shown in Figure A.7.

Table A.13. United States locations based on distance

Distance (km)	Location
[256 – 1,256]	Springfield, MA
(1,256 – 2,256]	Columbus, OH
(2,256 – 3,256]	Bloomfield, IL
(3,256 – 4,256]	Houston, TX
(4,256 – 5,256]	Pheonix, AZ
(5,256 – 6,256]	San Diego, CA

Like the domestic Canadian routes, the international routes also have exceptions. Table A.14 below lists these exceptions, which were employed to reduce the error between our results and CFAF data to <5%.

Table A.14. Routes selected to replace specific international routes

Original Route	New Route
Springfield, MA → Oyster Bed Bridge, PE	Albany, NY → Oyster Bed Bridge, PE
Springfield, MA → Priceville, NB	New Haven, CT → Priceville, NB
Columbus, OH → Oyster Bed Bridge, PE	Cleveland, OH → Oyster Bed Bridge, PE
Bloomfield, IL → Priceville, NB	Miami, FL → Priceville, NB
Bloomfield, IL → Oyster Bed Bridge, PE	Columbia, MO → Oyster Bed Bridge, PE
Houston, TX → Priceville, NB	Albuquerque, NM → Priceville, NB
San Diego, CA → Halifax, NS	Pheonix, AZ → Halifax, NS

All two-city pairings were input into Google Maps, and the distance traveled within the Maritimes was measured starting from the port of entry (i.e., the border of the three provinces that constitute the Maritimes) to the intended destination. Google Maps

alters routes due to traffic conditions, so it is important to note that the above route distances were all estimated during the time period from March 22 to 24, 2022. The following equation was repeated for each unique route to determine the percentage of distance driven in the Maritimes for each year from 2011 to 2017.

$$MP_r = \frac{MD_r}{TD_r} \tag{A.19}$$

where MP_r is the percentage driven in the Maritimes for each route, r, MD_r is the distance traveled in the Maritimes for each route, and TD_r is the total distance traveled for each route. These percentages are then applied to each route and the total distance traveled within the Maritimes is calculated each year with:

$$D_y = \sum_r MP_r * NS_{r,y} \tag{A.20}$$

where D_y is the distance traveled in the Maritimes for each year, y and $NS_{r,y}$ is the number of shipments for each route in each year. These yearly distances are multiplied by the fuel efficiency of a semi truck. The U.S. Department on Energy states the fuel efficiency of this type of truck is 5.29 miles per gasoline gallon equivalent [47]. Converting this to its diesel equivalency returns 5.9 MPG [109] which is what is used to calculate the total gallons of diesel consumed for that year. Gallons are then converted to cubic meters and then each year is plotted. Using the estimated values from 2050, it is determined that the amount of diesel needed is about 60.7 million cubic meters or about 213 billion cubic meters of hydrogen which is calculated as follows:

$$H_{Supp} = D_{2050} * \frac{35{,}811{,}696}{10{,}224} \tag{A.21}$$

Appendix B. Supporting information for Chapter 4

B.1. Data inputs for optimizing hydrogen-backed and diesel-backed microgrids

Table B.1 below shows the input parameters and their values for both the hydrogen and diesel microgrid models. Additional comments for of these can be found in the SI:

Table B.1. Parameter input values and references for optimization models

Technology	Parameter	Value	Reference
Diesel genset	CAPEX ($/kW)	900 – 1,000	[97]
	OPEX ($/kW)	114 – 149	
	Unit capacity (kW)	100, 500, 1,000, 2,000	Authors
	Max capacity (kW)	1E+9	
	Lifespan (years)	25	
	Fuel costs (USD/L)	2.0865	[99][a]
	Efficiency (%)	38	[77][b]
	Electrical conversion factor of diesel (L/kWh)	0.1	[109]
Diesel furnace	CAPEX ($/kW)	160	[97]
	OPEX ($/kW)	16[c]	Authors
	Unit capacity (kW)	17.58	
	Max capacity (kW)	1E+9	
	Lifespan (years)	20	
	Fuel costs (USD/L)	2.0865	[99] [a]
	Efficiency (%)	80	[119]
	Thermal conversion factor of diesel (L/kWh)	0.1	[109]
Hydrogen furnace	CAPEX ($/kW)	160	Authors[d]
	OPEX ($/kW)	16	
	Unit capacity (kW)	17.58	
	Max capacity (kW)	1E+9	
	Lifespan (years)	20	
	Efficiency (%)	80	
	Thermal conversion factor of hydrogen (kg/kWh)	0.03	[120]

Technology	Parameter	Value	Reference
RFC	CAPEX ($/kW)	460 – 2,490	[120]
	OPEX ($/kW)	6.9 – 37.35	
	Unit capacity (kW)	1,000, 20,000, 100,000	Authors
	Max capacity (kW)	1E+9	
	Lifespan (years)	10	[35]
	Electricity to hydrogen conversion factor (kg/kWh)	0.03	[120]
	Hydrogen to electricity conversion factor (kg/kWh)	0.023	[121]
	Water consumption range (LH_2O/kgH_2)	11 – 40.5	[98]
	Stoichiometric water consumption (LH_2O/kgH_2)	9	
Wind turbine	CAPEX ($/kW)	700 – 1357[e]	[122]
	OPEX ($/kW)	34 – 43[e]	
	Unit capacity (kW)	500, 800, 1,500	Authors
	Max capacity (kW)	1E+9	
	Lifespan (years)	25	[51, 52]

[a] Diesel prices of Hay River, NWT are used
[b] Efficiency is back calculated from diesel consumption numbers provided by the reference and NRCan's simulated electrical loads
[c] OPEX values are assumed to be 10% of the CAPEX
[d] These hydrogen furnace values are assumed to be the same as those from the diesel furnace
[e] Lower values are from conservative 2021 costs and higher values are from advanced 2030 costs.